Molecular characterisation of *Anopheles gambiae* haem oxygenase

Thesis submitted in accordance with the requirements of the University of Liverpool for the degree of Doctor in Philosophy

By

Christopher Stephen Spencer

March 2016

Supervisors

Dr Mark Paine

Dr Gareth Lycett

Dr Lu-Yun Lian

Declaration

This work has not previously been accepted in substance for any degree and is not being currently submitted in candidature for any degree.

Signed ……(Candidate)

Date ……

Statement 1

This thesis is the result of my own investigation, except where otherwise stated. Other sources are acknowledged and bibliography appended.

Signed ……(Candidate)

Date ……

Statement 2

I hereby give my consent for this thesis, if accepted, to be available for photocopying and for inter-library loan, and for the title and summary to be made available to outside organisations.

Signed ……(Candidate)

Date ……

“Everybody knows I’m known for dropping science”

Adam “Ad-Rock” Horovitz

Root Down

1995

Acknowledgements

This work would not have been possible without the guidance and support of my primary supervisor, Dr. Mark Paine. Mark's patience and knowledge of the scientific process has been invaluable in getting me across the finish line. I am similarly indebted to my secondary supervisors, Dr. Gareth Lycett and Prof. Lu-Yun Lian, who were happy to provide advice and technical expertise when required.

I would like to thank the plethora of people around LSTM and the University of Liverpool who helped me in one way or another, including (in no particular order) Rodolphe Poupardin, Alvaro Acosta Serrano, Kay Hemmings, Hanafy Ismail, Alister Craig, Ashley Warman, Shona Moore, Lee Haines, Sravan Pandalaneni, Pryank Patel, Evangelia Morou, Jonathan Thornton, John Morgan, Jo Solino, Olga Mayans and Dave Weetman. I am grateful to Graham Moores, Tadge Szestak, Walter Fabricio Silva Martins and Jacob Riveron Miranda for their kind gifts of cDNA. Thanks to staff at OPPF for their technical assistance.

Cristina Yunta Yanes, Jacob Riveron Miranda, Amy Lynd, Pat Pignatelli, Adriana Adolfi, Chris Williams and Kayla Barnes are people without whom Liverpool would have been an extremely drab affair, and I thank you all for making it a fun ride. Glauber Pacelli Gomes de Lima and Angela Hughes deserve extra credit for ensuring my chin is kept up. Eilidh Carrington deserves so many thanks for being such an incredible flatmate and friend.

This PhD would have been infinitely tougher without help from friends and family back home. Thanks to Nicola Spencer and Carl McLaren for their support. The CC also deserve my unreserved gratitude, particularly my friends Joe Windell ("it's taking you *how* long?"), Dave Livesey, who has cast an enthusiastic eye over some of the tastier sections, and particularly Saskia Whelan, who has always been invaluable for proof-reading, venting and always being there.

Abstract

Malaria control is heavily reliant on the use of insecticides for interventions such as Indoor Residual Spraying (IRS) and Long Lasting Insecticide Nets (LLINs). Widespread resistance to insecticides in the malaria vector *Anopheles gambiae* threatens these interventions. To ensure the continued effectiveness of malaria control strategies, novel insecticides and insecticide synergists must be formulated, and in order to do so, new insecticide targets must be investigated.

Digestion of huge volumes of vertebrate blood in the midgut of An. gambiae mosquitoes results in the production of large concentrations of free haem: a potentially cytotoxic molecule. Amongst the adaptations haematophagous arthropods have for limiting haem mediated toxicity is haem degradation by the haem oxygenase system. Haem oxygenase, with its obligate redox partner, cytochrome P450 reductase, catalyses the hydrolysis of haem into biliverdin, producing carbon monoxide and ferrous iron.

To investigate the biochemical properties of *An. gambiae* haem oxygenase (AgHO), the enzyme was cloned and expressed in *E. coli*. The purified AgHO was observed to catalyse the degradation of haem to biliverdin, releasing CO and Fe^{2+}, in the presence of insect and human CPR reducing systems. AgHO bound haem stoichiometrically, with a KD closer to that of *H. sapiens* and *C. diphtheriae* than that of *D. melanogaster*.

Application of the HO inhibitors Sn-protoporphyrin and Zn-protoporphyin to mosquitoes as a bloodmeal supplement revealed a dose-dependent reduction in egg laying capability of An. gambiae. It is unclear whether this is due to a detrimental effect on mosquito health because of haem mediated cytotoxicity, or if this reduction in reproductive fitness is due to a key role for AgHO in the reproductive system.

A range of truncated CPRs from insects (*An. gambiae, A.mellifera, C. quinquefasciatus, D. melanogaster, R. prolixus*) and *H. sapiens* were also cloned and expressed. The six enzymes were biochemically characterised side-by-side using cytochrome c reduction assays in order to determine whether there are any differences in activity between those CPRs in blood-sucking insects and others. There were no clear trends in terms of enzyme kinetics which associated with a phenotype of haematophagy. The insect enzymes studied had higher V_{max} values than *H. sapiens* with respect to both NADPH (1.6-7.8 fold higher) and cytochrome c (1.5-5.8 fold higher). Also compared were the enzymes' sensitivity to nucleotide analogue inhibitors and DPIC. HsCPR more sensitive to the nucleotide analogues than insect CPRs (by 2-30 fold). DPIC however was more inhibitory to insect CPRs by up to 20 times, giving it potential as an insecticide synergist. Again, there were no clear trends aligning inhibition profiles with a blood-feeding habit.

In conclusion, AgHO has been found to be a true haem oxygenase, with biochemical characteristics in keeping with well characterised HOs such as *H. sapiens* HO-1 and *C. diptheriae* HmuO. AgHO inhibition appears to play a key role in oviposition and mosquito fecundity, and therefore may be a potential target for insecticides and insecticide synergists. Taken together, these results suggest that knowledge of these enzyme targets may aid the future development of novel insecticides.

Contents

List of Figures

List of Tables

Abbreviations

2’ 5’ ADP	2’ 5’ adenine diphosphate
2’ AMP	2’ adenine monophosphate
aa	Amino acids
AaBV	*Aedes aegypti* biliverdin
AaCPR	*Aedes aegypti* cytochrome P450 reductase
AaHO	*Aedes aegypti* haem oxygenase
ACh	Acetylcholine
AChE	Acetylcholine esterase
AgBV	*Anopheles gambiae* biliverdin
AgCPR	*Anopheles gambiae* cytochrome P450 reductase
AgHO	*Anopheles gambiae* haem oxygenase
AmCPR	*Apis mellifera* cytochrome P450 reductase
ALA	δ-aminolevulinic acid
APS	Ammonium persulphate
BLAST	Basic local alignment search tool
bp	(Nucleotide) base pairs
BV-IX	Biliverdin IX
BV-Ixα	Biliverdin alpha
CCDS	Consensus coding sequence
cDNA	Complementary deoxyribonucleic acid
CO	Carbon monoxide
CPR	Cytochrome P450 reductase
CqCPR	*Culex quinquefasciatus* cytochrome P450 reductase

DmCPR	*Drosophila melanogaster* cytochrome P450 reductase
DmHO	*Drosophila melanogaster* haem oxygenase
DMSO	Dimethyl sulphoxide
DNA	Deoxyribonucleic acid
DPIC	Diphenyliodonium chloride
dT	Deoxythymine
EC	Enzyme Commission number
ECG	Enzyme Characterisation Group
EDTA	Ethylenediaminetetraacetic acid
EST	Expressed sequence tag
FAD	Flavin adenine dinucleotide
FMN	Flavin mononucleotide
g	Standard gravity
GmCPR	*Glossina morsitans* cytochrome P450 reductase
GRP94	Glucose regulated protein 94
HBP	Haem binding protein
HeLp	Haem lipoprotein
HO	Haem oxygenase
HO-1	Human haem oxygenase 1
HO-2	Human haem oxygenase 2
HO-3	Human haem oxygenase 3
HRP	Histidine rich protein
HsCPR	*Homo sapiens* cytochrome P450 reductase
IC_{50}	50% of maximal inhibitory concentration

IPTG	Isopropyl β-D-1-thiogalactopyranoside
IVCC	Innovative Vector Control Consortium
K_{cat}	Turnover number
kdr	Knockdown resistance
K_M	Michaelis constant
LB	Luria-Bertani medium
LSTM	Liverpool School of Tropical Medicine
MACE	Modified acetylcholine esterase
MCS	Multiple cloning site
MdCPR	*Musca domestica* cytochrome P450 reductase
mRNA	Messenger ribonucleic acid
$NADP^+$	Nicotine adenine dinucleotide phosphate (oxidised form)
NADPH	Nicotine adenine dinucleotide phosphate (reduced form)
NCBI	National Center for Biotechnology Information
Ni-NTA	Nickel-nitrilotriacetic acid
NMR	Nuclear magnetic resonance imagery
OD	Optical density
PBP/GOBP	Pheromone binding protein / General odorant binding protein
PCR	Polymerase chain reaction
PMV	Perimicrovillar intestinal membranes
POR	P450 oxidoreductase
QMEAN	Qualitative model energy analysis
rdl	Resistance to dieldrin
RHBP	*Rhodnius* haem binding protein
RNA	Ribonucleic acid

RnCPR	*Rattus norvegicus* cytochrome P450 reductase
RnHO	*Rattus norvegicus* haem oxygenase
RpBV	*Rhodnius prolixus* biliverdin
RpCPR	*Rhodnius prolixus* cytochrome P450 reductase
RpHO	*Rhodnius prolixus* haem oxygenase
SOC	Super optimal broth with catabolite repression
SDS-PAGE	Sodium dodecyl sulphate polyacrylamide gel electrophoresis
SnPP-IX	Tin protoporphyrin IX
TAE	Tris acetate EDTA
TEMED	Tetramethylethylenediamine
TB	Terrific broth
Tris	Tris(hydroxymethyl)aminomethane
UV	Ultra violet
Vis	Visible light
V_{max}	Maximum velocity (of reaction)
ZnPP-IX	Zinc protoporphyrin IX

Chapter 1 - Introduction

1.1 Background

Vector-borne disease accounts for over 17% of infectious disease, with a mortality of more than 1 million deaths per year [1]. Among the arthropod vectors, mosquitoes are responsible for most human death. Of the mosquito-borne diseases, malaria is considered to be the most important. Malaria is most common in tropical and subtropical regions, and has become established in some temperate climates too (See Figure 1.1, [2]).

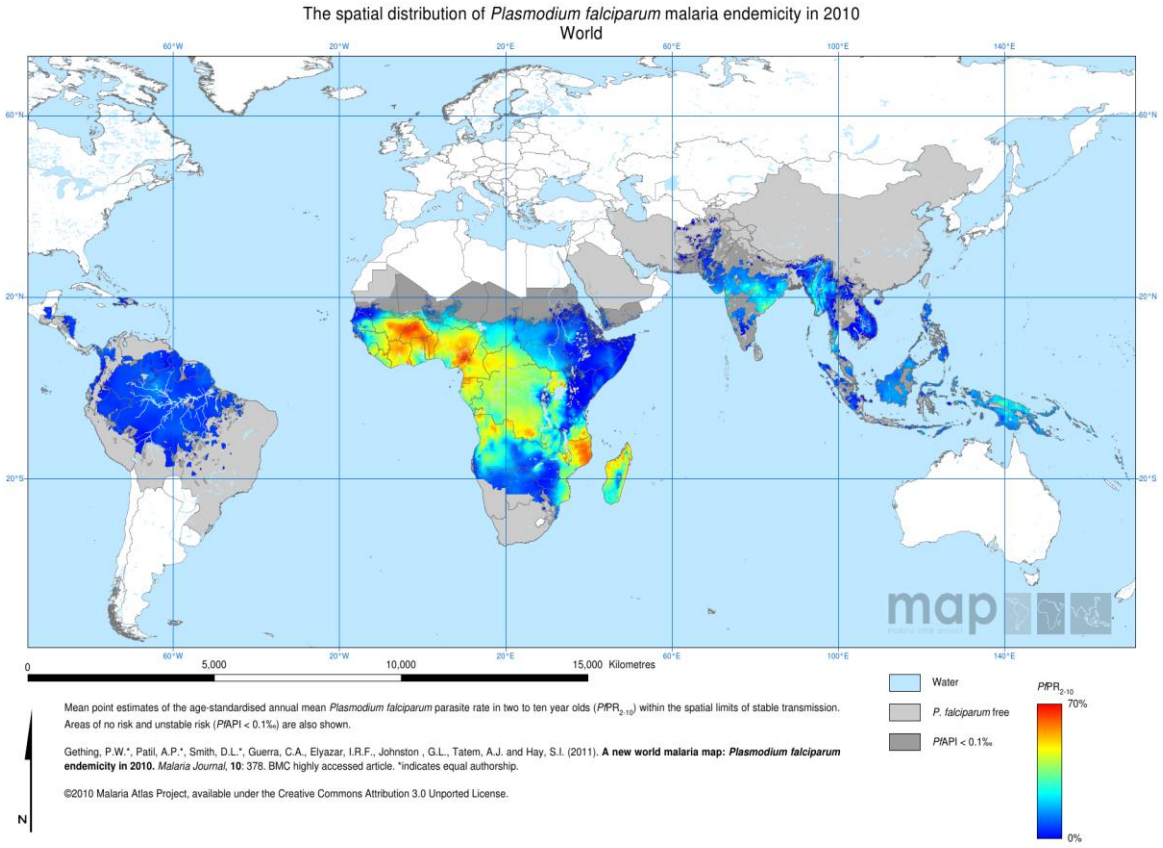

Figure 1.1. Global incidence of malaria in 2 -10 year olds [2]. This map reflects the tropical and sub-tropical regions where malaria is endemic

The estimated global incidence of malaria is huge; 2015 had an estimated 215 million cases, with 438,000 deaths [3]. Mortality is not the only problem with malaria infection – most of those infected each year are children, and those surviving the disease are prone to learning difficulties and brain damage. Infection of pregnant women is a major cause of maternal anaemia, low birth weights and infant death [4].

Malaria is caused by a protozoan parasites of the genus *Plasmodium*, which are transmitted by female *Anopheles* mosquitoes [3]. The major anopheline species in sub-Saharan Africa are *An. gambiae*, *An. arabiensis* and *An. funestus* [5]. Malaria remains one of the most important diseases in the world because of the numerous barriers to its control and eradication. There is currently no vaccine [6], *Plasmodium* parasites have developed resistance to numerous anti-malarial drugs [7, 8], and mosquito resistance to insecticide is a growing problem [9].

Malaria epidemiology is vitally dependent upon mosquito populations and their dynamics. The original Ross-MacDonald equation, the mathematical model which describes malaria epidemiology, relates to the mosquito in all of its transmission parameters, as do numerous of its successor models [10, 11]. It is clear that vector control is of paramount importance to breaking the malaria cycle, and that overcoming the hurdle of insecticide resistance in vector species is a key aspect. The first step towards the development of a novel insecticide is the identification of a new target.

1.2 Vector control methods

Given the establishment of resistance to *Plasmodium* species to anti-malarials and the importance of the vector life cycle to parasite transmission, vector control strategies continue to be a major preventative tool for the control of malaria and other vector borne diseases. There

is no single panacea for vector control in malaria, and accordingly, vector control in malaria endemic areas should involve numerous parallel efforts to minimise disease incidence.

1.2.1 Physical means of vector control

Non-chemical approaches to vector control are varied, and include strategies to both minimise mosquito populations, and to separate adult vectors from humans. Larval source management [12] is an approach which involves physical (elimination of breeding and hatching sites, such as stagnant water) and chemical means (larvicides such as pyriproxyfen) [13, 14] to reduce the populations of mosquito larvae, and therefore adult mosquito population. LSM is not always appropriate, particularly where mosquito breeding sites are either vast or ephemeral. It has been part of reductions in disease incidence, and it is argued [12] that it has great potential as part of an integrated vector control strategy.

Other physical means of transmission reduction include the employment of window screens [15] and untreated bednets [16] to separate human biting victims from mosquitoes. These methods have the potential to be effective due to the nocturnal and endophagic nature of *Anopheles* vector species – houses are the most common places for contact between night biting mosquitoes and humans [17]. Untreated bednets are not near as effective as those treated with insecticides however.

1.2.2 Insecticides

Long-lasting impregnated nets (LLINs) and indoor residual spraying (IRS) are the two front line means of targeting adult malaria mosquitoes indoors. Table 1.1 shows WHO approved insecticides for adult malaria mosquito control. These insecticides each fall into one of four categories dependent on their chemical structure; organochlorines, organophosphates, carbamates and pyrethroids.

Table 1.1. WHO approved insecticides for control of adult malaria mosquitoes [18]

Dates approved	Insecticide	Class	Application		P450 resistance
			IRS	ITN	
1940 – 1945	DDT	OC	X		r
1940 – 1950	Lindane	OC			
1951 - 1955	Malathion	OP	X		r
1961 – 1965	Fenitrothion	OP	X		r
	Propoxur	Ca	X		r
1966 – 1970	Chlorpiriphos-methyl	OP	X		r
1971 – 1975	Pirimiphos-methyl	OP	X		r
	Bendiocarb	Ca	X		r
	Permethrin	Pyr	X	X	R
1976 – 1980	Cypermethrin	Pyr	X	X	R
1981 – 1985	Alpha-cypermethrin	Pyr	X	X	R
	Cyfluthrin	Pyr	X	X	R
	Lambda-cyhalothrin	Pyr	X	X	R
	Deltamethrin	Pyr	X	X	R
	Bifenthrin	Pyr	X	X	R
1986 – 1990	Etofenprox	Pyr	X	X	R

OC, organochlorine; OP, organophosphate; Ca, carbamate; Pyr, pyrethroid; r, weak contribution to resistance; R, strong contribution to resistance.

1.2.2.1 Organochlorines

Organochlorine insecticides are chlorinated hydrocarbons which are divided into two categories: DDT-type compounds (DDT) and chlorinated alicyclics (lindane). Organochlorines have been banned for agricultural use since the 1970s due to their environmental persistence and long-term bioaccumulation in non-target organisms at all trophic levels. DDT was reapproved for use in IRS programs in limited quantities in 2006 [19]. The DDT mode of action is at the voltage-gated sodium channels (VGSC) in the nerve axon [20]. Here, the organochlorine molecule binds and prevents deactivation of the sodium gate. The axon membrane is prevented from depolarising, and Na^+ ions leak through the membrane. The affected nerve becomes hyperexcitable, resulting in spontaneous discharge. Chlorinated alicyclic insecticides also have the effect of nervous hyperexcitation, but via binding at the $GABA_A$ site on the GABA chloride ionophore complex, inhibiting Cl^- transport into nerves [20].

1.2.2.2 Organophosphates and carbamates

Phosphoric acid esters, termed organophosphates, have a toxic effect in animals by binding acetylcholinesterase (AChE). AChE is a class of enzymes which catalyses the hydrolysis of acetylcholine (ACh) – a neurotransmitter [21]. By binding to AChE, organophosphates inhibit the breakdown of ACh, allowing it to build up at nerve synapses leading to improper termination of nerve impulses.

Carbamates are esters derived from carbamic acid, and directly inhibit AChE, as organophosphates do [21].

1.2.2.3 Pyrethroids

Organic compounds similar to those pyrethrins naturally produced by certain *Chrysanthemum* species are called pyrethroids, and are among the most commonly used insecticides. They are significantly advantageous over other classes of insecticides in that they are generally harmless to humans and are not environmentally persistent. Pyrethroids work by binding to VGSCs whilst they are in an open conformations, resulting in a prolonged influx of Na^+ ions, similar to DDT-like organochlorines. This results hyperexcitiation of the nerves, and spontaneous nerve firing [20].

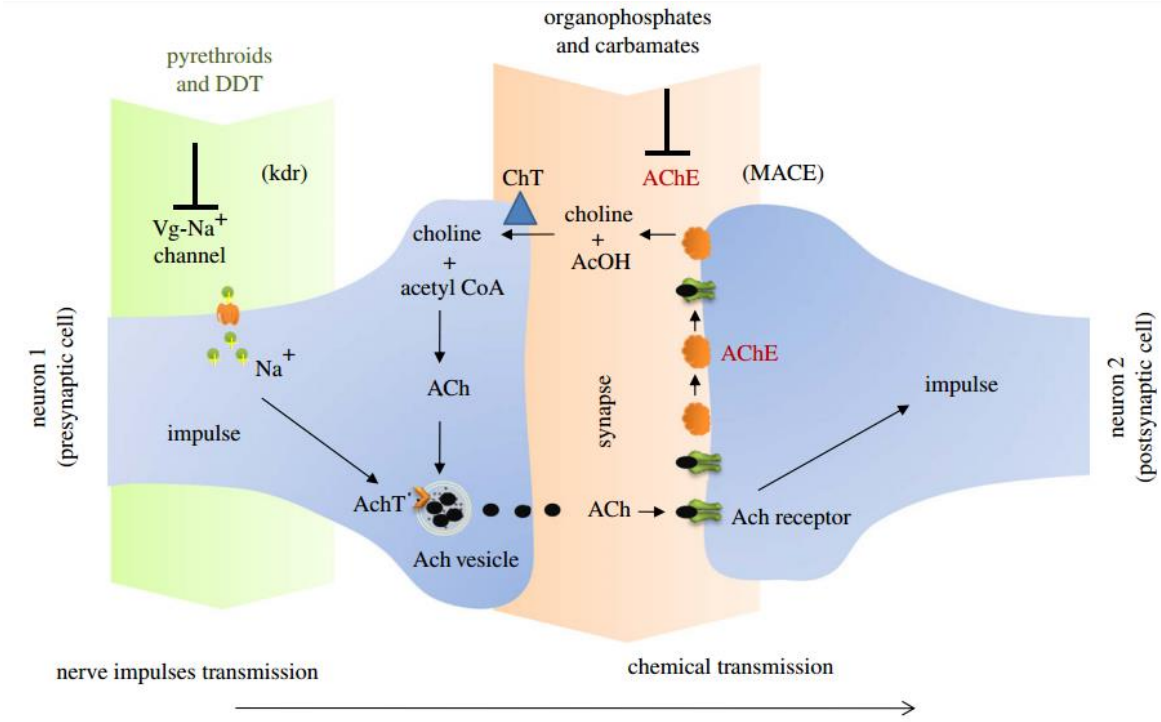

Figure 1.2. Modes of action of WHO approved insecticides (adapted from [22])

1.2.3.4 Pyriproxyfen and fecundity blocking insecticides

Pyriproxyfen does not belong to one of the four major classes of insecticides already discussed, rather it is a pyridine-based pesticide which acts as a juvenile hormone analogue [23]. It is

traditionally a larvicide, inhibiting the emergence of adult mosquitoes by targeting insect growth regulation. It also has great utility in IRS and LLINs, where it has multiple effects.

Firstly, mosquitoes can perform autodissemination [24]. Upon resting in a treated area, mosquitoes are exposed to pyriproxyfen, which they then take back to breeding sites. These breeding sites are then contaminated with pyriproxyfen, having a larvicidal effect.

Aside from its larvicidal effect, pyriproxyfen directly mediates mortality in adult mosquitoes, and decreases fecundity [25]. Juvenile hormone regulates insect ovarian development [26], and exposure to pyriproxyfen leads to abnormal hormonal regulation in ovarian development, improperly developed ovarian follicles, and sterility.

1.2.3 Insecticide resistance

The application of synthetic insecticides approved for public health use by WHO has dramatically reduced the risk of contracting arthropod-borne diseases. In fact, the 80% reduction in malaria incidence this century has come about as a direct result of the application of insecticides [27]. However, the widespread application of these insecticides has placed huge selection pressure on insect populations to develop adaptations to withstand these insecticides [28]. There has been resistance to each of the four major insecticide classes observed in many vector species.

Despite the fact that there are numerous WHO approved insecticides (Table 1.1), they only have two modes of action, as illustrated by Figure 1.2 [22]. This means that when resistance to one insecticide develops in an insect population, that adaptation can often confer resistance to other insecticides of the same class (crossresistance) or of a different class acting on the same target (multiresistance). Resistance in mosquitoes can be mediated by one of two mechanisms: metabolic resistance (degradation of the insecticide) or target-site resistance

(mutation of the target protein) [29]. Metabolic resistance involves detoxification enzymes such as esterases, cytochromes P450 and glutathione S-transferases chemically catabolising the insecticide molecules. The three known target-site resistance mutations are kdr (knockdown resistance – a mutation in the VGSC conferring DDT and pyrethroid resistance), rdl (resistance to dieldrin – allowing for resistance to chlorinated alicyclics) and MACE (modified acetylcholine esterase – conferring carbamate and organophosphate resistance) [18].

The spread of insecticide resistance, and the limited range of insecticide targets led to the establishment of the Innovative Vector Control Consortium (IVCC) [30]. The goals of the IVCC are to develop novel insecticides with novel modes of action, and to improve vector control delivery. Their target is to deliver three new insecticides by 2020, and they are on track to meet this target, however it is unlikely that these new insecticides will have reached the market by that time [31].

The threat posed by insecticide resistance is that it will undo the gains made in combatting malaria. It is of vital importance that future vector control strategies are not reliant upon insecticides with a single target, as has been the case for decades with pyrethroids. The insect bloodmeal has the potential to be an effective insecticide target.

1.3 Relevance of the bloodmeal to arthropod vectors

Haematophagy as a life strategy has arisen independently numerous times amongst arthropods [32], and accordingly, disease vectors are from a diverse range of arthropods, including arachnids (ticks), bugs (the kissing bug – *Rhodnius prolixus*) and true flies (mosquitoes, sandflies and tsetse flies). Haematophagy in these arthropods can be divided into obligate and optional, but only from the point of view of the individual insect, not from the point of view of the species. Obligate haematophages such as the kissing bug must feed on blood simply to

survive, however optional haematophages, like mosquitoes, can survive by feeding on nectar and fruit juices (indeed, male mosquitoes do not bloodfeed at all, and only feed on sugar sources). Optional haematophages do however need to feed on blood in order to develop eggs and form progeny. The bloodmeal is an essential aspect of the life cycle of all vector species, and is therefore an attractive target for novel insecticides.

The most obvious adaptations for a blood feeding habit are piercing or cutting mouthparts for mechanical disruption of vertebrate skin [33]. Other adaptations of blood-sucking insects include physiological adaptations which counter the responses of the vertebrate host. These include apyrase, which ameliorates a pain response [34]; peroxidase, which destroys vasoconstrictors [35] and hamadarin, an anti-factor XII [36]. Behavioural changes which aid in host location have also evolved. Some of the most important adaptations unique to blood-feeding insects are those which deal with the physiological impact of a huge influx of the pro-oxidant molecule, haem.

1.4 Haem and haem toxicity

Haem consists of an iron ion in the centre of a porphyrin ring (Figure 1.2). It is most commonly encountered as a prosthetic group in metalloproteins such as haemoglobin and myoglobin (where it functions in oxygen transportation and storage), and enzymes such as the cytochromes [37], certain peroxidases [38] and nitric oxide synthases [39] (where the function is electron transfer). Upon degradation of metalloproteins, the haem moiety is released. Free haem is toxic by way of two main mechanisms: prooxidant activity (the acceleration of free radical formation) and the physical disturbance of phospholipid bilayers [40].

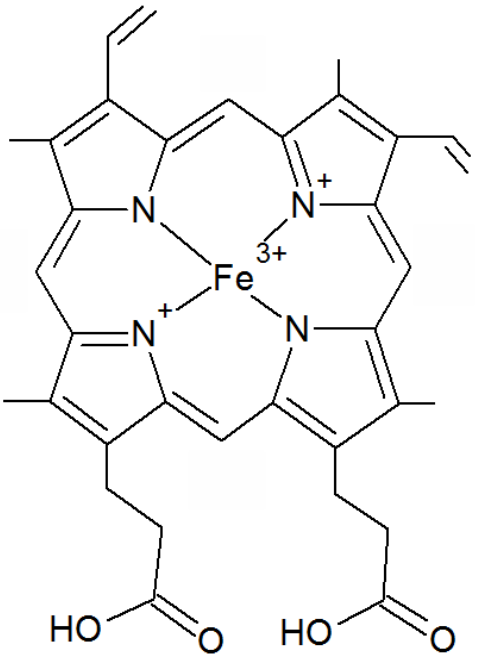

Figure 1.2 – Haem b

The haem mediated proliferation of free radicals in biological systems causes cytopathology through oxidation of lipids [41], degradation of proteins [42] and DNA strand scission [43]. The generation of these radicals is summarised in Figure 1.3 [44]. Free haem is particularly toxic due to the fact that it is a general peroxidative catalyst – with several routes towards the generation of radicals. Though free haem has been shown to promote the production of hydroxyl radicals *in vitro*, evidence suggests that haem mediated oxidative stress comes by way of the decomposition of organic hydroperoxides, rather than the generation of molecular hydrogen peroxide [45].

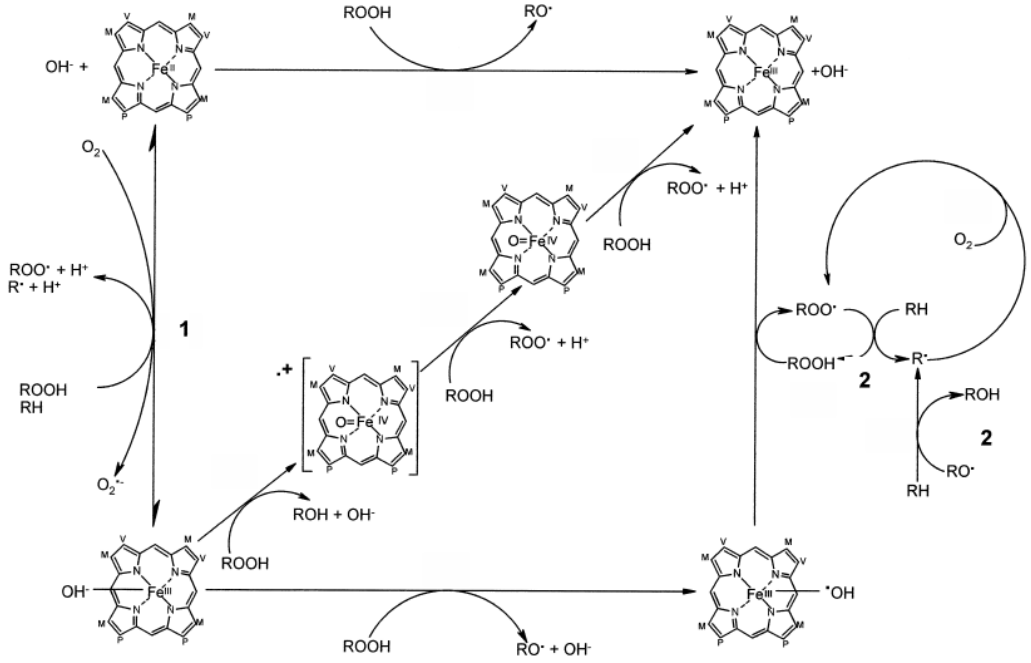

Figure 1.3. Overview of the radical reactions of the haem compounds haematin and ferrohaem. $O_2^{\cdot -}$, superoxide anion radical; ROOH, organic hydroperoxide; ROO·, lipid hydroperoxyl radical; -R·,alkyl radical; RO·, alkoxyl radical; RH, non-protein thiol (reduced glutathione, β-mercaptoethanol in **1** and unsaturated fatty acids in **2**) Adapted from [45]

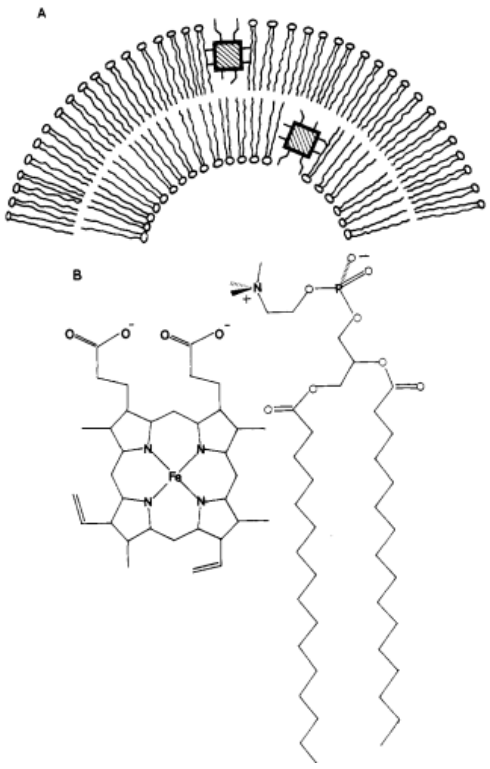

Figure 1.5. Possible orientation of haem in a phospholipid bilayer - At membrane level (**A**) and molecular level (**B**) [46].

The disturbance of phospholipid bilayers is brought about by haem's amphiphilic properties, as shown in Figure 1.4 [46]. Up to 97% of cellular haem can be membrane bound, conversely only up to 47% of cellular bilirubin (the product of mammalian haem degradation) will be membrane bound, emphasising the difference in solubility in the two molecules [47].

Female mosquitoes consume up to two times their own body weight in a bloodmeal [48-50]), producing haem at a concentration of *circa* 10mM [51]. Oxidative damage to membranes occurs maximally at 50-100μM, with effects on membrane permeability occurring about 100μM [40]. Mechanisms that have evolved to mitigate haem toxicity are vital for survival. These include aggregation of haem, use of anti-oxidants, haem binding proteins and the degradation of haem by haem oxygenases.

1.5 Mechanisms of haem detoxification

1.5.1 Haem aggregation

Once haemoglobin has undergone proteolysis and haem has been liberated, it becomes more insoluble. This can either result in membrane disturbance which is potentially harmful, or

aggregate formation, which reduces haem mediated toxicity by preventing membrane disturbance and minimising free radical formation *via* steric hindrance. Haem aggregates are an ordered complex first characterised in *Plasmodium falciparum* [52]. *Plasmodium* species form an aggregate called haemozoin, and that consists of dimeric haem units constructed with iron carboxylate bonds, which mass together through hydrogen bonds between propionate side chains on the haem porphyrin ring [53]. Similar haem aggregates occur in the mosquitoes *Aedes aegypti* [54] and *An. darlingi* [55], and the triatomine insect *R. prolixus* [56]. The mechanism of haem aggregation is best characterised in *R. prolixus*. Triatomines have perimicrovillar intestinal membranes (PMV); extracellular phospholipid membranes situated between the midgut epithelium and lumen that form a hydrophobic environment in which haem polymerises. [57]. There is debate as to whether the process of polymerising haem is protein mediated [58], membrane mediated [59] or is an autocatalytic process [60]. Two lines of evidence suggest that protein mediation may play a key role in aggregation. Firstly, *Plasmodium* histidine rich proteins (HRPs) mediate polymerisation activity *in vitro* [58], secondly, heating the triatomine PMV prevents polymerisation [56]. However, a likely scenario is that all three mechanisms are in play at the same time – for instance, a haemozoin 'primer' could be created by a haem-binding protein, and elongate itself through autocatalysis the rate of which could increase in a hydrophobic environment [51].

1.5.2 Haem binding proteins

Haem-binding proteins (HBPs) with an antioxidant role have been identified in the haemocoels of *R. prolixus* (*Rhodnius* haem-binding protein - RHBP) [61, 62] and the cattle tick *Rhipicephalus microplus* (haem lipoprotein - HeLp) [63, 64]. Whilst sharing a similar function, these two binding proteins have differences. The antioxidant mechanism for both is unclear; there are numerous examples of proteins which bind haem and augment the ability of haem to

mediate lipid peroxidation [65], therefore the ability to simply bind haem does not necessarily lead to detoxification. *R. microplus* HeLp has an important role in haem salvage and release, and hence maintenance of physiological haem levels, important, as *R. microplus* lacks a haem biosynthesis pathway. Conversely RHBP primarily acts as an antioxidant, but acts as a haem source only for embryonic development, as *R. prolixus* can synthesize its own haem. Structurally, the proteins are completely different. HeLp itself is a haemoprotein, possessing two haem moieties, and can bind a further six haem molecules. RHBP binds a single haem unit, suggesting a completely different evolutionary history. This is unlike haem oxygenases, which appear to be orthologous in different species (Chapter 3).

In mosquitoes, the haem binding protein AeIMUCI has been identified in the peritrophic matrix of *Ae. aegypti*. AeIMUCI has numerous analogues across the Insecta taxon, including in *An. gambiae*. Whether or not this *An. gambiae* analogue is a key aspect of gut detoxification is a matter of speculation. It may act as HeLp does, salvaging and releasing haem in a nutritional role, although as *An. gambiae* has a biosynthetic haem pathway, this may not be as crucial. This uncertainty illustrates a key point; that inhibition of the haem oxygenase enzyme as part of a control strategy may have different effects on different arthropod vectors, depending on the specific auxiliary strategies employed by each species.

1.5.3 Free radical attenuation

Rather than targeting haem itself, mechanisms may focus on the detoxification of generated free-radicals. Comparison of ESTs in *An. gambiae* [66-69] has shown increased expression of numerous genes coding for detoxification and haem metabolising enzymes 24 hours post blood feed. Prevalent amongst the stress proteins upregulated were those related to the thioredoxin reductase cascade. AgHO was notably absent from this list, indicating that it is not up- or down-

regulated by blood feeding, or that it was not identified. Stress response proteins such as Heat shock 70 and GRP94 are induced in *Ae. aegypti* [70], along with hexokinase, a glycolytic enzyme has been shown to act as an antioxidant in rats; preventing oxidative damage from free radicals generated by the mitochondria [71]. Superoxide dismutase and catalase, well known detoxificant enzymes, have been shown to be upregulated post-bloodmeal in *R. prolixus* [72] and *An. gambiae* [73].

Other sources of free-radical detoxification include smaller antioxidant molecules, most commonly uric acid. *R. prolixus* has displayed haem induced uric acid synthesis in the haemolymph [74], while xanthurenic acid has been identified as a detoxificant in *Ae. aegypti* [75].

1.6 The haem oxygenase reaction pathway

Haem oxygenase (EC 1.14.99.3), is diversely expressed by bacteria, plants and animals. While mammalian HOs have been extensively studied, the only insect haem oxygenases to have been cloned and characterised is *Drosophila melanogaster* haem oxygenase (DmHO) [76]. Haem oxygenation products have been identified in *R. prolixus* [77] and *Ae. aegypti* [78],

although RpHO and AaHO have yet to be individually expressed and functionally characterised.

Humans have three haem oxygenases; HO-1 is the best characterised haem oxygenase and is inducible in response to oxidative stress. HO-2 and HO-3 are less well studied. HO-2 is a constitutively expressed isoform involved with haem homeostasis, whilst HO-3 is not catalytically active, but could be involved in oxygen sensing [79].

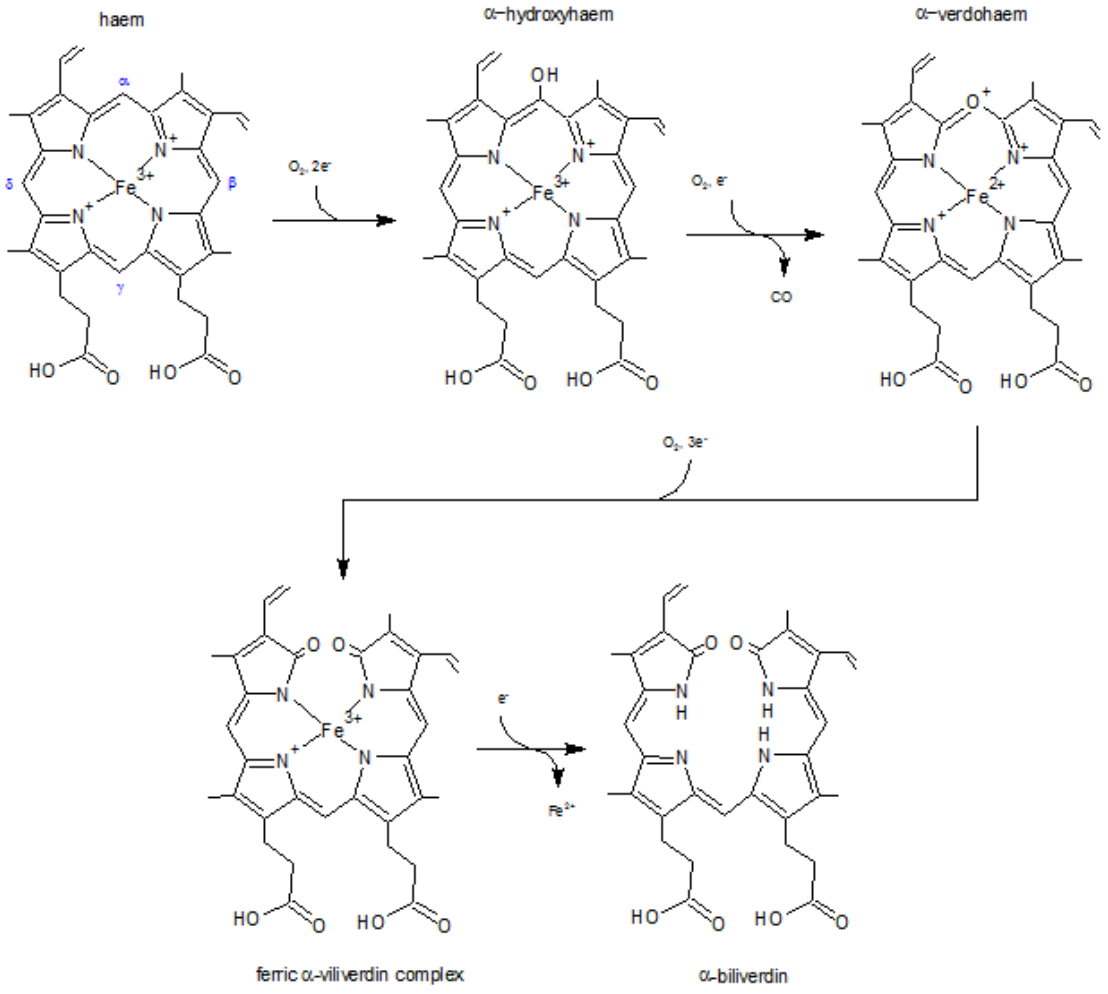

Figure 1.6. Schematic for HO-mediated haem degradation into BV IXα

Haem degradation by HO-1 occurs via a well-studied multistep mechanism [80]. The reaction requires electrons from NADPH [81, 82], and this transfer being mediated by

cytochrome P450 reductase [83]. The pathway begins with hydroxylation at one of the meso-carbons on the haem's porphyrin ring. Next is the oxygen-dependent removal of the hydroxylated meso-carbon as carbon monoxide-producing verdohaem, occurring alongside the reduction of the ferric complex to the ferrous state before complete elimination of the iron (Figure 1.5).

Figure 1.5 shows the hydroxylation and removal of the α-meso-carbon. Though this is the exclusive reaction pathway for HO-1; haem can be similarly oxidised in an enzyme-free, aerobic environment with ascorbate as a reducing agent [84]. In the enzyme-free reaction, all four meso-carbons are cleaved in equal proportion. Similarly, insect HOs can hydroxylate different meso-carbons. It has been established that some insects can hydroxylate and remove the γ-meso-carbon [85]; recombinant DmHO has been observed to hydroxylate α-, β- and δ-meso-carbons simultaneously *in vitro* [76]. Which carbon is hydroxylated i.e. the regiospecificity of the reaction, may be determined by structural motifs in the HO molecule.

1.6.1 Cytochrome P450 reductase

NADPH cytochrome P450 reductase (CPR, EC 1.6.2.4) is an integral membrane protein, and one of the few eukaryotic enzymes known to contain both FAD and FMN flavin cofactors [86]. CPR's physiological electron acceptors, are chiefly the cytochromes P450 [87]. As has been stated above, CPR is the also the obligate electron donor for haem oxygenase mediated haem degradation [83]. In this reaction system, electrons originate from NADPH. The NADPH cofactor binds in a pocket on CPR, which induces a conformational change in the enzyme, moving NADPH adjacent to FAD. Electrons are then passed from NADPH to FAD, then to FMN. The FMN cofactor is near to the edge of the enzyme, and close to the redox partner binding site. Here, FMN passes electrons to haemoproteins such as haem oxygenase [88] or cytochromes P450 [87]. In P450s, electrons drive the monooxygenation of drugs and xenobiotics [89], but in haem oxygenase these electrons are used to hydroxylate haem [80].

Study of *An. gambiae* cytochrome P450 reductase (AgCPR) is important, because it presents another potential target for novel insecticides and insecticide synergists [90, 91]. The fact that it is the obligate redox partner of two separate metabolic pathways (haem degradation and metabolic insecticide resistance) indicates that this enzyme holds great promise as an insecticide target. It has been shown that inhibition of CPR shuts down endoplasmic cytochrome P450 activity, which has a direct effect on the ability of an organism to metabolise and detoxify xenobiotics. In mice hepatic CPR knockout has been shown to impact drug metabolism [92]. Knockdown of CPR has been shown to increase the susceptibility of insecticide-resistant mosquitoes to permethrin [91] and similar effects have been observed in other insects, such as *Cimex lectularius* [93]. Whilst previous insect studies have focussed on the insecticide resistance phenotype, it is possible that CPR knockdown may be having other effects given its role in the haem degradation pathway. The CPR^- phenotype is non-lethal in mosquitoes and *C. lectularius*, but there may be more subtle phenotypes, such as diminished oviposition and increased oxidative stress.

1.6.2 Haematophage biliverdins and regiospecificity

R. prolixus and *Ae. aegypti* have been observed to produce modified biliverdins as a result of haem degradation (Figure 1.6 [77, 78]). *R. prolixus* has been shown to hydroxylate haem that has been modified to include two cysteinylglycine residues, at the γ-meso-carbon, yielding a BV IXγ. This activity is assumed to be through RpHO [77]. Similarly, haem degradation in the *Ae. aegypti* midgut yields a BV IXα modified downstream to include two glutamine residues [78]. The enhanced solubility of these molecules facilitate excretion, mirroring the mammalian strategy of converting biliverdin into more soluble bilirubin and then glucuronic acid. It can be

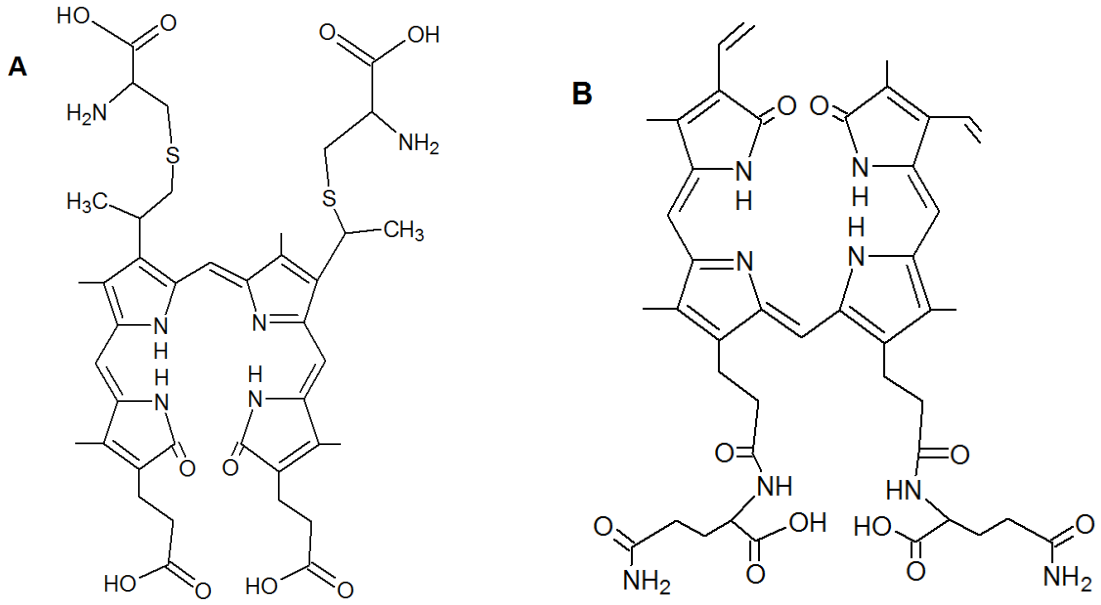

Figure 1.7. **Haematophage biliverdins**. **A**, *R. prolixus* biliverdin (RpBV). The porphyrin ring is oxidatively cleaved at the γ-meso-carbon after being chemically modified to include two cysteinylglycine residues [77]. **B**, *Ae. aegypti* biliverdin (AaBV). Here the porphyrin ring is cleaved at the α-meso-carbon, and then two glutamine residues are added sequentially post-cleavage [78].

expected that other haematophagous arthropods will modify biliverdin in similar ways, in order to solubilise the molecule.

1.7 Haem oxygenase in *Anopheles gambiae*

HOs are conserved across microbial and non-haematohphagous organisms, so while it is likely that *An. gambiae* haem oxygenase (AgHO) is a dietary detoxificant of blood, it may play other physiological roles in the blood feeding mosquito.

HO-1 and the other mammalian HOs primarily function in a homeostatic capacity to avoid toxicity from endogenous haem, such as during bruising [94] or in erythrocyte recycling in the spleen [95]. Dipterans do not contain haemoglobin instead they use an elaborate tracheal system to diffuse oxygen into the organism [96] (moreover, where arthropods do have an oxygen transportation protein, it is haemocyanin, which does not contain haem [97]). However *An. gambiae* and the other haematophages still require free haem for development, synthesis of haemoproteins, generation of pigments and other biological processes. As a result, HO is required to perform a role in haem homeostasis. Larger dietary haem concentrations in *An. gambiae* and other haematophages may require different reaction mechanisms and/or expression patterns in order to prevent oxidative stress.

1.8 Haem oxygenase as a detoxificant of dietary haem in *An. gambiae*

Haem degradation occurs in other haematophages - *Ae. aegypti* [78] and *R. prolixus* [77], and alongside *An. gambiae,* these insects have putative HOs in their genomes. It is uncertain whether or not HOs in these haematophages are significantly different in structure and function to the extensively characterised HO-1. Sequence analysis suggests that there is minimal variation around the active site. This is to be expected, because the substrate has not changed structurally only its location and concentration has. *R. prolixus* is a potential exception

however, as its HO appears to use a haem which has two cysteinylglycine residues attached to it. As *An. gambiae* has to deal with massive influxes of haem, it could be expected that there might be differences in affinity and reaction rates in AgHO. There might be differential expression patterns in AgHO, however this is yet to have been confirmed through EST analysis [66-69]. It could be expected that AgHO is differentially regulated in response to oxidative stress like human HO-1.

1.9 Haem oxygenase as a vector control target

Assuming AgHO plays a key role in *An. gambiae* blood digestion, then it presents a potential "Achilles heel", that might be exploited as part of a vector control strategy. Inhibition of haem aggregation in *R. prolixus* leads to oxidative stress, however does not lead to insect death [56]. Thus the mode of action of an HO inhibitor might not necessarily lead to an instant knockdown or killing effect, as is seen in traditional insecticides with neurotransmitter targets. Known inhibitors of haem oxygenase include zinc and tin protoporphyrins (ZnPP and SnPP) [98], which compete for the active site of haem oxygenase. The use of porphyric insecticides was first proposed with the haem biosynthesis pathway as a target [99], the mode of action – accumulation of porphyrins and oxidative stress – is expected to be the same as in haem oxygenase inhibition, as evident by inhibition of haemozoin synthesis and RpBV production in *R. prolixus* fed with SnPP-IX, presumably due to RHBP and RpHO inhibition [100]. A major effect of feeding *R. prolixus* with such inhibitors is a significant reduction in oviposition. Inhibition of AgHO may therefore have a similar detrimental impact on oviposition, which makes it ideal for a vector control strategy.

1.10 Research Objectives

It is unknown what the specific role of AgHO is, though it seems likely that it plays an important physiological role in haem catabolism, and other processes such as egg development. AgHO has not yet been characterised, and this is essential in order to understand its biological role(s) and its potential as a target for vector control. Thus, the main aim of this study is to clone and characterise AgHO with respect to haem degradation in *An. gambiae*. The *in vitro* characterisation will examine the haem oxygenase enzyme itself, as well as its redox partner, AgCPR. The *in vivo* approach will examine the role of haem oxygenase in a biological context.

More specifically, the objectives of this project are:

i. An *in silico* investigation into haem oxygenase, and its similarities and differences with respect to other enzymes,
ii. Cloning and expression of AgHO,
iii. Biochemical characterisation of recombinant AgHO, including verification of putative AgHO as a classical haem oxygenase by identification of its reaction products,
iv. Comparative characterisation of insect and human CPRs, including AgCPR,
v. Examination of the *in vivo* role of AgHO using classical haem oxygenase inhibitors.

Chapter 2 – General Materials and Methods

2.1 RNA extraction

RNA extraction from tissues was carried out using the RNAqueous® Micro Kit from Thermofisher. Extraction was performed on insect and mammalian tissues according to the RNAqueous® protocol.

2.2 cDNA synthesis

cDNA synthesis was conducted on extracted RNA using the Superscript III First Strand Synthesis kit from Thermofisher Scientific. The reaction mixture was set up in a 50µL tube according to Table 2.1. As the cDNA to be synthesised would use mRNA as a template, the oligo(dT) priming method was used.

Table 2.1. Reaction composition of first strand DNA synthesis – RNA volumes are approximate. Total RNA should be no more than 5µg.

Component	**Volume (µL)**
RNA	2
50 µM oligo$(dT)_{20}$ primer	1
DEPC treated H_2O	6
10mM dNTP mix	1
Total	**10**

The mixture was incubated at 65°C for five minutes and then placed on ice for at least one minute. The cDNA synthesis mix in Table 2.2 was prepared, and added to each RNA/primer mixture.

Table 2.2. cDNA synthesis mix

Component	**Volume (µL)**
10X reaction buffer	2
25mM $MgCl_2$	4
0.1 M DTT	2
RNaseOUT	1
Superscript III RT	1

The reaction mixture was incubated for 50 minutes at 50°C, before being terminated by incubating at 85°C for 5 minutes and afterwards placed on ice. 1µL RNase H was added to the tube and incubated for 20 minutes at 37°C.

2.3 Primer design

As can be expected, primer design was largely dictated by the nucleotide sequence of the cDNA to be amplified. There were three rules followed when designing proteins. Firstly, it was ensured that primers were 18-30 base pairs in length in order to ensure specificity to the appropriate sequence. Second, the nucleobase furthest to the 3' was always a guanine or cytosine. Lastly, the melting temperature of the reverse and forward primers were aimed to be

within 2°C of the one another, but this rule was circumvented in favour of the other two in instances where it was otherwise impossible.

2.4 Primer synthesis

Primers were designed as per the "Primer design" protocol above and were ordered from and synthesised by Eurofins Genomics.

2.5 Polymerase chain reaction (PCR)

Polymerase chain reactions were typically carried out in a 25µL reaction volume with the composition outlined in Table 2.3. The enzyme system used was Phusion HF by Thermofisher.

Table 2.3. PCR Reaction components

Component	**Volume (µL)**	**Final Concentration**
Nuclease-free H_2O	Add to 25µL	-
5X HF buffer	5	1X
10mM dNTPs	0.5	200µM
10µM forward primer	0.5	0.2µM
10µM reverse primer	0.5	0.2µM
Template DNA	< 2.5	< 125ng per reaction
10mM $MgCl_2$	< 1	< 200µM

Phusion DNA polymerase	0.25	0.02U/µL

This is the standard PCR enzyme mixture. $MgCl_2$ was only used when templates were proving difficult to amplify. Thermal cycling of the reaction mixture was carried out on a thermal cycler according to the sequence shown in Table 2.4.

Table 2.4. PCR thermal cycling timetable

Cycle stage	**Temperature (ºC)**	**Time (s)**	**Cycles**
Initial denaturation	98	30	1
Denaturation	98	10	35
Annealing	Variable	30	
Extension	72	30	
Final extension	72	600	1
Hold	4	∞	-

If PCR yields were low, the cycle number was increased to 40. The annealing temperature was based on the melting temperatures of the forward and reverse primers. If the forward and reverse primers had different melting temperatures, the lower of the two was used at the annealing stage, although primer design tries to avoid this becoming a problem.

2.6 Agarose gel electrophoresis

All gels were made using Tris Acetate EDTA (TAE) buffer with 0.5-2.0% agarose by mass and 0.5mg mL^{-1} ethidium bromide. Set gels were submerged in TAE and DNA samples were applied to wells at a volume of 15µL per well. 5µL DNA ladder was added in at least one well per gel (GeneRuler 1kB, Hyperladder I or Hyperladder IV, depending on availability and expected fragment size). Samples were run at 90 – 120 volts for as long as required for appropriate resolution.

2.7 Restriction digest

All restriction digests were carried out using Fast Digest enzymes from Thermofisher. The reaction mixture was set up according to Table 2.5.

Table 2.5. Reaction composition of restriction digest

Component	**Volume (µL)**
DNA (up to 1µg)	2
Restriction Enzyme 1	1
Restriction Enzyme 2	1
Fast Digest 10x Buffer	2
H_2O	16
Total	**20**

The mixture was then incubated at 37ºC for 1 hour. The enzymes were inactivated by incubation at 65ºC for ten minutes.

2.8 DNA ligation

Plasmid inserts were prepared for ligation by creating sticky ends, i.e. performing restriction digests according to the MCS of the plasmid. Plasmids were linearized using the same restriction enzymes.

The ligation reaction was catalysed by T4 DNA ligase (Thermofisher), according to the reaction mixture outlined in Table 2.6.

Table 2.6. Reaction composition of DNA ligation – DNA volumes are approximate. Insert DNA concentration should be in a 3:1 ratio with plasmid DNA.

Component	**Volume (µL)**
10x T4 DNA ligase buffer	2
Plasmid DNA	1
Insert DNA	3
Nuclease free H_2O	13
T4 DNA ligase	1
Total	**20**

The reaction was incubated for 10 minutes at room temperature.

2.9 *Escherichia coli* transformation

E. coli cells were of two strains – BL-21* (DE3) One Shot® for expression and DH5α for subcloning. All cells were purchased from Thermofisher Scientific. 10ng DNA was added to a

single vial containing 50µL competent cells. Cells were mixed by being gently tapped, and then incubated on ice for 30 minutes. Cells were transformed *via* heatshock by being introduced to a waterbath prewarmed to 42ºC for 30 seconds. The cells were then immediately returned to the ice. 250µL 37ºC SOC medium was added to the cell mixture, then the vial was incubated at 37ºC, shaking at 200rpm for 1 hour. The grown mixture was then pipetted onto an LB agar plate containing appropriate antibiotic (100µg/mL ampicillin unless otherwise stated), and incubated overnight at 37ºC. All transformation work was conducted under a hood with care taken to ensure proper sterile technique.

2.10 Plasmid purification by Miniprep

The Miniprep kit was purchased from Qiagen, and uses their proprietary buffers, tubes and protocols.

Bacteria with plasmids to be isolated were picked from single colonies and grown overnight at 37ºC in 5mL LB broth containing the appropriate antibiotic. Bacteria were then pelleted by centrifugation at 5000rpm for 6 minutes.

The pelleted bacteria were resuspended in 250µL buffer P1 and transferred to a 1.5mL Eppendorf tube. 250µL buffer P2 was added and the tube was gently mixed by inversion. 350µL buffer N3 was added and immediately mixed by gentle inversion. Tubes were next subjected to centrifugation at 13,000*g* for 10 minutes.

The supernatants from the centrifugation step were carefully pipetted into a QIAprep spin column and centrifuged at 13,000*g* for 60 seconds. The flow-through was discarded, and 0.5mL buffer PB was added to the column and centrifuged at 13,000*g* for 60 seconds. The flowthrough was discarded, 0.75mL buffer PE was added to the column, and it was centrifuged

at 13,000*g* for 60 seconds. The flowthrough was discarded, and the column was again centrifuged at 13,000*g* for 60 seconds.

The spin column was moved to a fresh 1.5mL Eppendorf tube. 50µL buffer EB was added, and the column was rested for three minutes. Isolated plasmid was recovered by centrifuged at 13,000*g* for a final 60 seconds. Plasmid concentrations were estimated by Nanodrop spectroscopy.

2.11 DNA sequencing

DNA sequencing was performed externally by the University of Sheffield's DNA sequencing service and by Source BioScience. Everything to be sequenced was sent in duplicate, with the appropriate forward and reverse primer pairs. Sequencing primers were the initial PCR primers in the case of PCR amplicons, and plasmid primers in the case of cloned or subcloned plasmid constructs.

2.12 Preparation of growth media

Luria-Bertani (LB) broth was made with 10g tryptone, 10g NaCl and 5g yeast extract, dissolved in 1L H_2O. Terrific broth (TB) was made with 12g tryptone, 24g yeast extract, 2.2g KH_2PO_4, 9.4g K_2HPO_4 and 4mL glycerol, dissolved in 996mL H_2O. LB agar plates were made with 10g tryptone, 10g NaCl, 5g yeast extract and 15g agar, dissolved in 1L H_2O.

Once dissolved, all media and the glassware they are stored in and/or were grown in were autoclaved to ensure sterilisation. Care was taken to ensure that autoclaving occurred as soon as possible after the media was dissolved, such that bacterial growth was prevented. Antibiotic was added to the media when it had reached a temperature of 50ºC. LB agar was

poured into plastic agar plates after having had antibiotic added, but before the liquid had begun to solidify.

Any SOC medium used was that packaged along with competent cells and was therefore not prepared by me.

2.13 Protein expression

Unless otherwise stated, bacterial protein expression starts with a fresh transformation of BL-21* *E. coli* cells (LifeTechnologies). Single transformed colonies are used to inoculate 10mL TB containing the appropriate antibiotic. Unless otherwise stated, this antibiotic is ampicillin at a concentration of 100µg mL^{-1}.

After an overnight incubation at 37ºC with shaking at 180rpm, the 10mL culture is used to inoculate 1L of TB with antibiotic in a 2L Erlenmeyer flask. This culture is then incubated at 37ºC with shaking at 180 rpm for approximately 5 hours. The optical density (OD) at 600nm of 300µL of the culture was then checked on an Epoch spectrophotometer. Once the culture had an OD of 0.3 – 0.5 Abs, the shaking incubator's temperature was reduced to that required for expression (25ºC for pOPIN constructs, 16ºC for pCold constructs) with shaking reduced to 160 rpm. Once this temperature was reached by the incubator, the OD was checked again. Once the OD of the culture had reached 0.7 Abs, the culture was induced by addition of IPTG to a final concentration of 0.5mM. The culture was incubated further for at least another 16h, depending on the protein being expressed. Bacteria were harvested by centrifugation at 8000rpm for 10 minutes.

2.14 Creation of cell lysate for protein purification

The pellet obtained from the protein expression protocol was placed on ice and resuspended in 25mL ice cold lysis buffer (note that the lysis buffer is different depending on which protein is expressed, see results chapters for details). Once resuspended, PMSF to a final concentration of 1mM was added to each resuspended pellet. These pellets were sonicated on ice at an amplitude of 60-80% for twenty seconds, then left to stand for ten seconds, with this being repeated for a period of seven minutes. The lysates created were then centrifuged at 30000*g* for 25 minutes, after which time the supernatant was purified. All steps take place on ice where possible.

2.15 Ni-NTA protein purification

Ni-NTA columns were created by adding 2mL shaken Ni-NTA resin into a plastic elution column containing a filter disc. The ethanol storage solution runs through the column, leaving an Ni-NTA column with 1mL resin bed volume. This column was then rinsed with 20mL H_2O, followed by 20mL wash buffer.

The supernatant from the creation of cell lysate protocol was filtered through a PORE SIZE filter before being applied to the resin, which was sealed at the bottom. The lid was replaced, and the resin/supernatant mixture was incubated, shaking at 4^{o}C for one hour.

The column was affixed to a clamp stand and held over a falcon tube, the lid and stopper were removed, and the flowthrough was collected.

10mL wash buffer was used to rinse the resin, and the flowthrough was collected in a separate tube. This step is repeated, with the flowthrough collected in another separate tube.

10mL elution buffer was used applied to the resin, and 10 1mL fractions were collected in Eppendorfs. Aliquots of these fractions were applied to an SDS-PAGE gel to assess purity and presence of the protein of interest.

2.16 Sodium dodecyl sulphate polyacrylamide gel electrophoresis (SDS-PAGE)

SDS-PAGE gels were made by first allowing a 12.5% acrylamide resolving gel to set, then pouring a 3% acrylamide stacking gel on top.

The resolving gel was made using the reactants described in Table 2.7. After mixing, these reactants had 100µL fresh 0.1g mL^{-1} ammonium persulphate (APS) and 10µL TEMED added to catalyse polymerisation. The solution was poured between two pairs of glass plates up to 1.5cm below the top, and 100µL 2-propanol was pipetted onto the solution. The 2-propanol is immiscible with the gel solution, and floats on top of it, thereby making the resolving gel flat on top. The gel was allowed to set by leaving it to stand at room temperature for 1 hour.

The stacking gel was made using the reactants described in Table 2.7. Again, after mixing these reactants had 50µL fresh 0.1g mL^{-1} APS and 5µL TEMED added. The 2-propanol was poured off from the resolving gel, and the stacking gel solution was poured in. Gel combs were slotted into the top of the glass plate cassettes so that wells would be formed. The stacking gel was left to stand for half an hour so that the gels would set.

Table 2.7. SDS-PAGE gel composition. Enough for two 12 x 8cm gels, 0.75mm thickness

Resolving gel		**Stacking gel**	
Component	**Volume**	**Component**	**Volume**
30% acrylamide bis	4.16mL	30% acrylamide bis	0.625mL
H_2O	3.14mL	H_2O	3.0mL
1.5M Tris HCl, pH 8.8	2.50mL	0.5M Tris HCl, pH 6.8	1.25mL
10% SDS	100µL	10% SDS	50µL

After having set, gels to be run were placed in a gel tank, clamped in place, and then submerged in SDS-PAGE running buffer (made from a dilution of 10x stock, the stock was 144g glycine, 30.2g Tris base and10g SDS, dissolved in 1L H_2O).

All protein samples to be run were of a volume of 25µL, mixed with 25µL 2X Laemmli buffer (950 µL BioRad premixed 2X Laemmli buffer, 50µL β-mercaptoethanol) in microcentrifuge tubes. These sample tubes were incubated at 95^{o}C for 10 minutes in order to denature the protein samples.

Up to nine protein samples can be run on one gel (each gel has ten wells, at least one is ear marked for PageRuler^{+} Prestained Protein ladder from Thermofisher). 25µL of each denatured protein sample was pipetted into each well.

The gel was subjected to a voltage of 60V until the dye front had moved into the resolving gel, after which time the voltage was increased to 90V. The gel was allowed to run until the dye front reached the bottom of the gel (approximately an hour and a half).

2.17 Protein dialysis

Protein samples were applied to a Pur-A-Lyzer™ Midi Dialysis Kit tubes (Sigma-Aldrich) in aliquots of 50-800µL. The dialysis tubes were then floated in 1L of cold dialysis buffer (different according to which protein was used) and incubated at 4°C for at least 16 hours.

For samples in a volume of more than 4mL (for instance, haemoglobin), the sample was pipetted into a rinsed length of dialysis tubing which was secured at both ends with clamps. The tubing was submerged in 10L cold H_2O, and incubated overnight at 4°C.

2.18 Quantification of protein concentration

Protein concentration was quantified using the Bradford method, specifically the Quick Start™ Bradford assay (BioRad). This assay required BSA protein standard at ten concentrations from 0.1 – 1.0 mg mL^{-1}. 5µL of each standard was added in triplicate to separate wells in a 96-well plate, plus one set containing no standard.

5µL of the protein sample to be quantified was added to empty wells on the plate. In cases where the protein concentration was completely unknown, the sample was diluted 1 in 5, 1 in 10 and 1 in 20, to try and ensure that the absorbance value obtained for the sample wells could be located in the linear portion of the standard curve generated by the BSA standards.

Next 45µL of H_2O was added to each well, followed by 200µL Quick Start™ Bradford reagent. This was allowed to stand at room temperature for five minutes, before absorbance at 595nm was measured on a plate spectrophotometer.

The BSA standards were used to generate a standard curve, which was used to calculate the protein concentration, in mg mL^{-1} of the samples.

2.19 Concentrating protein samples

When protein samples were in volumes too high (such as application to a desalting column) or concentrations too low, they were concentrated by use of an Amicon Ultra-15 Centrifugal Filter Unit, with a 10kDa pore size (this is well below all the proteins studied). No more than 15mL protein was applied to the column, then it was spun down at 4000*g* for fifteen minutes at a time in a centrifuge pre-chilled to 4^{o}C. The process was repeated until the protein sample was of either the volume or concentration required.

2.20 Buffer exchange/desalting

Buffer exchange took place on either a PD-10 desalting column or a PD Minitrap G-25 column (both from GE Healthcare). Columns were rinsed through with 5 times bed volume H_2O, followed by five times bed volume of the final sample buffer. Sample was then applied, flowthrough discarded, and sample eluted in final buffer. For PD-10, sample volume was 2.5mL, and final buffer volume was 3.5mL, for the PD Minitrap G-25 column, sample volume was 0.5mL and final buffer volume was 1mL.

2.21 Plate spectrophotometry

All 96-well plate based assays were performed using disposable 96-well plates (Nunc), and on either an Epoch Microplate Spectrophotometer (BioTek) or a FLUOstar Omega plate reader (BMG Labtech) for temperature dependent assays.

2.22 Homology modelling of proteins

All homology models were performed using the SWISS-MODEL workspace [101-104], using specified templates. Images were created and manipulated using PyMOL [105]. Estimations of surface electrostatics were performed using PyMOL also, and are hence a qualitative rather than quantitative measure of surface potential. Table 2.8 shows the quality scores for models created.

Table 2.8. Quality scores for protein homology models generated

Model	Page	GMQE	QMEAN4
AgHO	47	0.59	-4.05
AgHO docked with AgCPR	50	0.62	-7.77
AgCPR docked with AgHO	50	0.78	-6.93

2.23 *An. gambiae* rearing

Mosquito eggs were rinsed into a plastic tray containing c. 300mL distilled H_2O and allowed to hatch. Once hatched, larvae are fed daily with a pinch of TetraMin fish food flakes which had been ground into a powder. Larval populations are split down and divided amongst multiple trays to avoid larval density becoming a detriment to health.

After approximately 8 – 10 days, pupation will have occurred. At this stage, pupae are manually removed from the larva trays with a Pasteur pipette and placed into a smaller plastic pot containing c. 50mL distilled H_2O. This pot is placed into a BugDorm 2.0 adult mosquito cage and adults are allowed to emerge.

Adult mosquitoes are allowed to feed via cotton wool soaked in 10% sucrose water *ad libitum*. If eggs are required from the adults they are blood fed. Adults can be blood-fed from 2 days post-emergence.

Blood feeding took place either using human blood purchased from the NHS and administered using a Hemotek feeding apparatus set to 37ºC, or directly from a human limb which was in contact with the cage wall. Feeding was allowed to take place, in the dark, for 1 hour (Hemotek) or 15-10 minutes (human). A plastic pot containing water soaked cotton wool in contact with a 12.5cm diameter circle of Whatman filter paper was placed in the blood-fed cage two days post bloodmeal. The paper was left in the cage for a further two days to allow mosquitoes to lay. This egg paper was then rinsed into a larva tray.

In circumstances where mosquito adults were anaesthetised, the mosquito cage was refrigerated at 4ºC for one hour. The mosquitoes were then manually moved to a petri-dish which had be pre-chilled on ice. The mosquitoes remained on ice until the anaesthetic effect was no longer required, at which point they would be returned to standard rearing conditions.

Chapter 3 - Cloning and Expression of AgHO

3.1 Introduction

In spite of studies into the numerous adaptations haematophagous insects have to a haem-rich diet, such as haem aggregation [54-56] and haem-binding proteins [61, 63], haem catabolism in disease vectors is poorly characterized. Several HOs have previously been cloned and expressed, including mammalian (human and rat [82, 106, 107]), bacterial (*Neisseria* and *Corynebacterium* [108, 109]) and *D. melanogaster* [76] HOs. These studies vindicate the use of a heterologous *Escherichia coli* expression system, and will provide a platform for preliminary structural characterization using *in silico* modelling, and strategies for cloning and functional characterization of AgHO.

Whilst HO activity was originally studied using isolated liver microsomes [110], cloning and expression of diverse HOs has since been successfully performed in *E. coli*. Heterologous expression in bacteria allows for easy purification of active HO enzyme in order to study its activity. Many HO studies also incorporate the expression of a CPR enzyme to act as the redox partner, although artificial redox partners, such as ascorbic acid have also been used [76]. As bacteria do not have a true CPR enzyme, other redox partners have been expressed to study their HOs, such as flavodoxins, putidaredoxins, *E, coli* NADPH reductase, and human CPR [109].

When expressed in *E. coli* systems, the HO is always in a truncated form, missing its N-terminal transmembrane domain, with the exception of bacterial enzymes, which lack this domain altogether. When studying cytochromes P450, the CPR and P450 enzymes are full length and are coexpressed. The P450 system is then studied using isolated bacterial membranes. This is because the membrane domains of these enzymes are required for efficient

docking of the enzymes and P450 activity. This strategy has not been employed for study of HOs, because P450s are easy to quantify on the membrane spectrally; a characteristic not present in HOs.

Human HO-1 is among the best studied of the haem oxygenases. Its full length, membrane bound form has proved intractable to work with, so studies of HO-1 are invariably carried out on its truncated form. HO-1 has been expressed in an *E. coli* system, and purified using ion exchange chromatography, using previous insights gained from expression of rat HO [106, 107]. A fusion protein of human HO-1 and human CPR was created and purified in the same way, and was found to have oxygenase activity 2 times higher than that of HO-1 and CPR separately [107]. *E. coli* expression systems have also been used as a basis for crystallisation trials. Crystallisation has been successfully carried out in rats [111] humans [80] and numerous bacterial species [112]

D. melanogaster has been successfully expressed and characterised as a truncated form called DmΔHO, alongside a similarly truncated cytochrome P450 reductase, DmΔCPR [76]. As with human HO-1 expression, truncation led to successful expression of soluble protein. DmΔHO expression did not turn culture medium or bacterial colonies green with biliverdin accumulation, unlike previously expressed mammalian and bacterial HOs. This implies that DmΔHO may be unable to use endogenous *E. coli* reductases as redox partners. Another difference between DmΔHO and HO-1 is interaction with CPR. Whereas HO-1 interacts well with CPR, electron transfers between DmΔHO and DmΔCPR is inefficient.

The first aim of this chapter is to analyse *in silico* the attributes of AgHO and compare it with better known HOs such as human HO-1. The second aim is to clone and express a functional AgHO enzyme for use in biochemical characterisation.

3.2 Materials and Methods

3.2.1 AgHOΔ31 expression

Protein expression was carried out according to the protocols in Chapter 2, with the exception that all buffers contained 150mM NaCl, 50mM Tris pH 8.0. Lysis buffer and wash buffer also contained 50mM imidazole, elution buffer contained 400mM imidazole**.**

3.2.2 AgHO activity assay

AgHO reactions were carried out in a final volume of 90µL containing phosphate buffered saline, 10µM AgHO:haem complex, 10µM AgCPR and 250µM NADPH. NADPH, AgCPR and AgHO were omitted from each control system.

The AgHO:haem complex was created by incubating AgHO with a twice equimolar concentration of haem in a volume of 500µL. The mixture was allowed to stand for five minutes before applying to a PD Minitrap G-25 column and eluted.

The reaction was initiated with addition of NADPH, and immediately subjected to scanning UV-Vis absorption spectroscopy in the range 350-800nm and repeated 30 minutes after addition of NADPH.

3.2.3 Codon optimisation of synthetic AgHO

The AgHO DNA sequence was modified to retain the correct amino acid sequence, but with a codon bias more suited to *E. coli* expression. A range of restriction sites were added for compatibility with pCold-II and other expression vectors, see Appendix 3.4 for the full codon optimised sequence and added restriction sites.

The holding vector pMK contained a kanamycin selection marker allowing for single tube restriction digest and ligation into Amp^+ expression vectors could be performed.

3.2.4 Synthetic AgHO expression

Synthetic AgHO was excised from pMK using NdeI and EcoRI. The reaction mixture was then incubated with linearized pCold-II and ligated using T4 ligase. The mixture was then used to transform DH5α *E. coli* cells, which were plated on Amp^+ LB plates. The pCold-IIAgHO was isolated from these cells *via* Miniprep.

Protein expression was carried out according to the protocols in Chapter 2, with the exceptions that all buffers contained 150mM NaCl, 50mM Tris pH 8.0, 0.1% Triton X100. Lysis buffer contained 50mM imidazole and 0.5% Triton x100, wash buffer contained 50mM imidazole, elution buffer contained 400mM imidazole**.**

3.3 Results

3.3.1 Identification and sequence analysis of AgHO

The putative AgHO gene, AGAP003975 was identfied by querying the genome database VectorBase for the words “heme oxygenase.” The gene is located on the 2R chromosome, and contains a single intron. The size of the genomic sequence is 867bp. The coding sequence is 750bp, coding for a 249aa, 29.5kDa protein [66, 113]. Figure 3.1 compares the AgHO amino acid sequence with other haem oxygenases identified *via* blast or by literature search. Table 3.1 shows the amino acid identity and similarity between the HOs in Figure 3.1. Appendix 3.1 shows a phylogram of these haem oxygenases.

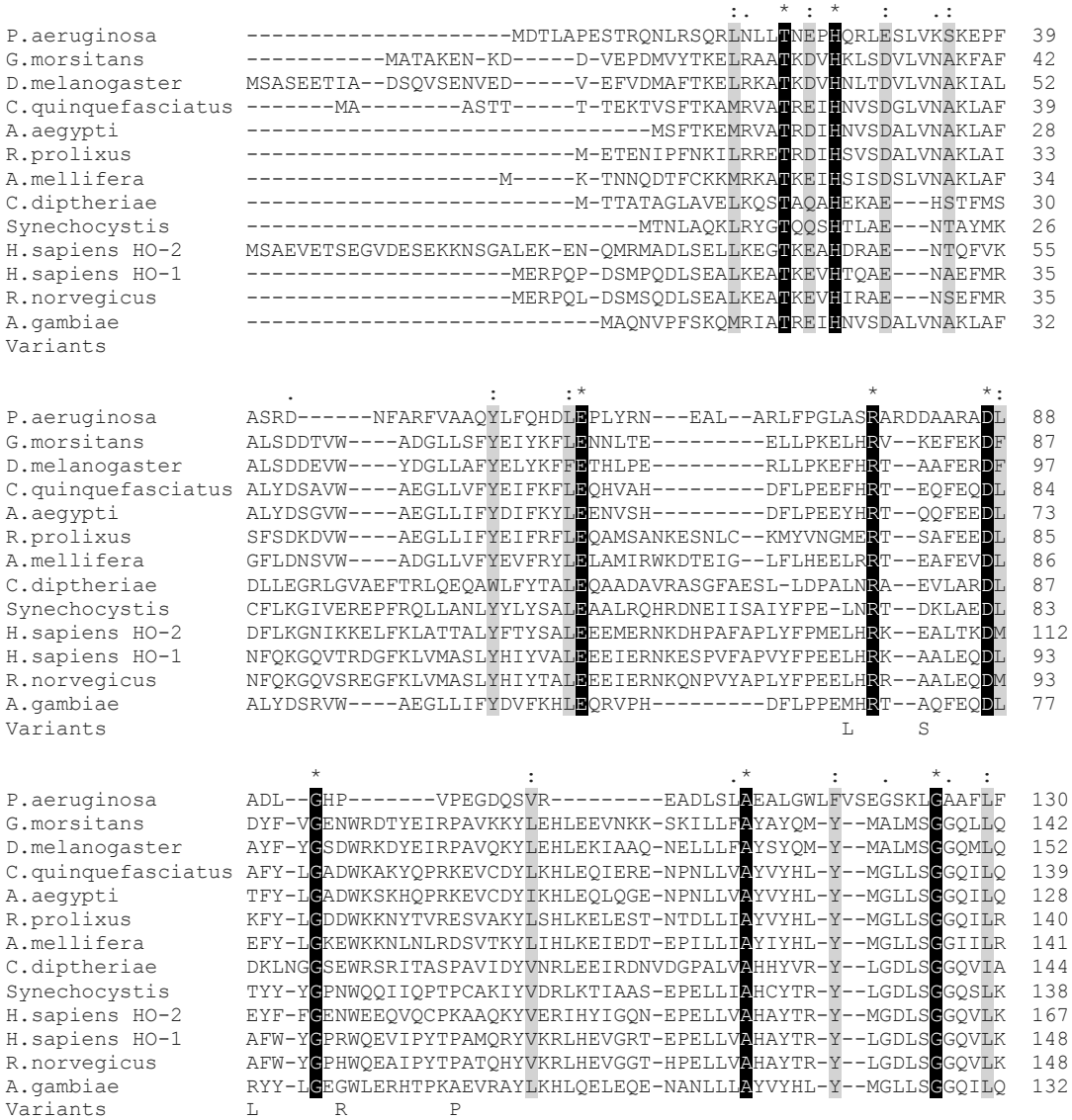

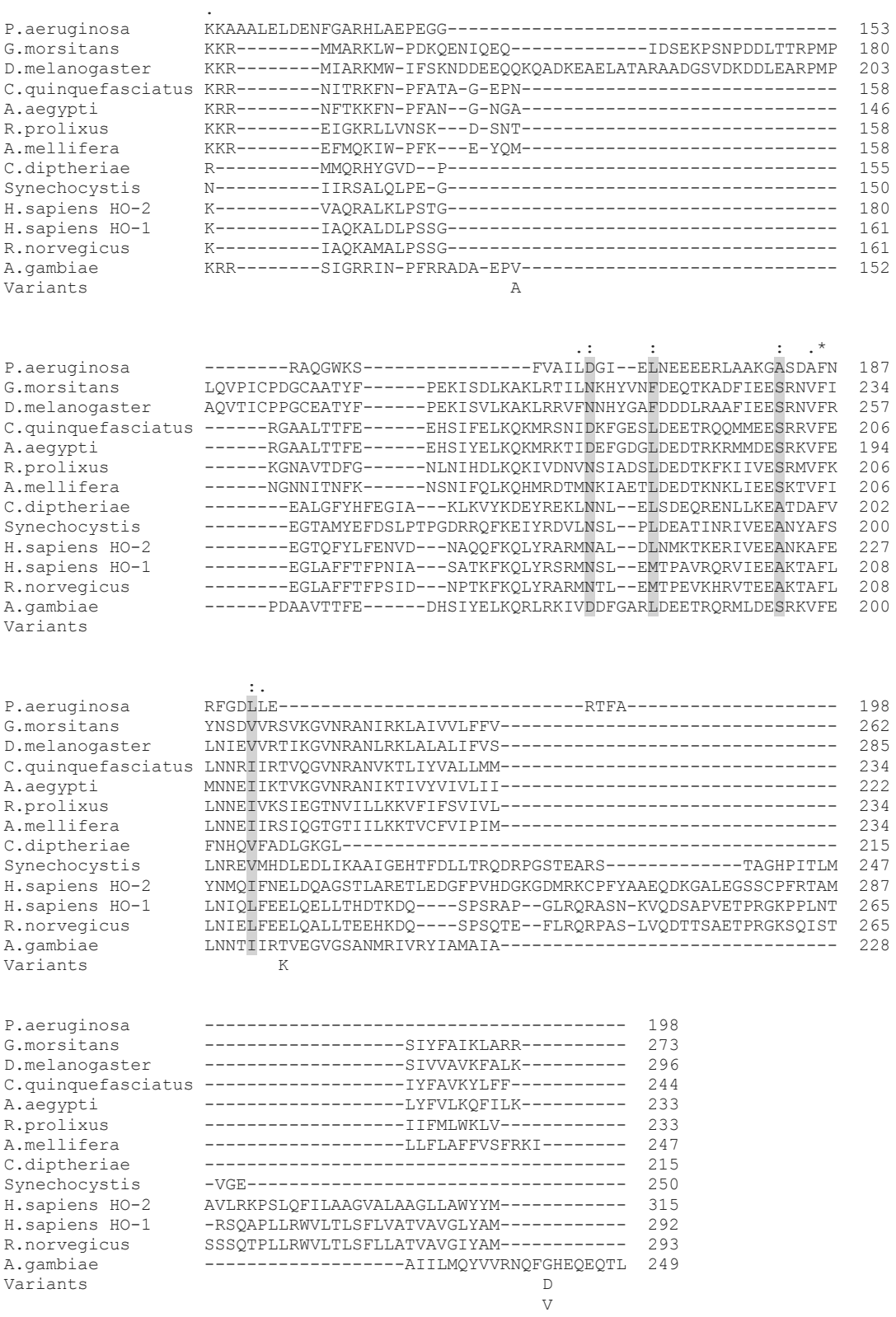

Figure 3.1. Alignment of putative and confirmed haem oxygenases. Included are haematophagous insects (*An. gambiae, An. funestus*, *C. quinquefasciatus, R. prolixus*, *G. morsitans*), non-haematophagous arthropods (*A. mellifera, D. melanogaster*), mammalian (*H. sapiens, R. norvegicus*) and bacterial HOs (*C. diphtheriae, Synechocystis*) Amino acid residues that are identical white on a black background, conservative divergences are grey

Table 3.1. Amino acid identity and similarity between AgHO and other haem oxygenases

Haem oxygenase	% Identity with AgHO	% Similarity with AgHO
P. aeruginosa	18.68	43.00
G. morsitans	36.94	61.25
D. melanogaster	36.54	54.75
C. quinquefasciatus	61.88	79.50
Ae. aegypti	62.23	79.75
R. prolixus	44.03	69.25
A. mellifera	40.48	69.00
C. diptheriae	19.06	47.75
Synechocystis	19.67	45.50
H. sapiens HO-1	21.68	33.00
H. sapiens HO-2	21.68	40.50
R. norvegicus	20.08	39.00

Also shown in Figure 3.1 are the polymorphic variant amino acids observed as a result of the high SNP frequency in *An. gambiae* [114]. None of these mutations are on residues predicted below to be involved with catalytic activity.

Table 3.2 shows those amino acid residues which have previously been implicated as being important for HO function, and highlights differences in sequence between HO-1 and AgHO.

Table 3.2. Functional residues in HO-1 and conservation in AgHO

HO-1 Residue	**AgHO residue**	**Function**	**Conservation**
K18	R12	Propionate binding	Conservative divergence
T21	T15	Propionate binding via water molecule	No divergence
H25	H19	Proximal haem iron binding	No divergence
A28	S22	Proximal haem contact	Conservative divergence
E29	D23	Proximal haem contact	Conservative divergence
Y134	Y118	Distal haem contact	No divergence
T135	H119	Distal haem contact	Non-conservative divergence
R136	L120	Distal haem contact	Non-conservative divergence
G139	G123	Distal haem binding residue, provides binding flexibility (contact is on amino acid backbone), ligand discrimination, opening and closing of active site	No-divergence
S142	S126	Distal haem contact	No-divergence

G144	G128	Distal haem binding residue, provides binding flexibility (contact is on amino acid backbone), ligand discrimination, opening and closing of active site	No-divergence
L147	L131	Distal haem contact	No-divergence
K149	K133	Interaction with CPR	No-divergence
K153	I137	Interaction with CPR	Non-conservative divergence
R185	I175	Interaction with CPR	Non-conservative divergence
F207	F199	Proximal haem binding (not on either binding helix)	No-divergence
F214	I206	Haem α-meso carbon binding	Semi-conservative divergence

Figure 3.1 shows the high levels of conservation of the H25 and T19 residues, which may stress their importance in haem binding. A28 and E29 are a point of divergence between putative HOs. Visible in Figure 3.1 is the predicted distal haem binding pocket of HO (bases 139-144), another highly conserved region. HOs are somewhat unique in the fact that, rather than incorporating haem as a prosthetic group, HOs use haem as the cofactor for its own degradation [80, 115]. This sets HOs apart from the classical haemoproteins such as catalases

and cytochromes P450. Bases G139 and G144 provide HO-1 with flexibility and allow the distal helix to get closer to the haem than in other haemoproteins [80]. The backbone atoms of these amino acids directly contact haem in HO-1. G144 is 100% conserved, while G139 is conserved in all enzymes bar *G. morsitans, D. melanogaster* and *Pseudomonas aeruginosa.* In human HO-1, semi-, non- and conservative mutants of either G139 or G144 yielded loss of oxygenase activity, likely *via* displacement of the distal helix [116]. An exception is the G139A mutant, which still catalyses haem – note that *G. morsitans* and *D. melanogaster* both have alanine at this position. The other mutants effectively turned HO-1 into a peroxidase, indicating that a role of these conserved residues is to supress ferryl species formation [116] The flexibility of the distal haem helix is likely due to the fact that glycine and alanine are the smallest two amino acids, and their conservation in AgHO implies the flexibility of the pocket is important in *An. gambiae* as well as in humans. Y134, T135, R136, S142 and L147 are distal helix residues which contact haem [80]. Y134 has 100% conservation and L147 has one semi-conservative mutation in *C. diphtheriae*.

3.3.2 Structural prediction of AgHO

In order to inform design of AgHO expression constructs, *in silico* analysis of the gene was carried out. Figure 3.2 shows the predicted structure of AgHO. Due to low quality scores in comparison with human HO-1, interpretation of individual residue function must be treated

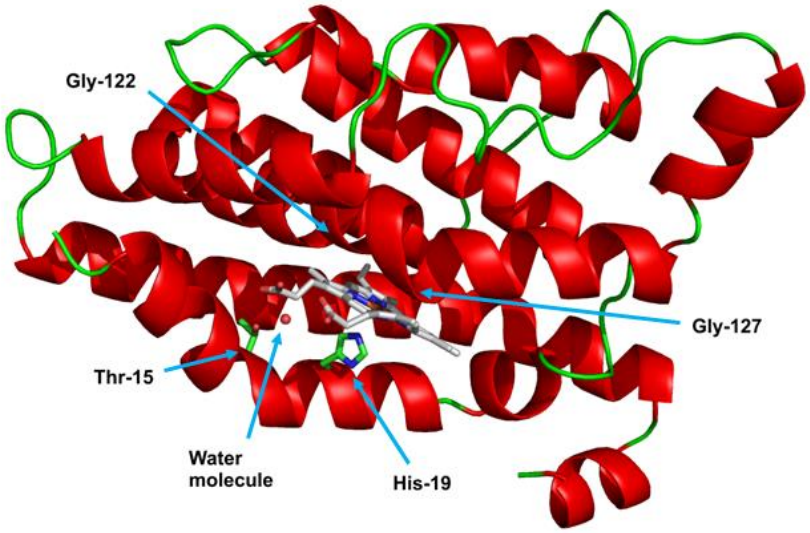

Figure 3.2. Haem binding residues in AgHO

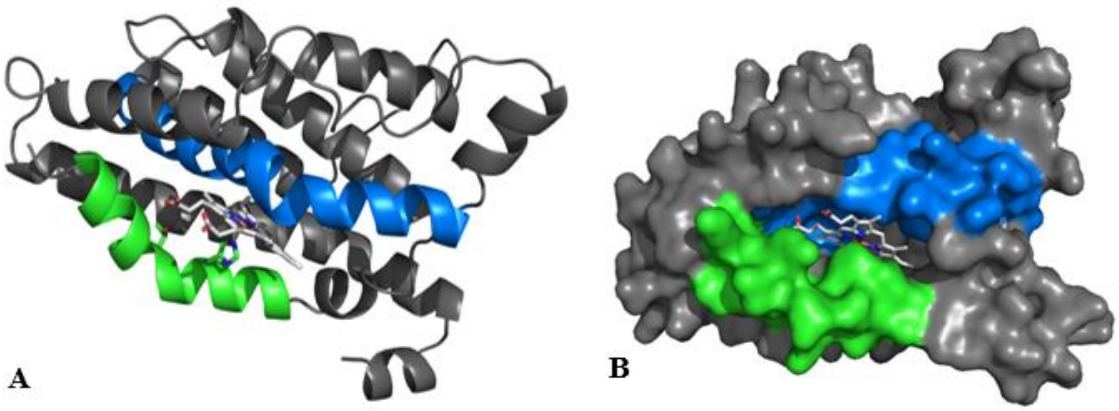

Figure 3.3. Structure of the haem binding pocket - Highlighted are the proximal (green) and distal (blue) helices which make up the haem binding pocket, **A** shows the two helices which make up the pocket, **B** shows the surface of the pocket

with caution, however, predictions of surface structure to indicate potential binding sites with AgCPR may be made.

The crystal structure of human HO-1 reveals that haem is bound between two α-helices (proximal and distal) [80]. These helices are conserved in AgHO, and contain the important haem binding residues highlighted in Table 3.2 (K18, T21, H25, A28, E29, Y134, T135, R136, G139, S142, G144 and L147). Human HO-1 residues G122 and G127 are conserved in AgHO, and Figure 3.4 shows that they are involved with distal helix flexibility – a conserved structural motif between HO-1 and AgHO.

The predicted surface charge of AgHO is illustrated in Figure 3.5. The positive potential at the iron centre of the haem is visible and is essential for haem coordination to the H19 residue. Also visible is a clearly positive area corresponding with the binding domain of the propionate haem chains, and the negative region corresponding with the opposite end of the haem molecule, adjacent to the haem α carbon. Given that these domains are associated with

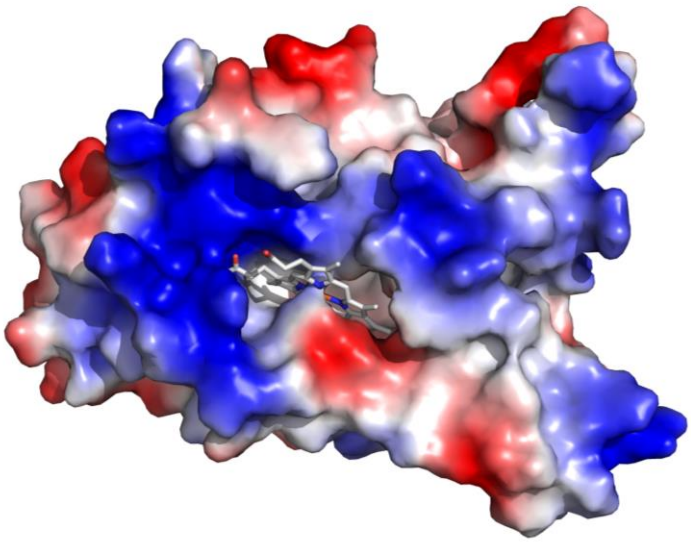

Figure 3.4. **Surface electrostatic potential of AgHO binding pocket** Blue indicates positive potential, red indicates negative potential, white is neutral

haem binding and orientation this suggests a role for these positively charged amino acids in haem orientation.

Human HO-1 exhibits regiospecificity in the production of BV-IXα which seems dependent on propionate charge interactions [80]; these are important in orienting the α-meso-carbon for hydroxylation in human HO-1. Conserved amino acids implicated in propionate binding are K18, K22, Y134, K179 and R183, of these, Y134 and K179 are conserved in eukaryotes. Because of conservation around this domain across humans and insects, it is unlikely that the divergent regiospecificity observed in some insects is because haem is not positioned in the same orientation.

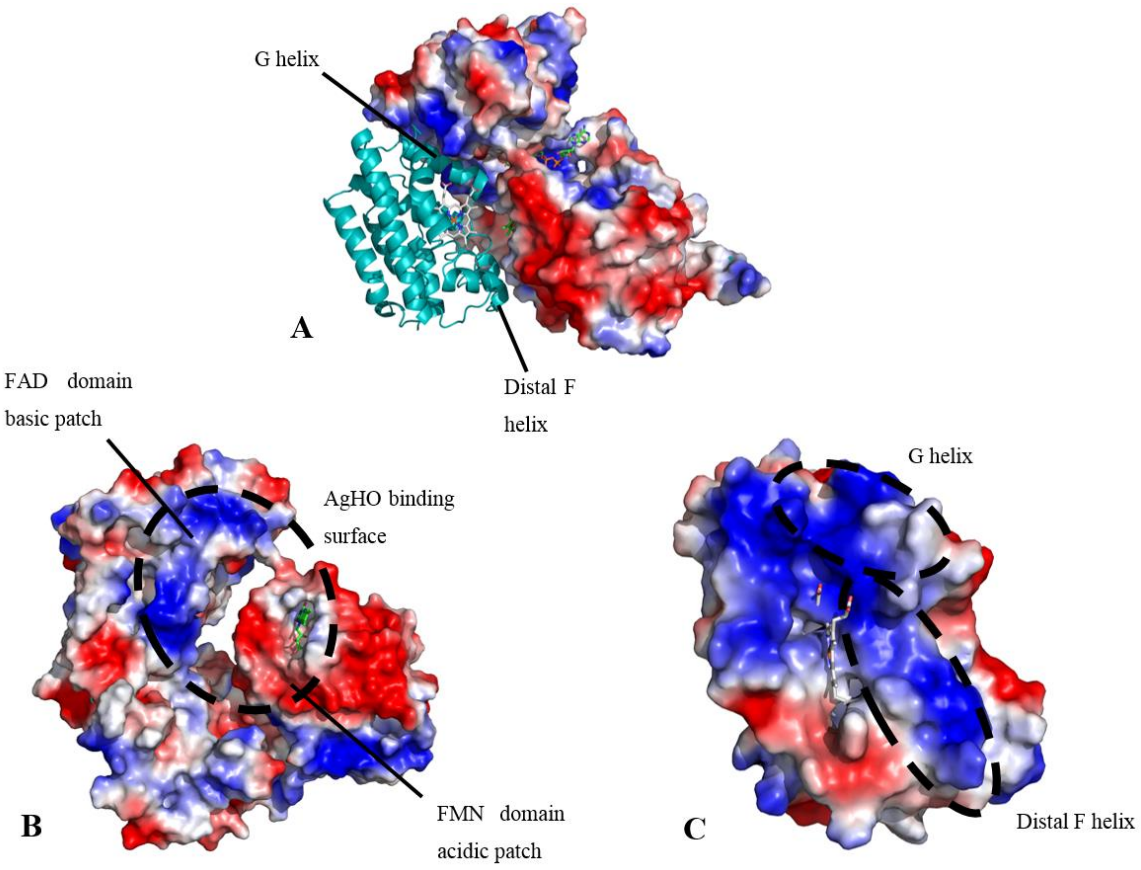

Figure 3.5.Surface electrostatic potential of AgHO in putative docking conformation with AgCPR, based on structural homology with RnHO and RnCPR – A, AgHO (blue) docked with AgCPR (surface model); **B,** Putative AgHO docking surface on AgCPR; **C,** Putative AgCPR-docking helices on AgHO; Blue indicates positive potential, red indicates negative potential, white is neutral.

Note that for these structures, the terminal transmembrane domains are missing. The transmembrane domains and therefore the membrane these proteins are situated on would be located downwards relative to the enzymes.

In order to examine the docking of AgHO with its redox partner, AgCPR, homology models were created using the crystal structure of *Rattus norvegicus* HO and CPR in binding conformation [88]. Rat CPR has a modified hinge region (four residues removed) to produce an "open" conformation, capable of electron transfer to HO. Figure 3.5 shows the structure of AgHO and AgCPR resulting from this modelling.

The predicted AgHO binding surface on AgCPR shows that negative and positive patches are visible on the FMN and FAD domain surfaces respectively. The areas associated with HO binding provide FMN close proximity with HO bound haem, allowing electron transfer to haem.

Eukaryotic HOs contain C-terminal transmembrane domains that is not shared with bacterial HOs, and likely contributes to CPR docking [117].

3.3.3 Cloning of AgHO from *An. gambiae* cDNA

In order to clone the full length AgHO coding sequence, primers were designed complementary to the 5' and 3' ends of AgHO, with modifications to allow for ligation into the pJET1.2 holding vector (BamHI and HindIII restriction sites). The designed primers are shown in Appendix 3.2.

mRNA was isolated from homogenised *An. gambiae* and used to synthesise cDNA. This cDNA which was used as a template for amplification and cloning (Figure 3.6). The AgHO insert in pJET1.2 was sequenced using amplification primers and the dideoxy-termination method, and found to be identical to AGAP003975.

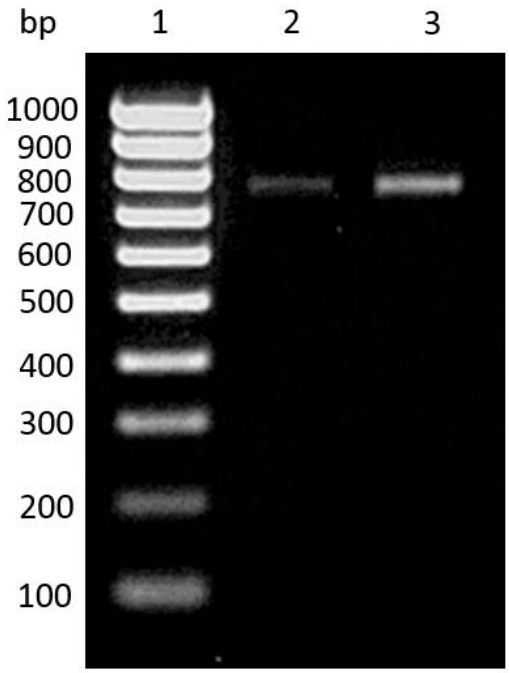

Figure 3.6. Isolation of AgHO from *An. gambiae* cDNA Lane 1, molecular mass markers; Lanes 2, AgHO amplified from cDNA; Lane 3, AgHO amplified from AgHO-pOPIN-F

For expression, AgHO was subcloned into the pOPIN-F expression vector according to the protocols in Chapter 2. AgHO contains a C-terminal transmembrane domain [117]. Previously expressed recombinant HOs have been expressed using constructs which were truncated at the C-terminus [76, 106, 107]. The full length sequence, plus a series of truncations from the C-terminus were therefore produced to optimise protein solubility, as summarised in Appendix 3.3.

The truncation series was created by PCR. The primers for this PCR are described in Appendix 3.2, and the AgHO:pJET1.2 plasmid was used as a template. Each of these amplicons was subject to restriction digest with BamHI and HindIII before being ligated into pJET1.2. These plasmids were transformed into competent *E. coli* and miniprepped to increase copy number. The truncated and full length AgHO inserts were removed from the pJET1.2 holding vector by restriction digest (BamHI and HindIII), and ligated into linearised pOPIN-F. The inserts were confirmed by sequencing using the initial amplification primers.

Table 3.3. TMPred analysis highlights two possible transmembrane regions The first region is deep in the centre of the enzyme, the second corresponds with identified transmembrane regions in previously expressed HOs

Starting aa	**Finishing aa**	**Length of domain (aa)**	**Score**	**Orientation**
112	128	17	797	i-o
219	237	19	1906	o-i

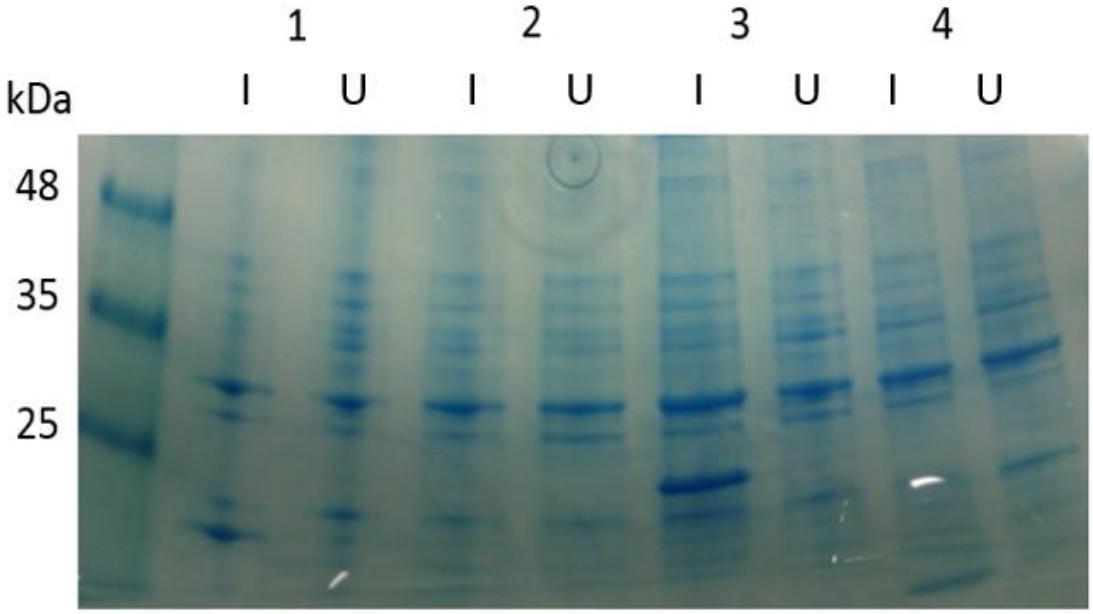

Figure 3.7. AgHOΔ31 expresses soluble protein. SDS PAGE gel of cell lysates of different AgHO truncation constructs. **1**, AgHOΔ10; **2**, AgHOΔ15; **3**, AgHOΔ31; **4**, AgHOΔ46; **U**, uninduced control culture; **I**, induced culture.

AgHOΔ31 is the only construct which yields soluble enzyme

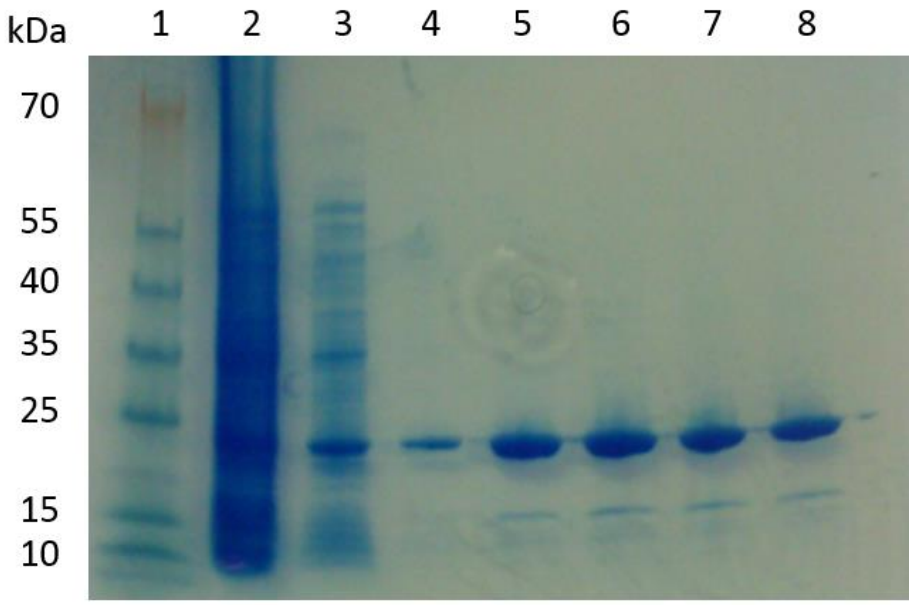

Figure 3.8. SDS-PAGE gel of purification of AgHOΔ31

Lane 1, molecular mass markers; Lane 2, Ni-NTA column flowthrough (unbound protein); Lane 3, Wash buffer flowthrough; Lanes 4-8, AgHOΔ31 elutions

Only AgHOΔ31 expressed soluble protein, as shown in Figure 3.7 (hereafter referred to as AgHOΔ31). This construct was then used as a starting point to scale up expression. Optimal expression (shown in Figure 3.8) occurred with a 48 hour incubation post-induction, producing ~2mg total pure protein per litre of cell culture (See Appendix 3.4 for time course).

In order to determine if AgHOΔ31 was catalytically active, the protein was incubated with haem and spectral measurements done to determine haem catabolism. As shown in Figure 3.10, the characteristic decrease in Soret peak absorbance (380-400nm) associated with haem catabolism is not observed with AgHOΔ31. MdCPR, HsCPR, and the artificial electron donor ascorbic acid were used also, and no reactivity was observed. Also absent was a biliverdin peak at 680nm.

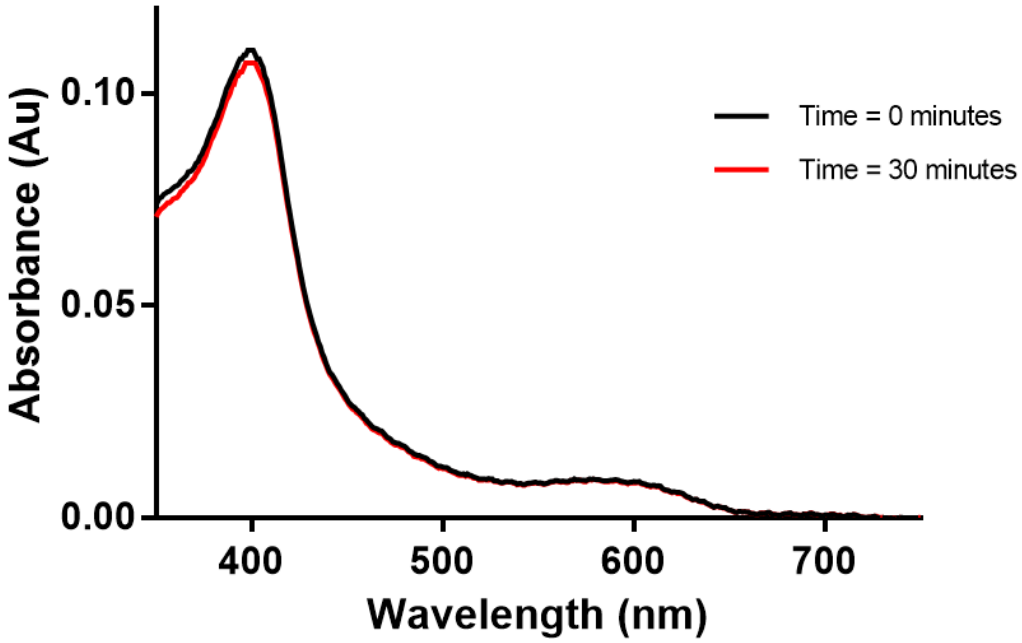

Figure 3.9. **Absorption spectra of AgHOΔ31 in complex with haem shows the enzyme is inactive** 30 minute incubation of AgHO with haem, AgCPR and NADPH revealed no significant changes to the haem spectrum characteristic of haem catabolism

Analysis of AgHOΔ31 by ^{1}H 1D NMR indicated misfolded protein. Although this construct was not used further for biochemical studies, the amounts produced were sufficient for the production of antibodies. Polyclonal rabbit antisera against AgHO (α-AgHO) was produced by Davids Biotechnologie (Appendix 3.4 for antibody validation).

3.3.5 Expression and purification of codon optimised AgHO

Due to low yield and catalytic inactivity, a codon optimised AgHO was designed and synthesised (Appendix 3.6). The soluble truncation of AgHO may have had an effect on the conformation of the catalytic domain of AgHO. As full length AgHO would not express normally, the DNA sequence was altered to take advantage of codon redundancy; producing the same amino acid sequence, but with a codon bias more similar to that of *E. coli*. Expression trials showed that the ideal growth conditions for AgHO occurred with a 48 hour incubation post-induction, producing ~5mg total pure protein per litre of cell culture.

3.3.6 Activity assay of codon optimised AgHO

The UV-Vis spectra in for the assay clearly show reduction in the haem Soret region at 380-400nm (Figure 3.10), indicative of haem catabolism. There was also a modest reduction in the haem α/β peaks at 560-610nm, and an increase in the 660-700nm region, which is associated with formation of biliverdin. Taken together, this is an indication of enzyme activity thus AgHO was used for further biochemical analysis.

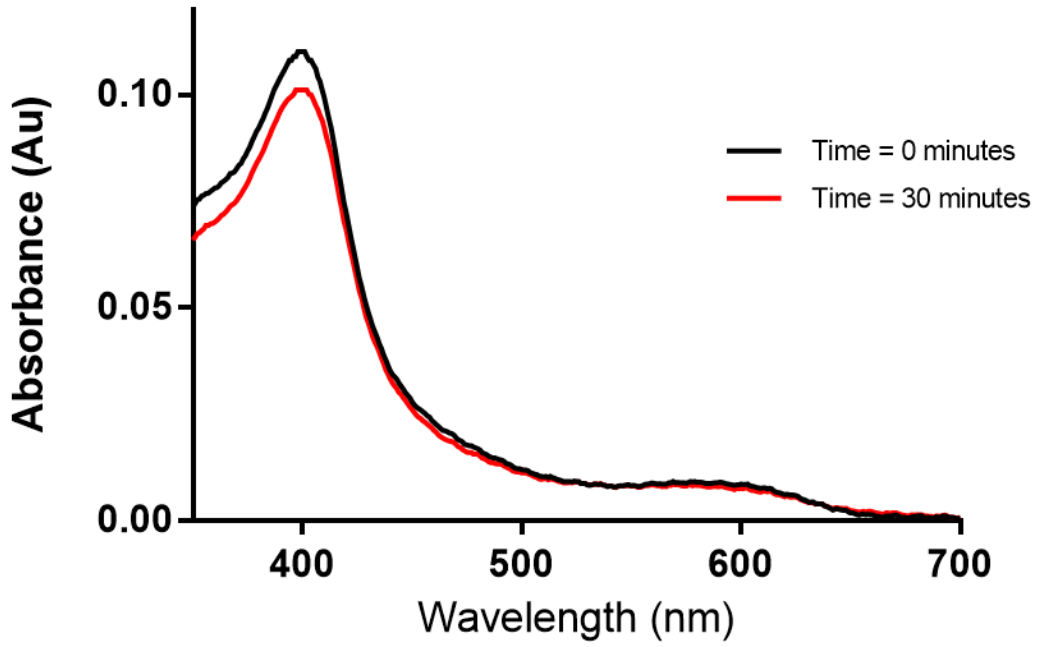

Figure 3.10. Changes in the absorption spectra of codon optimised AgHO in complex with haem show the enzyme is catalytically active 30 minute incubation of AgHO with haem, AgCPR and NADPH revealed a clear reduction at the haem Soret peak

3.3.7 Antibody generation

Since the inactive AgHOΔ31 was shown to be misfolded, 500µL protein at a concentration of 0.5mg mL^{-1} was sent to Davids Biotechnologie for generation of polyclonal rabbit antisera, and affinity purified α-AgHO antibody. These antibodies were tested and found to be specific to AgHO.

3.4 Discussion

This chapter describes the cloning and expression of AgHO. Sequence analysis shows that AgHO shares 23% amino acid sequence identity with *Homo sapiens* HO-1 and 67% structural identity. The four residues previously found to be important for haem binding are conserved in AgHO: T15, H19, G122 and G127. T15 is on the proximal haem binding helix and indirectly contacts haem via a water molecule. H19 is also on the proximal helix directly coordinates with haem iron. G122 and G127 are located on the distal helix of the haem binding pocket. These are important because they contact the haem porphyrin ring *via* the amino acid, and also they mediate flexibility of the distal helix itself. From the structural homology model, the flexibility of this helix appears to help in giving the pocket its shape [80].

Analysis of the electrostatic surface of the protein reveals how AgHO may bind haem and how it may dock with AgCPR. An acidic area containing the residues R12, R16, Y118, K169 and R173 forms the "entrance" to the haem binding pocket. The positive potential of this domain of the protein, its conservation in HO-1 and the position of the haem substrate in the crystal structure of HO-1 suggest that these residues are responsible for correctly orientating the haem in the haem binding pocket. Presence of this orientation domain, and the fact that the biliverdin product isolated from the closely related *Ae. aegypti* is a modified biliverdin α implies that AgHO likely hydrolyses biliverdin at the α-position only.

Structural analysis also confirmed that AgHO is a membrane bound protein with a C-terminal hydrophobic transmembrane domain. Knowledge of the extent of this domain was used to inform the design and construction of a series of expression plasmids truncated at the 3' end to varying extents. These expression plasmids were used in expression trials to obtain a soluble and catalytically active recombinant AgHOΔ31. One of the expression constructs yielded mg quantities of protein, but a lack of catalytic activity and 1D NMR analysis showing that this enzyme was misfolded meant it was not suitable for biochemical characterisation. The

fact that this misfolding occurred across different batches, and with different expression conditions suggests that the misfolding may have been because of the C-terminal truncation.

Instead, the full length AgHO was cloned, but failed to express when using the native cDNA sequence amplified from *An. gambiae*. A codon optimised version of the gene was thus created. Full length AgHO was successfully expressed from this construct, with a significant yield and catalytic activity.

This construct was used for the biochemical characterisation of AgHO as described in the next chapter. According to structural analysis, AgHO has the characteristic features of a true haem oxygenase, such as a haem binding pocket and a potential CPR docking domain, but biochemical analysis, such as confirmation of reaction products, must occur before AgHO is confirmed as a true haem oxygenase.

Chapter 4 – Biochemical analysis of *Anopheles gambiae* haem oxygenase

4.1 Introduction

Haem is of key importance to all insects. Most insects use haem as a nutrient in embryonic development [118, 119], and as the prosthetic group in haemoproteins such as nitric oxide synthase [120], catalase [72] and the cytochromes P450 [121, 122].

As discussed in Chapter 1, haem is also potentially toxic, due to its ability to interrupt phospholipid membranes and participate in the generation of ROS which damage proteins, nucleic acids and membranes. Though other haem detoxification methods [54, 56, 62] and haem biosynthesis itself [118] are relatively well characterised in insects, haem degradation by enzymatic oxygenation is less well known. There is only one instance of the isolation and characterisation of an insect HO, *D. melanogaster* [76]. Due to its potentially key role in bloodmeal detoxification, the biochemical characterisation of *An. gambiae* haem oxygenase is an important area of research, one which this chapter will focus on.

The characterisation of *D. melanogaster* HO (DmΔHO) was conducted on an *E. coli* expressed enzyme which had been truncated at the N-terminus to remove the transmembrane domain, and was studied alongside a similarly truncated CPR (DmΔCPR) [76]. This study suggests that DmΔHO had haem oxygenase activity and is a true HO, however it is one which has a different active site structure to other known HOs such as human and rat. The DmΔHO reaction was found to degrade haem to biliverdin, carbon monoxide and iron in the presence of both the DmΔCPR/NADPH reducing system, and an artificial ascorbate reducing system.

Differences observed between DmΔHO and mammalian HOs include the way in which haem binds at the active site. Mammalian and cyanobacterial HOs have been observed to bind haem *via* a histidine residue at the proximal face, and a water molecule at the distal face. This binding mode is supported by homology modelling of AgHO, although this is not surprising given that the template is human HO. EPR spectroscopy has shown that the haem-DmΔHO lacks the six-coordinate high-spin binding mode as in other HOs, and that the haem iron is not involved in binding. DmΔHO catalysis leading to haem degradation is therefore predicted to be different to mammalian systems, with the proximal histidine residue being unimportant for catalytic activity. A similar observation has been made previously from site directed mutagenesis of HmuO from *Corynebacterium diphtheriae*. Here, the H20A mutant had its binding histidine removed, and was still capable of the initial meso-hydroxylation of haem, but not the whole reaction pathway [123].

DmΔHO produces three biliverdin isomers (α, β, δ), which distinguishes it again from other known haem oxygenases, which only produce biliverdin-α. The distal binding site helix in human HO-1 sterically prevents access of the hydroperoxy species to the β-meso, δ-meso and γ-meso carbons, which explains the regiospecificity of human HO-1. DmΔHO producing three isomers is another piece of evidence for a structurally different active site.

This chapter aims to describe the biochemical characterisation of recombinant AgHO and verifies its ability to degrade haem to produce the three reaction products associated with HO mediated haem degradation: biliverdin, carbon monoxide and ferrous iron. This chapter also characterises the binding of haem by haem oxygenase to experimentally confirm the presence of structural motifs identified in Chapter 3. Finally, the pH and temperature optima of AgHO are determined in order to help place this enzyme into a physiological context.

4.2 Materials and Methods

4.2.1 Creation of the AgHO-haem complex

The first step to spectroscopic analysis of the AgHO reaction is to create an AgHO-haem complex. AgHO was mixed in a 1:2 molar ratio with haem. *In silico* analysis shows that AgHO only has one haem binding site, therefore a 1:2 molar ratio equates to a 2x excess of haem. After being mixed with haem, the AgHO was applied to and eluted from a PD Minitrap G-25 column for buffer exchange. The protein complex was then concentrated such that it could be used in assays.

4.2.2 Spectral analysis of AgHO complex variants

In vivo, the iron requires electrons from NADPH (*via* CPR) in order to be reduced, however *in vitro* haem iron can be reduced artificially by creating a reducing environment and introducing carbon monoxide forming a complex of ferrous haem and carbon monoxide. The ferrous CO complex was created by adding sodium dithionite powder to an aliquot of the ferric complex (creating a reducing environment [124]), the solution was then saturated with CO by bubbling the gas through the solution [109, 125, 126].

The ferrous dioxyhaem complex was created by passing the ferrous-CO complex over a sephadex G25 column removing excess reductant and carbon monoxide.

All complexes were scanned spectroscopically from 750nm – 350nm in 90µL in a quartz cuvette, at a concentration of 10µM, in a buffer of 150mM NaCL, 50mM Tris, pH 7.4, 0.1% Triton x100.

4.2.3 Calculation of the extinction coefficient of the haem-AgHO complex

The extinction coefficient was calculated using the pyrimidine haemochrome method [127, 128]. 10µM AgHO-haem complex in a buffer of 150mM NaCl, 50mM Tris, pH 7.4, 0.1% Triton x100 was mixed 1:1 with a solution of 0.2 M NaOH, 40% (v/v) pyridine, 500 µM potassium ferricyanide in a final volume of 1mL and placed in a 1mL quartz cuvette. The solution was observed *via* scanning absorption spectroscopy from 700nm to 350nm to obtain the oxidised spectrum.

Approximately 5mg sodium dithionite was added, and the solution was mixed thoroughly. The pyridine haemochrome spectrum was recorded repeatedly until it stopped changing, and the concentration of heme was determined from the extinction coefficient at 557 nm, using the value of 34530 M^{-1} cm^{-1}.

4.2.4 Haem binding assessment by titration

Haem binding was assessed by increasing the concentration of haem whilst keeping the AgHO concentration fixed. The reaction mixture (100µL solution, 10µM AgHO in a buffer of 150mM NaCl, 50mM Tris, pH 7.4, 0.1% Triton x100) was placed in a 90µL quartz cuvette. The reference cuvette contained only buffer.

Change in absorbance of the complex was tracked via scanning absorption spectroscopy from 700nm to 350nm, with the reference cuvette in the blank chamber. 2µL of a 100µM solution of haem was added to sample and reference cuvettes, and after five minutes, the sample was observed again. This was repeated until the haem concentration in each cuvette was 20µM.

4.2.5 Cytochrome P450 reductases used for biochemical analysis of AgHO

The CPRs used in this chapter are AgCPR, MdCPR and HsCPR. AgCPR were expressed according to the protocols outlined in Chapter 2. The AgCPR plasmid was provided by Mark Paine (LSTM) [90]. MdCPR was provided by Evangelia Morou (University of Crete). HsCPR was from Sigma.

4.2.6 Identification of biliverdin as an AgHO reaction product

The reaction mixture (100µL solution, 10µM AgHO-haem complex, 3µM CPR, 300µM NADPH in a buffer of 150mM NaCL, 50mM Tris, pH 7.4, 0.1% Triton x100) was placed in a 90µL quartz cuvette. The reference cuvette contained only buffer and CPR. The reaction was initiated with addition of NADPH, and absorbance from 750nm to 350nm was immediately measured. Absorbance was measured every ten minutes for two hours.

Control systems were used which each omitted one reactant of NADPH, CPR, and AgHO to ensure that haem degradation was not spontaneous, non-enzymatic or CPR driven.

4.2.7 Identification of CO as an AgHO reaction product

The final reaction mixture was 100µL containing 10µM AgHO-haem complex, 3µM MdCPR, 300µM NADPH, 150µM myoglobin in a buffer of 150mM NaCL, 50mM Tris, pH 7.4, 0.1% Triton x100. All components except for myoglobin and NADPH were placed in in a 90µL quartz cuvette, and then blanked. The reference cuvette contained only buffer and CPR. Myoglobin was added to the sample cuvette, the reaction was initiated with addition of NADPH, and absorbance from 600nm to 350nm was immediately measured. Absorbance was measured every ten minutes for two hours.

Control systems were used which each omitted one reactant of NADPH, CPR, and AgHO.

4.2.8 Identification of ferrous iron as an AgHO reaction product

This reaction relies on 3-(2-Pyridyl)-5,6-diphenyl-1,2,4-triazine-*p*,*p'*-disulfonic acid, better known as Ferrozine [129]. Ferrozine binds iron, producing a distinct change in absorption at 562nm as it does so.

The reaction mixture (100µL solution, 10µM AgHO-haem complex, 3µM MdCPR, 250µM Ferrozine, 300µM NADPH in a buffer of 150mM NaCL, 50mM Tris, pH 7.4, 0.1% Triton x100) was placed in a 90µL quartz cuvette. The reference cuvette contained only buffer and CPR. The reaction was initiated with addition of NADPH, and absorbance from 750nm to 350nm was immediately measured. Absorbance was measured every ten minutes for two hours.

Control systems omitted, in turn, NADPH, CPR, and AgHO. The Ferrozine assay proved reliable, and was used to determine pH and temperature optima.

4.2.9 AgHO pH experiments

Each reaction mixture (200µL solution, 10µM AgHO-haem complex, 3µM MdCPR, 250µM Ferrozine, 300µM NADPH in a buffer of 150mM NaCL, 50mM Tris, 0.1% Triton x100) was placed in a well in a Nunc 96-well plate. There were six different pHs for the 50mM Tris buffer; 6.5, 7.0, 7.5, 8.0, 8.5, 9.0. Four reaction wells were set up for each buffer – three experimental wells and one control well. The reaction was initiated with addition of NADPH, the control wells had buffer added rather than NADPH. Absorption at 562nm was measured every 15 seconds for 5 minutes.

4.2.10 AgHO temperature experiments

Each reaction mixture (200µL solution, 10µM AgHO-haem complex, 3µM MdCPR, 250µM Ferrozine, 300µM NADPH in a buffer of 150mM NaCL, 50mM Tris pH 7.4, 0.1% Triton x100) was placed in a well in a Nunc 96-well plate. Four reaction wells were set up– three experimental wells and one control well. The spectrophotometer was set to 20^{o}C, then the plate was introduced and allowed to equilibrate to the correct temperature for five minutes. The reaction was initiated with addition of NADPH, the control wells had buffer added rather than NADPH. Absorption at 562nm was measured every 15 seconds for 5 minutes. The experiment was repeated at 25^{o}C, 27.5^{o}C, 30^{o}C, 32.5^{o}C, 35^{o}C, 37.5^{o}C and 40^{o}C.

4.3 Results

4.3.1 Spectral analysis of the AgHO-haem complex

Using the AgHO-haem complex, the mode of the haem binding can be investigated. Human HO-1 has been observed to allow water, carbon monoxide and oxygen to co-ordinate to haem

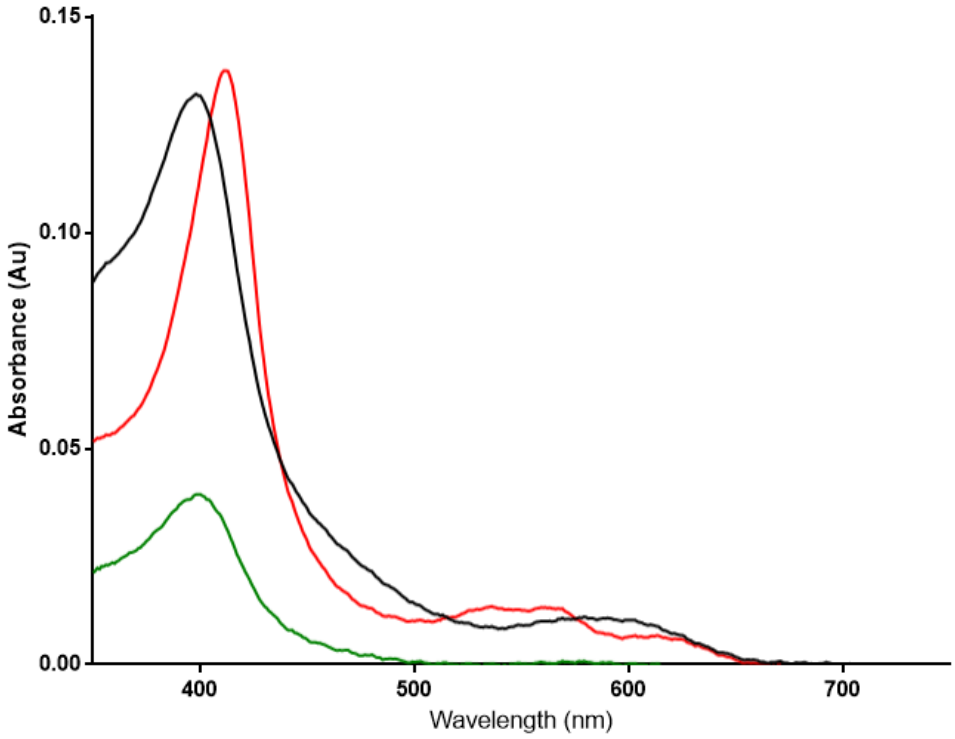

Figure 4.1. Spectral shift of the AgHO-haem complex under different redox conditions – black is the ferric haem complex, red is the ferrous carbon monoxide-haem complex and green is the ferrous dioxyhaem complex

iron at the sixth "vacant" valence position, the others being four nitrogens in the porphyrin ring, and the proximal helix histidine [80]. DmΔHO has been observed not to bind in this way, however, and does not coordinate with histidine [76]. From the structural models in the previous chapter, it appears as though AgHO binds via histidine similar to HO-1 and dissimilarly to DmΔHO. In the AgHO-haem complexed form, haem iron is in a ferric state.

Table 4.1. Absorption maxima for haem complex spectra verify mode of haem binding

Complex	Soret peak maximum (nm)	α peak maximum	β peak maximum
Ferric haem	398	603	579
Ferrous CO-haem	412	564	535
Ferrous Dioxyhaem	400	570	-

The spectra in Figure 4.1 show changes in haem-AgHO complex absorbance based on the oxidation state of haem iron. The absorption maxima for peaks of interest are shown in Table 4.1. The ferric form of the complex had a Soret Peak at 398nm, with smaller peaks in the visible region at 603nm and 579nm. Bubbling CO through the enzyme solution in the presence of sodium dithionite reduced the iron to a ferrous-CO form, with a Soret maximum at 412nm, and smaller peaks at 564 and 535nm in the visible range. Exchange of the gas phase of the solution by passing through a Sephadex G-25 column indicated a conversion of the ferrous-CO form to a ferrous dioxy form with Soret peak at 400nm and diminished α/β peaks.

These changes correspond with haem-HO spectra observed for bacterial and eukaryotic haem oxygenases [106, 107, 109, 110].

4.3.2 Study of binding affinity of AgHO for haem

The extinction coefficient of the AgHO-haem complex was calculated using the pyrimidine haemochrome method [127, 128]. The extinction coefficient at 398nm (ε_{398}) was calculated to be 105.73mM^{-1} cm^{-1}. This value was used to accurately estimate the concentration of the AgHO-haem complex during the calculation of the dissociation constant.

The binding affinity of AgHO haem was examined by titrating haem into cuvettes containing AgHO (sample) and buffer (control) and monitoring the absorption spectrum. Figure 4.2 shows the absorption spectra across this titration, and Figure 4.3 shows the absorption maxima across the titration.

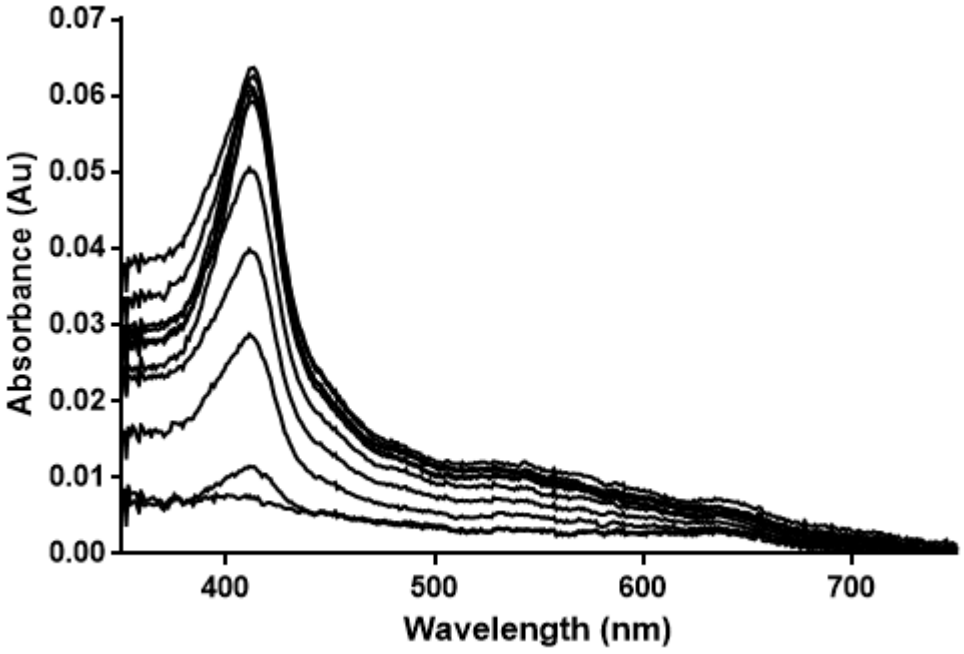

Figure 4.2. AgHO haem titration spectra Optical absorption spectra for 10μM AgHO titrated with 2-20μM of haem.

These data show that AgHO binds haem in a 1:1 stoichiometry since the Soret peak absorbance increases up to the point at which there is an equimolar concentration of AgHO and haem in the cuvette. After this point, continuing to add haem to both sample and reference cuvettes yields no increase at the Soret peak due to the fact that AgHO binding sites are saturated. Use of a one-site binding model estimates the dissociation constant (K_D) for AgHO for haem to be 3.9 ± 0.6 μM.

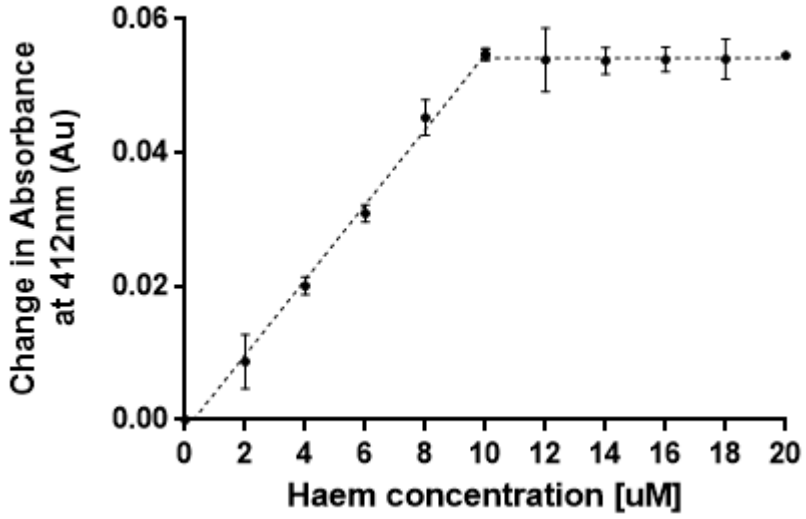

Figure 4.3. Stoichiometry of haem binding to AgHO – Absorbance of the AgHO-haem complex at 412nm as a function of 412nm absorption

4.3.3 Identification of biliverdin as an AgHO reaction product

Figure 4.4 shows haem catabolism with AgHO and three different CPRs: AgCPR, MdCPR and HsCPR. Each of the experiments shows a reduction in absorption at the haem Soret peak (398nm) and at the haem α/β peaks (603nm, 579nm), indicating catabolism of haem. Each experiment also shows the appearance of a broad absorption peak centred at 680nm, corresponding with one of the observed absorption peaks for biliverdin.

AgCPR the lowest rate of activity of the CPRs tested as measured by the extent of the reduction of the Soret peak over two hours. This may be related to a lack of N-terminal membrane anchor, in comparison with MdCPR and HsCPR, which were both full length. Control systems did not yield reduction in absorption at the Soret peak or α/β peaks, there was also no recorded increase at 680nm. From this point forward, only MdCPR was used.

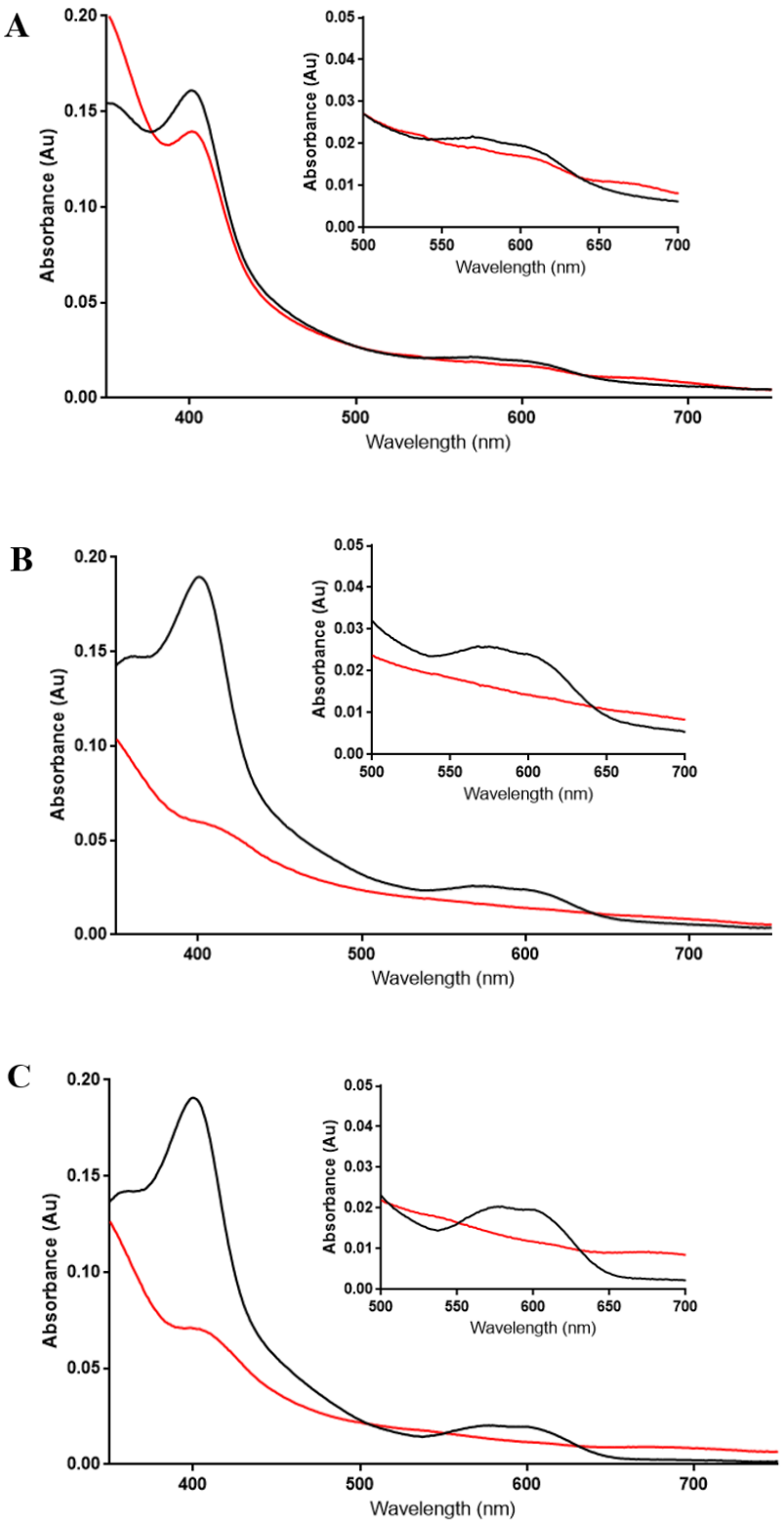

Figure 4.4. Absorption spectra showing detection of biliverdin as a reaction product of AgHO mediated haem catabolism A is with AgCPR, **B** is with MdCPR and **C** is with HsCPR. Black is the spectrum at time 0 (immediately after initiation of reaction by addition of NADPH), red is 2 hours after initiation

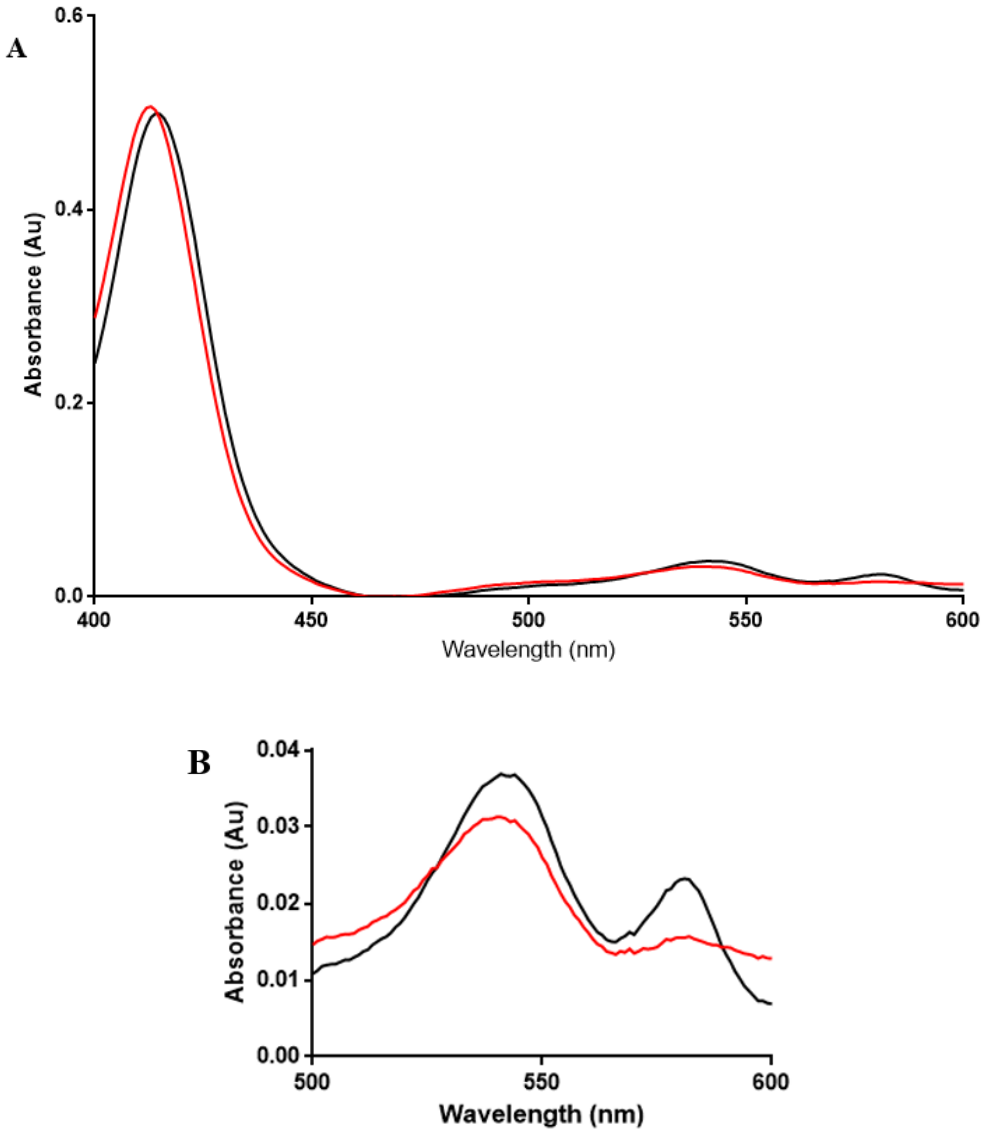

Figure 4.5. Spectral shift of myoglobin Soret peak shows production of CO by AgHO mediated haem catabolism – **A -** Soret peak absorbance maximum shifting to a higher wavelength as a result of CO binding, **B -** increase in absorbance at myoglobin α/β peaks as a result of CO binding

Red is immediately after reaction initiation by addition of NADPH to control and sample cuvettes, black is 30 minutes after reaction initiation.

4.3.4 Identification of carbon monoxide as an AgHO reaction product

Carbon monoxide is produced by HO mediated haem catabolism. It is undetectable by absorption spectroscopy, but can be observed indirectly by measuring CO binding to myoglobin.

Figure 4.5 shows the spectral differences of myoglobin brought about by the production of CO by haem catabolism. The myoglobin Soret peak shifts to a higher wavelength and the myoglobin α/β peaks have increased absorption. These changes are characteristic of CO binding to a haemoprotein. Control systems which were not initiated by NADPH, or which had no CPR reducing equivalent produced no such spectral changes in myoglobin.

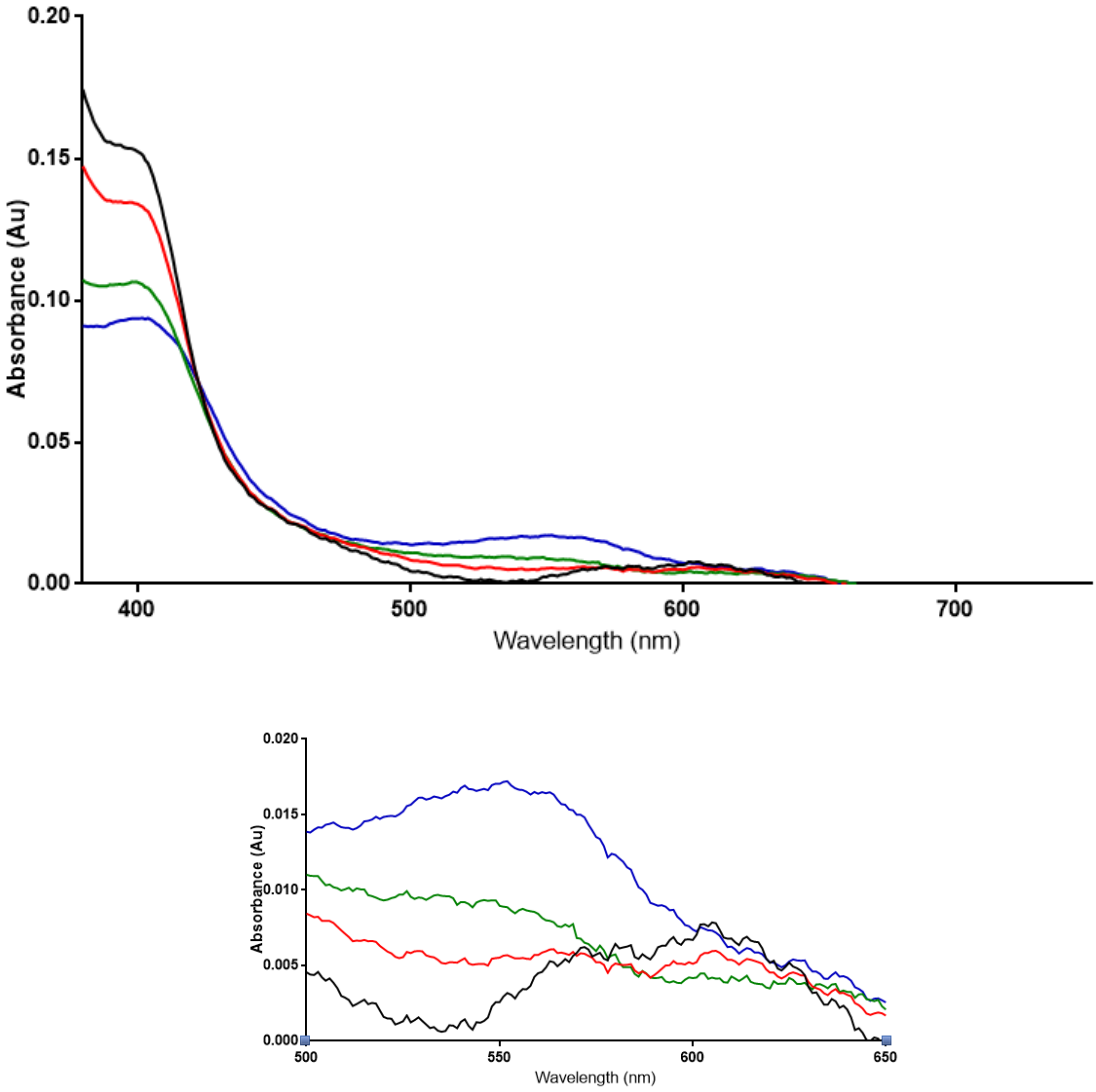

Figure 4.6. Increase in absorption at 562nm shows Ferrozine binding to ferrous iron produced by AgHO mediated haem catabolism – **A -** Soret peak absorbance decreasing with haem catabolism, whilst absorbance at 562nm increases due to formation of Ferrozine-ferrous iron complex; **B –** Increase in absorbance at 562nm due to formation of Ferrozine-ferrous iron complex.

Black is immediately after reaction initiation by addition of NADPH to control and sample cuvettes, red is 10 minutes after reaction initiation, green is 20 minutes after reaction initiation, blue is 60 minutes after reaction initiation.

4.3.5 Identification of ferrous iron as an AgHO reaction product

As with CO detection, ferrous iron is not directly observable using absorption spectroscopy. Therefore ferrozine is used; ferrozine is an organic compound that binds Fe^{2+} ions [129].

Figure 4.6 illustrates the release of Fe^{2+} by haem when degraded by AgHO. The peak centred at 562nm is characteristic of formation of a ferrozine - metal ion complex which is magenta in colour. The only possible ferrozine ligand in this reaction system is Fe^{2+}, therefore the 562nm peak comes about due to ferrous iron being released during AgHO mediated haem catabolism.

This reaction is ideal to examine other parameters of the AgHO reaction, such at temperature and pH optima as the 562nm peak is in a region of the absorbance spectra area far removed from potentially interfering peaks. Also, it will bind iron at a constant rate over a wide pH range (4-10) [129].

4.3.6 Effect of pH on AgHO

The ferrozine assay was repeated across a range of pHs in order to examine the effect of pH on AgHO activity. The results are shown in Figure 4.7.

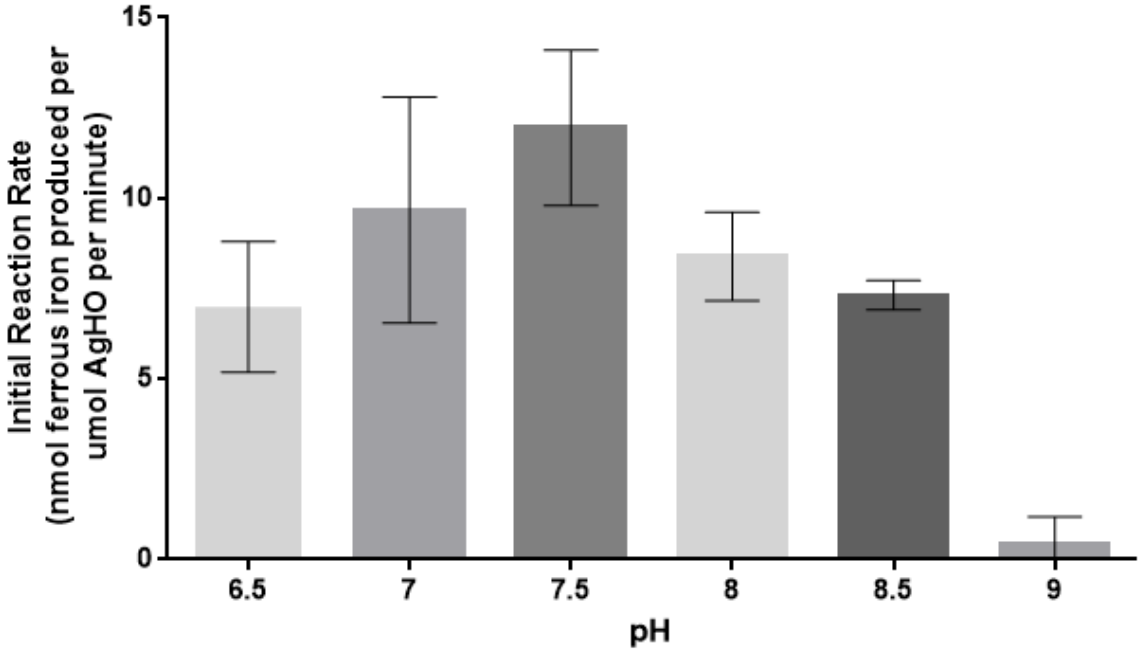

Figure 4.7. The pH optimum for AgHO activity is pH 7.5 – Using formation of Fe^{2+}-ferrozine complex to measure the AgHO reaction rate shows that activity is highest at around pH 7.5.

AgHO has the highest reaction rate at pH 7.5 (ANOVA; $F(5,12) = 4.568$, $p = 0.0145$), mirroring physiological conditions. Reaction rate drops off rapidly at pH 9, possibly due to inhibition of AgHO binding to haem *via* haem propionate groups, or due to denaturation of the functional conformation of AgHO.

4.3.7 Effect of temperature on AgHO

The ferrozine assay was repeated across a range of temperatures in order to examine the effect of temperature on AgHO activity. The results are shown in Figure 4.8.

Highest activity was measured at 27.5ºC (ANOVA; $F(7,16) = 4.459$, $p = 0.0063$), with activity minimal at 20ºC.

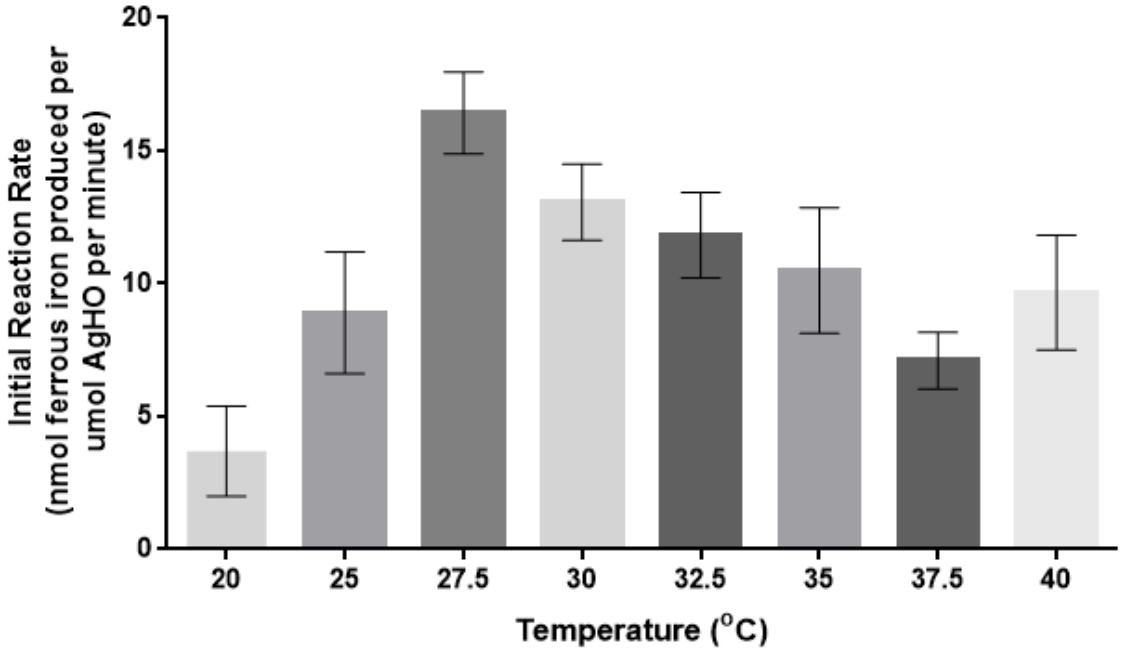

Figure 4.8. The temperature optimum for AgHO activity is 27.5ºC – Using formation of Fe^{2+}-ferrozine complex to measure the AgHO reaction rate shows that activity is highest at around 27.5ºC.

4.4 Discussion

This chapter represents the first time that a haematophagous insect HO has been isolated and characterised *in vitro*. Binding studies confirmed that AgHO binds haem in a 1:1 stoichiometry. Similarities in Soret and α/β peak maxima between AgHO, rat and *Corynebacterium* haem oxygenases [107, 109] provide evidence that the AgHO binding site is similar, with H19 at the proximal haem face and coordination *via* a water molecule with T15.

The K_D of AgHO was estimated to be 3.9 ± 0.6 μM using a one-site binding model. This value is comparable to previously measured dissociation constants of 2.5 ± 1 μM for *C. diphtheriae* HmuO [109] and 0.84 ± 0.2 μM for human HO-1 [130], however it is far lower than the 27 ± 1 μM value obtained for DmΔHO [76]. The disparity between AgHO and DmΔHO may have arisen due to the unique nature of DmΔHO binding, which does not appear to be shared by AgHO.

Analysis of the AgHO reaction shows that AgHO is a true haem oxygenase, in that it conforms to the previously observed haem degradation pathway of haem being hydrolysed to form biliverdin, carbon monoxide and ferrous iron. Biliverdin has been observed to be produced from enzymatic haem degradation, measured by increases at 680nm wavelength, as the haem Soret peak at 398nm decreases in absorbance. Carbon monoxide and ferrous iron production have been observed indirectly by their effects on the absorbance of myoglobin and ferrozine respectively. Haem catabolism was found to be inefficient when using a truncated AgCPR, compared to full length HsCPR and MdCPR. This suggests that the hydrophobic tail of CPRs are an important aspect of HO:CPR docking. Further experiments using truncated HsCPR and MdCPR would be useful to determine the accuracy of this hypothesis.

The data obtained on AgHO driven haem degradation in this chapter have been qualitative. Quantitative analysis of HO reactions are difficult, particularly without employing

biliverdin reductase. Biliverdin reductase (BVR) is a mammalian enzyme not present in *An. gambiae* which catalyses the conversion of biliverdin to bilirubin, a spectroscopically distinct reaction product with a Soret peak at 460 nm. Mammalian haem oxygenase studies have successfully employed biliverdin reductase to examine kinetic parameters of HOs. Use of BVR in AgHO systems did not yield any results, possibly due to divergent BVR binding residues in AgHO inhibiting BVR:AgHO docking [82].

Ferrozine has only once been used as a substrate for measuring haem oxygenase activity [131]. Here it has been found to have a number of advantages for the characterisation of AgHO activity. Firstly, the change in its absorbance that arises when ferrozine binds ferrous iron is away from other, potentially interfering spectroscopic peaks, such as the Soret peak. Secondly, it can be easily employed in a microplate style assay, thus facilitating examinination of variables such as temperature and pH parameters on enzyme activity, as its complexation with iron is stable across most biologically relevant temperatures and pHs. With further work, this assay may be able to accurately examine the kinetics of AgHO with respect to haem, something that is otherwise intractable given the spectroscopic changes when haem is bound by AgHO, and following catabolism. Another advantage is direct comparison between HOs, without the need for BVR. Comparing the reaction rates of HOs using BVR is confounded by the fact that both the reaction rate of haem degradation and the BVR:HO docking is being measured simultaneously, whereas the ferrozine assay only measures liberation of ferrous iron. The assay also has potential for future work with haem oxygenase inhibitors.

The pH and temperature parameters discovered for AgHO are consistent with the physiological context of AgHO. Vertebrate blood has a pH of 7.4, increasing to 7.6 when ingested by *Anopheles*. Moreover, eukaryotic cytosol pH is 7.4. The temperature optimum for AgHO was 27.5^{o}C, which corresponds to the behaviour of blood fed mosquitoes that seek

temperatures in the range of 26-28^{o}C at which to rest [132]. The high AgHO activity during the post-bloodmeal resting phase might aid in rapid digestion.

Chapter 5 – Development of a bioassay to investigate the *in vivo* role of AgHO

5.1 Introduction

As has been discussed in previous chapters, the disposal of excess haem is a vitally important process which prevents the oxidative damage that high concentrations of haem can inflict [40-43]. Given the huge quantities of haem released by *An. gambiae* over the course of haemoglobin digestion, it is clear that mechanisms to limit haem toxicity are of key importance. These mechanisms are yet to have been studied in detail in *An. gambiae*. Some, such as formation of haem aggregates, have arisen independently in numerous species as diverse as blood flukes [133], malaria parasites [52], and haematophagous insects including *R. prolixus* [56], *Ae. aegypti* and *An. gambiae* [134]. Other defence mechanisms include haem binding proteins, which have been investigated in blood feeding insects [61, 135], but not *An. gambiae*.

Disposal of haem is carried out by the haem oxygenase enzyme in an extremely wide range of species, from bacteria to mammals. It makes sense that AgHO acts in concert with other mechanisms (aggregation, haem binding proteins) to ameliorate haem-mediated toxicity. It has been observed that in haematophagous insects [77, 78], including *An. gambiae* (data not shown), that the bloodmeal changes from a red to a green colour, and in other insects, this has been associated with a reduction in haem concentration and an increase in biliverdin IX concentration. This is likely the result of haem oxygenase activity.

Having expressed recombinant AgHO and examined its haem oxygenase activity *in vitro*, the next step is to examine its *in vivo* role and insecticide target potential. AgHO knockout can be achieved by gene knockout or *via* inhibition of enzyme activity. Time constraints precluded the use of RNAi, therefore this chapter aims to estimate the in vivo role of AgHO

via inhibition of AgHO activity by ingestion of inhibitors. Previous studies in *R. prolixus* have shown that tin protoporphyrin inhibits haemozoin formation and haem degradation, resulting in the promotion of oxidative stress and reduction in reproductive capacity [100]. These results show that haem analogues may be used to inhibit HO activity and examine physiological outcomes. The aim of this chapter, is to develop a viable bioassay to apply AgHO inhibitors to *An. gambiae* mosquitoes. The second aim is to use this assay to study the role of the AgHO mediated haem degradation pathway using a range of haem analogues – zinc protoporphyrin (ZnPP), tin protoporphyrin (SnPP) and copper protoporphyrin (CuPP).

5.2 Materials and Methods

5.2.1 Feeding inhibitory globins to *An. gambiae* as part of a bloodmeal

5.2.1.1 Preparation of inhibitory globins

Inhibitory globins were made using the acidified butanone method [100, 136]. A solution of 50mg mL^{-1} bovine haemoglobin was dialysed against ddH_2O for 16 hours at 4°C. The pH of the protein solution was adjusted to 2.0 with dropwise addition of 1M HCl. The haemoglobin was placed in a 50mL falcon tube on ice alongside falcon tubes containing butanone.

Once ice cold, the butanone was mixed gently with the protein solution and left on ice, shaking at 40rpm for 2 hours. The mixture was left to stand for ten minutes to allow the two liquid phases to separate. The organic phase was removed using a serological pipette and analysed for haem content on a spectrophotometer. This process was repeated at least three times, until no more haem was detected in the organic phase. The aqueous phase was extensively dialysed against ddH_2O for 16 hours at 4°C to remove any remaining butanone.

The dialysed globin product was mixed in an equimolar mount of 5mM ZnPP-IX dissolved in DMSO to make the metalloporphyrin-globin complex, referred to hereafter as ZnPP-globin.

5.2.1.2 Feeding inhibitory globins to mosquitoes

Cohorts of *An. gambiae* mosquitoes, strain Kisumu, were bloodfed on heparinized human blood supplemented with 0μM, 40μM, 100μM and 400μM ZnPP-globin. The inhibitor supplement was in a volume of 500μL, added to 4.5mL blood. The mosquitoes were fed *via* hemotek bloodfeeders, for two hours, in darkness. Mosquitoes were visually confirmed to have fed. Those individuals which had not fed were excluded. 25 individuals from each feeding group were isolated and kept under standard conditions (see Chapter 2), and fed 10% sucrose

ad libitum. After two days, an egg paper was introduced to allow mosquitoes to lay. After two further days, the egg paper was removed and laid eggs were counted.

5.2.2 Microinjection of protoporphyrin into *An. gambiae*

5.2.2.1 Determination of ZnPP amount to microinject

In order to establish a quantity of ZnPP to microinject into *An. gambiae* thoraces, the bloodmeal volume was weighed. This was achieved by cold-anaesthetising mosquito cohorts before a bloodfeed, and weighing them. The mosquito cohort was then allowed to bloodfeed as normal. After the bloodfeed, the mosquitoes would be anaesthetised and weighed again. An average bloodmeal size was determined by calculating the difference in the mass of the cohort. The mosquitoes are not allowed access to 10% sucrose during the bloodmeal here, to ensure that changes in weight are strictly related to the bloodmeal and not sugar consumption. These calculations are outlined in Table 5.1, where bloodmeal volume is calculated based on a blood density of 1.06 g cm^{-3}. These figures are in line with previously reported mosquito bloodmeal sizes

Table 5.1. Bloodmeal sizes in *An. gambiae*, strain Tiassale

Mass of 50 mosquitoes, pre-bloodmeal (g)	**Mass of 50 mosquitoes, post-bloodmeal (g)**	**Mass of 50 bloodmeals (g)**	**Mean mass of *An. gambiae* bloodmeal (mg)**	**Mean volume of *An. gambiae* bloodmeal (µL)**
0.0583	**0.145**	**0.0868**	**1.74**	**1.64**

5.2.2.2 Microinjection of ZnPP

Based on the calculations in Table 5.1, 65 nL 10mM ZnPP was injected into the thoracic cavities of *An. gambiae* strain Tiassale mosquitoes whilst cold-anaesthetised. 10mM NaOH was used as a solvent. As previously, surviving mosquitoes were isolated in groups of ten (one group injected with an equivalent of 400μM ZnPP, the other with an equivalent volume of NaOH solvent) and kept under standard conditions and fed 10% sucrose *ad libitum*. After two days, an egg paper was introduced to allow mosquitoes to lay. After two further days, the egg paper was removed and laid eggs were counted.

5.2.3 Feeding free protoporphyrin to An. gambiae as part of a bloodmeal

10mM ZnPP stocks were made by dissolving ZnPP in 50mM NaOH. The ZnPP was added to blood in a volume of no more than 200μL in 5mL heparinized human blood. Final concentrations of ZnPP in blood were 0μM, 40μM, 100μM and 400μM ZnPP.

Cohorts of *An. gambiae* mosquitoes, strain Tiassale, were fed the inhibitor-supplemented blood *via* hemotek bloodfeeders, for two hours, in darkness. Mosquitoes were visually confirmed to have fed. Those individuals which had not fed were excluded. 25 individuals from each feeding group were isolated and kept under standard conditions (see Chapter 2), and fed 10% sucrose *ad libitum*. After two days, an egg paper was introduced to allow mosquitoes to lay. After two further days, the egg paper was removed and laid eggs were counted.

5.3 Results and Discussion

5.3.1 Trials of AgHO inhibition methods

5.3.1.1 Effect of bloodmeal ZnPP-globin on An. gambiae fecundity

Figure 5.1 shows preliminary data suggesting that application of ZnPP-globin could have a dose dependent effect on oviposition rates in *An. gambiae*. Increasing concentrations of ZnPP-globin over the range chosen yield a measurable reduction in oviposition, therefore this is a potentially viable bioassay.

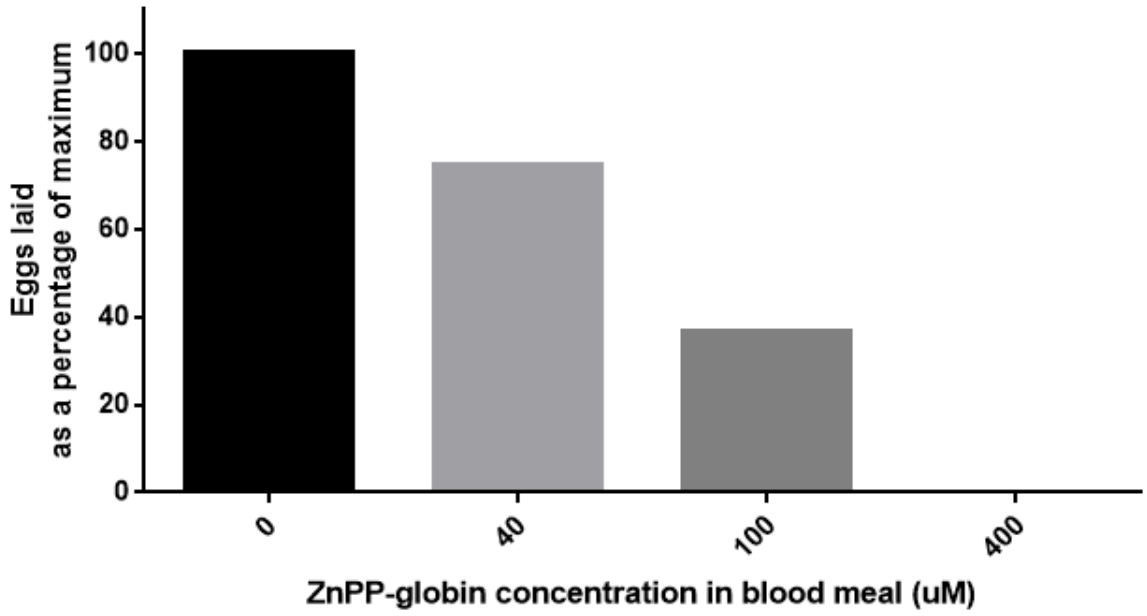

Figure 5.1. Dose dependent response of oviposition to concentration of ZnPP-globin in the bloodmeal (experiment performed once)

5.3.1.2 Effect of microinjected ZnPP on An. gambiae

Table 5.2 shows that injection of ZnPP has a detrimental effect on *An. gambiae* fecundity, meaning that it has potential as a bioassay. Table 5.3 shows that up to 90% of mosquitoes were unable to be resuscitated following microinjection. There is not a significant difference between mortalities in different treatment cohorts, indicating that mortality here is due to either the procedure itself (mechanical damage from thoracic microinjection) or the NaOH solvent. This solvent cannot be changed, as an equimolar amount of OH^- is a requirement for dissolving ZnPP. An alternative solvent, DMSO, is incompatible with the microinjection apparatus. The mortality during fecundity analysis is estimated after ten surviving mosquitoes from the microinjection procedure are isolated and provided with sugar water.

Table 5.2. Effect of microinjected ZnPP on fecundity

Equivalent concentration of ZnPP (μM)	**Eggs laid by cohort of ten mosquitoes**
0	407
400	0

Table 5.3. Effect of microinjected ZnPP on mortality

Equivalent concentration of ZnPP (μM)	**Mosquito mortality within 1 hour of microinjection procedure**	**Mosquito mortality during fecundity analysis (96 hours)**
0	89%	20%
400	90%	20%

5.3.1.3 Effect of bloodmeal ZnPP on mosquito fecundity

Figure 5.2 shows that like ZnPP-globin, free ZnPP has a dose dependent effect on mosquito fecundity. Again, increasing concentrations of ZnPP over the range chosen yield a measurable reduction in oviposition, therefore this is a potentially viable bioassay.

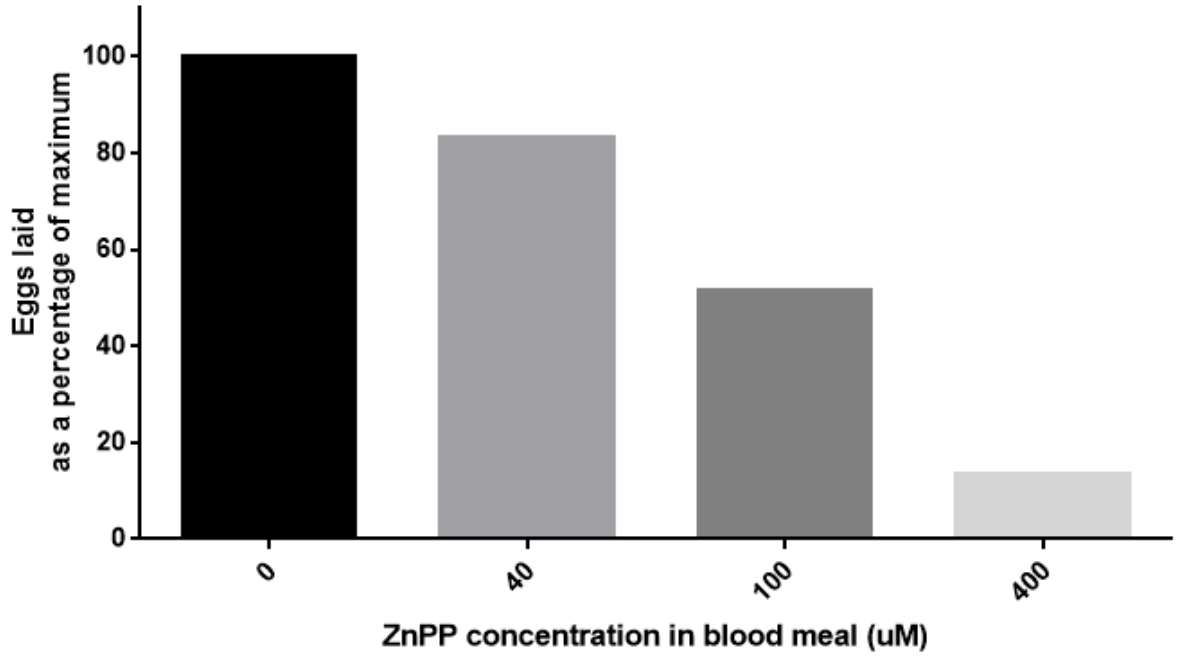

Figure 5.2 – Dose dependent response of oviposition to concentration of ZnPP in the bloodmeal (experiment performed once)

5.3.1.4 Evaluation of methods of in vivo haem oxygenase inhibition

All the tested protocols for *in vivo* AgHO inhibition yield a phenotype in which oviposition is inhibited by high concentrations of ZnPP. However, each assay has advantages and disadvantages.

Application of ZnPP-globin has the advantage of being ingested similar to natural ingestion of haemoglobin. It resulted in a measurable phenotype (reduction in oviposition). The

major shortcoming of this protocol is the creation of the inhibitory globin. The process is very resource-wasteful, expensive and time-consuming. Also, haem removal from the globin is not 100% efficient, and is difficult to quantify. It is therefore difficult to estimate how accurate the inhibitory globin concentration is. There is no guarantee that the inhibitory globin is formed as predicted; this assay may simply involve the application of inhibitory protoporphyrin in conjunction with globin protein. Furthermore, a battery of controls would be required to conclusively state that the inhibition occurring is due to the inhibitor itself, or because other factors, such as diluted nutrient, application of malformed globin or trace amounts of solvents such as DMSO or butanone.

Though microinjection of protoporphyrin directly into the mosquito thorax did achieve a differential phenotype between control and inhibitor treatments, the bioassay is a poor one. Firstly, since the injection is into the thorax and not into the bloodmeal bolus itself, the treatment is not representative of AgHO application in the midgut. This makes the calculation of an equivalent of 400μM in the bloodmeal is irrelevant. This is also a very time consuming assay. The biggest concern is mosquito mortality. The fact that only ten percent of mosquitoes survive the injection procedure makes this assay extremely wasteful in terms of live mosquito resources. There is also a concern that the effects of inhibitors are exaggerated, as the mosquito system is dealing with massive mechanical damage, in addition to the hypothesised oxidative stress.

The best assay is the feeding of free protoporphyrin *via* the bloodmeal. It has most of the advantages of the protoporphyrin-globin assay, with none of the drawbacks. One potential shortcoming is the fact that the application of inhibitor is not the same as in the globin assay, i.e. there is no digestion of haemoglobin to release inhibitor. In this respect it may not be as accurate at estimating the normal *in vivo* function of AgHO. However, in terms of potential for

insecticide development, it is just as useful. The free protoporphyrin feeding bioassay is the one which will be used for the remainder of the *in vivo* inhibition analysis.

5.3.2 Effect of HO inhibitors on oviposition

Three different haem-analogues were applied as in section 5.2.3: ZnPP, SnPP and CuPP. Both zinc [98] and tin [137] protoporphyrins are canonical haem oxygenase inhibitors, and copper protoporphyrin is a canonical control for haem oxygenase inhibition - that is, it does not inhibit the haem oxygenase reaction, but does participate in other physiological processes which other inhibitors do, such as inhibition of guanylyl cyclase [138]. Figures 5.3 and Figure 5.4 show that there is a dose dependent response in which, as the concentration of inhibitory protoporphyrin in the bloodmeal increases, oviposition rates decrease. This trend is present in both ZnPP (ANOVA; $F(3,8) = 40.44$, $p < 0.0001$) and SnPP (ANOVA; $F(3,8) = 135.2$, $p < 0.0001$) , and appears to be more potent in SnPP, in line with previous mammalian studies [137].

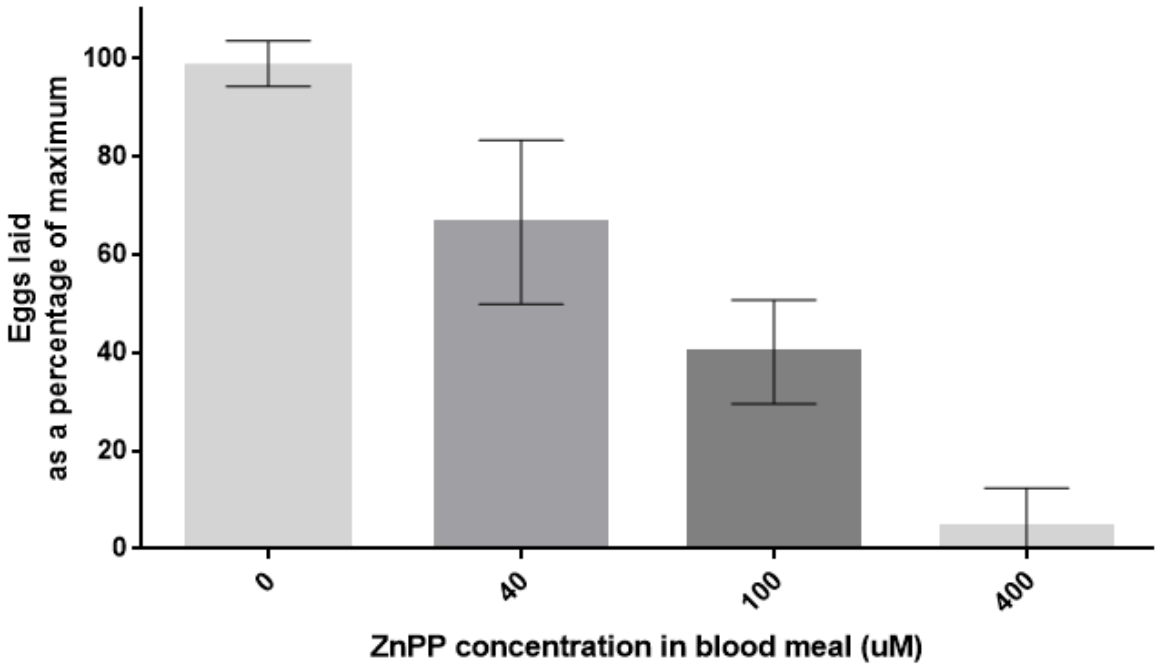

Figure 5.3. Dose dependent response of oviposition to ZnPP in the bloodmeal

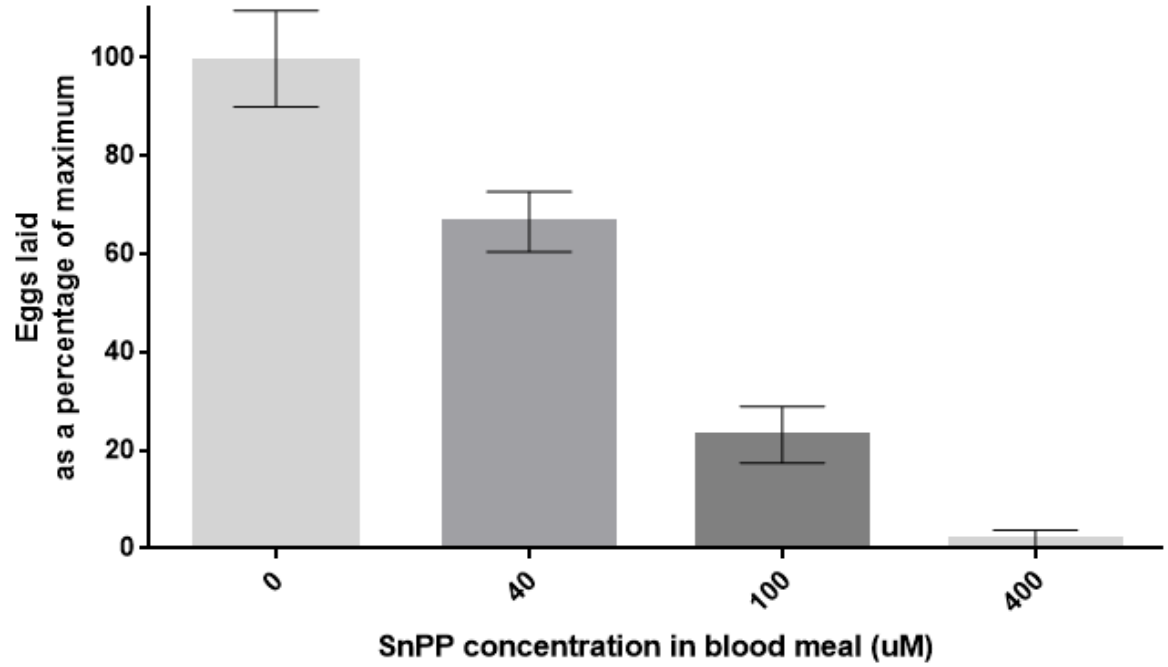

Figure 5.4. Dose dependent response of oviposition to SnPP in the bloodmeal

Figure 5.5 shows the application of CuPP to mosquitoes *via* the bloodmeal, and shows an insignificant effect on fecundity (t-test, t(4) = 0.69, P = 0.53). There seems to be a small impact on fecundity, possibly related to background effects of protoporphyrin feeding, but too insignificant to draw conclusions from, other than that CuPP works as a negative control in *An. gambiae* as it does in mammalian systems.

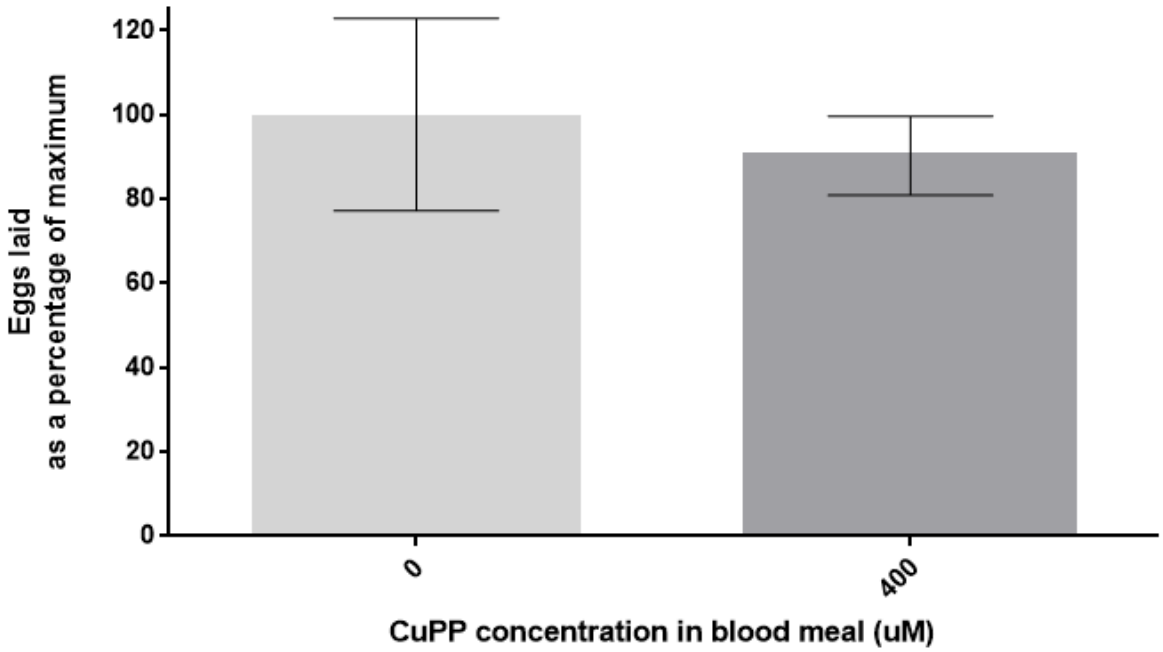

Figure 5.5. Increasing CuPP concentration in the bloodmeal does not effect oviposition

5.4 Conclusion

This chapter represents the first time a HO inhibitor's effects on mosquitoes have been estimated, and points towards the utility of using HO inhibitors in vector control. The role of AgHO as a dietary detoxificant is shown here. Use of the CuPP negative control suggests that the effect on oviposition by ZnPP and SnPP is due to inhibitory effects on the haem degradation pathway, as opposed to effects on other physiological processes, such as the guanylyl cyclase pathway.

What has not yet been ascertained is the specific mode of action of these inhibitors in a physiological context. Whilst it seems clear that these inhibitors compete for the active site of haem oxygenase [139], it is not necessarily clear why this should have an effect on oviposition. One possibility is oxidative stress on the mosquito. It has been shown that inhibition of haem oxygenase with SnPP-globin leads to an increase in oxidative stress in *R. prolixus* [100], and oxidative stress is a known factor towards decreased reproductive fitness in insects [140]. Another factor to look at is the reaction products of haem oxygenase, and whether or not these are essential for any aspect of oogenesis. The fate of biliverdin is largely unknown, however in *Ae. aegypti*, 7% of total blood meal iron is directed to egg formation [119]. It may follow that without sufficient iron from haem degradation, oogenesis is arrested. Another possibility is lack of carbon monoxide. Haem degradation is a key source of carbon monoxide, and given its role as a signalling molecule, a lack of endogenous CO may inhibit signals involved with oviposition behaviour or nutrient trafficking in oogenesis.

Chapter 6 – Functional comparison of insect and human cytochrome P450 reductases

6.1 Introduction

NADPH-dependent cytochrome P450 reductase (EC 1.6.2.4) is a membrane bound enzyme required for electron transfer from the NADPH electron donor to a number of diverse electron acceptors, including flavoproteins like squalene monooxygenase, and haemoproteins such as the cytochromes P450, cytochrome b_5 and haem oxygenase. Transfer occurs along the pathway NADPH → FAD → FMN → haem.

CPRs from numerous organisms have been expressed and characterised, including *H. sapiens, R. norvegicus, Petroselinum crispum, Musca domestica* and *An. gambiae*. In most organisms except plants (which contain multiple CPR genes [141]), CPR is a single gene, believed to have evolved as a result of gene fusion between an FMN- and an FAD-containing flavoprotein [142]. These two domains remain functionally and structurally distinct, and can be heterologously expressed as functionally active separate enzymes.

In total, there are four CPR domains [142]. There are the two major catalytic domains, the FMN-binding domain, structurally similar to flavodoxins, and the NADPH/FAD-binding domain, which is structurally similar to ferredoxin-$NADP^+$ reductase. There is also a linker domain that likely plays a role in positioning the two catalytic domains for optimal electron transfer [87]. The fourth domain is the transmembrane region, which is relatively structurally unknown owing to difficulties in its crystallisation.

The FMN-binding domain is the point at which electrons are transferred from the CPR enzyme cofactors to the haem moiety on the electron accepting enzyme. In cytochromes P450,

electrons are further transferred to perform a monooxygenase reaction which catabolises their substrate. In haem oxygenase, the transferred electrons are used for haem degradation. Accordingly, the FMN-binding domain contains negatively charged residues important for binding at the haem pockets of HO and P450s [86, 143, 144].

CPR enzymes have high levels of conservation at residues involved in cofactor binding and orientation. HsCPR and AgCPR have an amino acid similarity of 53.3% and an amino acid identity of 54.1%. However, despite such high conservation, differences in cofactor binding are evident between these two CPRs that suggest that AgCPR may be a target for selective inhibition.[90]. It has been found that AgCPR has a K_D for 2' 5' ADP which is ten-fold lower than that of HsCPR, explaining why it fails to bind 2' 5' ADP-Sepharose columns (these columns can usually be used to affinity purify CPRs [86, 144, 145]). It was also found that HsCPR was more sensitive to inhibition by nucleotide analogue inhibitors (such as 2' 5' ADP) which bind at the NADPH binding site.

These differences may be a random reflection of the phylogenetic distance between HsCPR and AgCPR, or alternatively, they may be due to differences in biology. Examination of these two CPRs, alongside other haematophagous and non-haematophagous insects may inform which of these explanations is more likely.

This chapter aims to address the question of whether AgCPR is a selective target for inhibition, and to what extent differences in cofactor binding or other biochemical aspects differ amongst insects. Given the predicted importance of haem oxygenase for haem detoxification, the question of whether there are functional differences separating the CPRs of haematophagous and non-haematophagous insects is raised, particularly as regards possible preferences for HO interaction over interaction with P450s.

6.2 Materials and Methods

6.2.1 High-Throughput Expression Screening

The screening procedure was conducted according to standard OPPF procedures [146].

DNA was available from sources in the Vector Department at Liverpool School of Tropical Medicine. mRNA *Apis mellifera* was obtained from Dr Graham Moores at Rothamsted Research Institute, *H. sapiens* cDNA was obtained from the Parasitology Department at LSTM. Where the source material was mRNA, it was used as a template for cDNA synthesis. The HsCPR amino acid sequence was used for a Blast query in order to identify the CPRs shown in Table 6.1. Their cDNA sequences are shown in Appendix 6.1.

Table 6.1. CPR accession numbers

CPR	Accession Number	Database used
AaCPR	AAEL003349-RA	Vectorbase
AgCPR	AGAP000500-RC	Vectorbase
AmCPR	XP_006569767.1	Beebase
CqCPR	CPIJ014664	Vectorbase
DmCPR	NP_477158.1	Flybase
GmCPR	GMOY007231-RA	Vectorbase
HsCPR	NP_000932.3	NCBI CCDS database
RpCPR	RPRC005729-RA	Vectorbase

cDNA templates were used as templates for PCR amplification using KOD Hot Start DNA polymerase (except in the repeated PCR of AmCPR, where Phusion Flash DNA polymerase was used) Since the protocol uses pOPIN expression primers and the InFusion enzyme system. Primers were designed to be complementary to the gene fragment of interest (in this case, the CPR cDNA) at the 3', and to the pOPIN cloning site at the 5'. Primers are detailed in Appendix 5.3. PCR products were analysed using agarose gel electrophoresis.

The PCR products were purified using AMPure XP Magnetic Bead Purification. Because the templates were held in pJET1.2, which has the same antibiotic resistance marker as pOPIN-F (amplicillin), the reaction products were DpnI treated to eliminate false positives with ampicillin selection on agarose plates.

The purified inserts were next cloned into linearised pOPIN-F using lyophilised InFusion recombinase by mixing followed by incubation at 42^{o}C for 30 minutes. These newly created plasmids were then immediately used to transform OmnimaxII *E. coli* cells. These cells were grown overnight at 37^{o}C on LB agar containing ampicillin, X-Gal and IPTG.

Two positive white colonies were picked per construct and used to inoculate Power Broth and grown overnight at 37^{o}C, shaking at 220rpm. These cultures were used for Miniprep and for creation of glycerol stocks. The Minipreps were verified using PCR with KOD Hot Start DNA Polymerase.

Constructs were verified for correct coding sequence by sequencing before expression. Each plasmid was used to transform, separately, B834(DE3) and Rosetta(DE3)LysS *E. coli* cells. The transformed cells were grown overnight at 37^{o}C on LB agar containing the appropriate antibiotic(s).

Individual colonies were picked and used to inoculate Power Broth and grown overnight at 37^{o}C, shaking at 220rpm.

The cultures were used to inoculate either fresh Power Broth or Overnight Express Instant TB Medium, these cultures were grown at 37^{o}C, shaking at 220rpm for 3-5 hours, until the OD reached 0.5. At this point the Power Broth cultures were moved to an incubator set to 20^{o}C, shaking at 220rpm. Once the cultures had equilibrated to the lower temperature, they were induced by addition of IPTG. Overnight Express cultures were moved to an incubator set to 25^{o}C, shaking at 220rpm. This culture autoinduces. Both sets of cultures were left in the incubators for 24 hours.

These cultures were subjected to freeze-thaw and lysozyme cell lysis followed by Ni-NTA purification. The purified cell lysates were visualised using SDS-PAGE.

6.2.2 Scaled up expression and purification of CPRs

Expression was carried out largely as described in Chapter 2. The cell line used for transformation was BL-21*, and the growth medium was TB. After IPTG induction, incubation was carried out at 25^{o}C for 16h. Purification was carried out as described in Chapter 2; the wash buffer used was 150mM NaCl, 50mM Tris HCl pH 7.4, 20mM imidazole, and the elution buffer was 150mM NaCl, 50mM Tris HCl pH 7.4, 200mM imidazole.

Pooled pure fractions had their protein concentration determined by Bradford assay, and were reconstituted with FMN at a concentration of 2:1 FMN:CPR. The CPRs were then applied to a PD-10 column to desalt and remove excess unbound flavin, as per the protocols in Chapter 2. The PD-10 column was pre-equilibrated with 150mM NaCl, 50mM Tris HCl pH7.4, which was also used to elute the protein from the column.

The CPR activity assay was performed at regular intervals over the course of the purification procedure to ensure that active CPR was present. The samples tested were the cell lysate post sonication, the initial Ni-NTA flowthrough (to ensure that a significant amount of

enzyme was not being lost), the eluted Ni-NTA fractions, the pooled sample, and the PD-10 eluate.

6.2.3 Cytochrome P450 reductase activity assay

CPR activity was measured by cytochrome c reduction when using NADPH as an electron donor. 1µL of the enzyme source (cell lysate, Ni-NTA column flowthrough fractions, or pooled purified enzyme) was added to 150µL of 100mM cytochrome c in a 96 well plate in duplicate. 150µL of H_2O was added to one well as a negative control, 150µL of 100mM NADPH was added to the other. Absorbance at 550nm was immediately monitored every 20 seconds for 5 minutes. The slope of the curve was compared between the initiated reaction well and the negative control in order to confirm CPR activity.

6.2.4 Spectral analysis of CPRs

For the oxidised spectrum, 1.5µM of purified CPR in a sample buffer (150mM NaCl, 50mM Tris HCl, pH 8.0) was placed in a 1mL quartz cuvette and scanned from 700 – 380nm in a Cary 4000 absorption spectrophotometer. For the reduced spectrum, NADPH was added from a 5mM stock to a final concentration of 1.5µM, and the sample scanned immediately. The solution was incubated at room temperature for 30 minutes and scanned again to obtain the air-stable semiquinone spectrum [90].

6.2.5 Cytochrome c kinetics

The rate of change of absorbance of horse heart cytochrome *c* (Sigma-Aldrich, UK) at 550 nm was measured at 25°C using a Biotek Epoch platereader essentially as described [90]. 0.75 pmol purified CPR was pre-incubated with 0–110 µM cytochrome *c* (dissolved in 0.3 M

potassium phosphate buffer; pH 7.7 in a total volume of 200µl for 2 min at 25°C. Reactions were initiated by the addition of NADPH to a final concentration of 50 µM and rates measured in triplicate for 2 mins, a linear reaction range.

6.2.6 NADPH kinetics

The rate of change of absorbance of horse heart cytochrome *c* (Sigma-Aldrich, UK) at 550 nm was measured at 25°C using a Biotek Epoch platereader essentially as described [90]. 0.75 pmol purified CPR was pre-incubated with 50 µM cytochrome *c* (dissolved in 0.3 M potassium phosphate buffer; pH 7.7 in a total volume of 200µl for 2 min at 25°C. Reactions were initiated by the addition of NADPH to a final concentration of 0-160 µM and rates measured in triplicate for 2 mins, a linear reaction range.

6.2.7 Inhibition measurement

Measurement of cytochrome *c* reduction was carried out at 25°C with 50 µM cytochrome *c* and 0.75 pmol purified AgCPR or hCPR essentially as described [90] using 0.3 M potassium phosphate buffer, pH 7.7, and different concentrations of 2′, 5′-ADP, 2′-AMP, NADP or diphenyliodonium chloride (Sigma-Aldrich, UK). Reactions were initiated by the addition of NADPH to the final concentrations shown in Table 6.2 corresponding to their apparent K_M values.

Table 6.2. Final concentration of NADPH in each inhibition experiment – Concentration corresponds with the experimentally determined K_M value for the CPR

CPR	AgCPR	AmCPR	CqCPR	DmCPR	HsCPR	RpCPR
NADPH concentration (μM)	13	21	34	31	4	25

6.3 Results

6.3.1 Identification of candidate species for CPR analysis

CPR candidates were selected from a range of available species that would allow the study of haematophagous, non-haematophagous and mammalian enzymes. The species chosen were *An. gambiae*, *Ae. aegypti*, *C. quinquefasciatus*, *D. melanogaster*, *G. morsitans* and *R. prolixus.*

6.3.2 High throughput expression of CPR

Each CPR had two variants to be screened: a full length gene and an N-terminal truncation to enhance solubility [90, 147]. The limits of this N-terminal domain were defined by alignments with previously truncated CPRs, namely AgCPR and HsCPR.

As PCR is often the rate limiting step of an expression screen, the full length genes were amplified and cloned into pJET2.1 to be used as PCR templates.

All of the initial amplifications were successful with the exception of AmCPR constructs. These underwent a second attempt at PCR amplification, this time with a range of annealing temperatures. The PCR was successful for AmCPR with a higher annealing temperature (62^{o}C).

These amplicons were cloned into pOPIN-F. Miniprepped pOPIN-FCPR plasmids were subjected to PCR to confirm that the cloning was successful. Only full length AaCPR and full length DmCPR failed to be cloned and transformed correctly. The fact that pOPIN-F primers and the InFusion method were used eliminates the need to check that the insert is in the plasmid in the correct orientation, as would be necessary with traditional T4 ligase mediated cloning.

All the successfully cloned CPRs were used in expression trials. Figure 6.4 shows the cell lysates from these expression trials after being subjected to Ni-NTA purification. AmCPR,

CqCPR, DmCPR, HsCPR and RpCPR all had constructs with successful expression. Successful expression came from those constructs with the N-terminal transmembrane domain removed (see Appendix 6.4 for truncation details). These five CPRs were taken forward for scaled up expression and characterisation. AaCPR and GmCPR had negligible expression, and were discontinued. The pOPIN-AgCPR also failed to express, therefore a pETM-11-AgCPR expression clone was provided by Dr. M. Paine for expression [90].

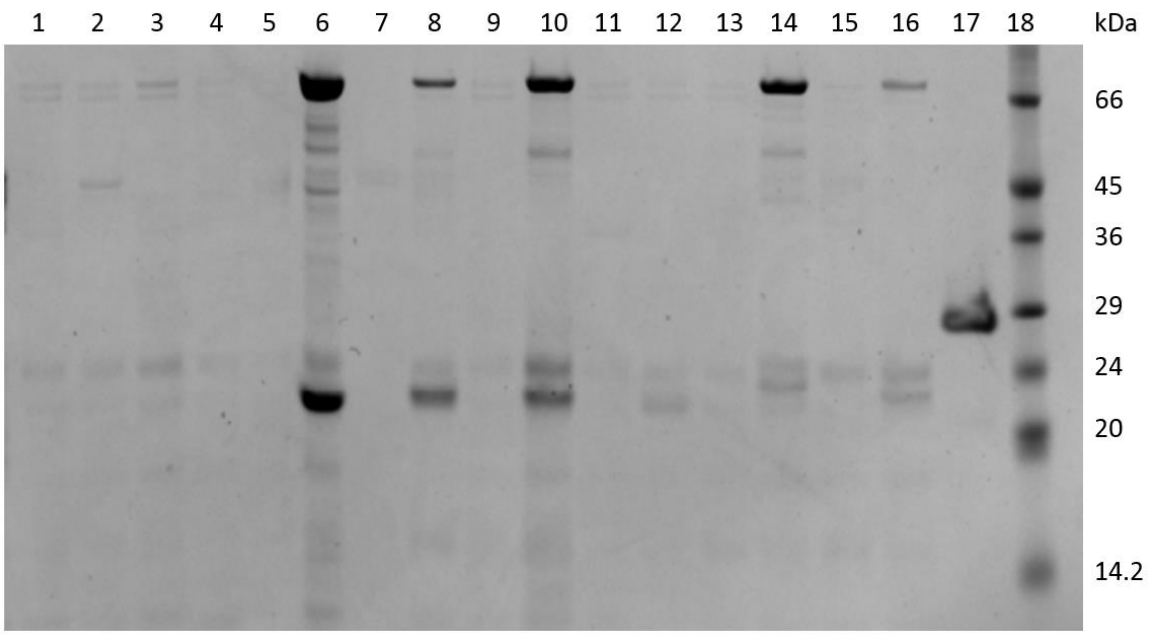

Figure 6.1 Ni-NTA purified CPRs from OPPF expression screening

Lane 1, AaCPR; Lane 2, truncated AaCPR; Lane 3, AgCPR; Lane 4, truncated AgCPR; Lane 5, AmCPR; **Lane 6, truncated AmCPR**; Lane 7, CqCPR; **Lane 8, truncated CqCPR**; Lane 9, DmCPR; **Lane 10, truncated DmCPR**; Lane 11, GmCPR; Lane 12, truncated GmCPR; Lane 13, HsCPR; **Lane 14, truncated HsCPR**; Lane 15, RpCPR; **Lane 16, truncated RpCPR**; Lane 17, GFP Control; Lane 18, molecular weight markers

Bold typeface denotes those expressions which were judged to be successful, and would have their expression scaled up.

6.3.3 Expression and purification of CPRs

Scaled up expression was attempted with each of the successfully expressed CPRs from the OPPF screen and with AgCPR.

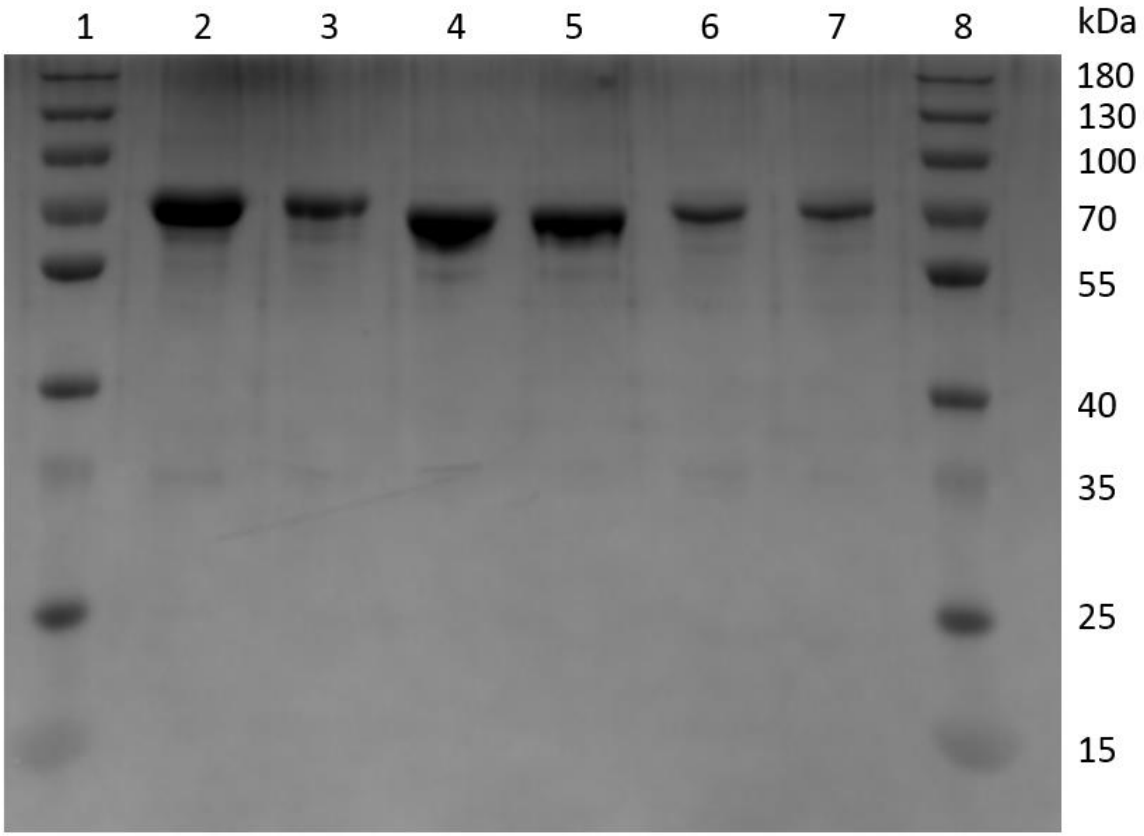

Figure 6.2. Pooled Ni-NTA purified CPRs from scaled up expression

Lane 1, molecular weight marker; Lane 2, AgCPR; Lane 3, AmCPR; Lane 4, CqCPR; Lane 5, DmCPR; Lane 6, HsCPR; Lane 7, RpCPR; Lane 8, molecular weight marker

Figure 6.4 shows the purified protein expressed by the CPR constructs (Appendix 6.4). Yields for these soluble CPR proteins are described in Table 6.3. All the CPRs were tested for cytochrome c reductase activity and found to be functionally active.

Table 6.3. Yields of expressed CPRs

CPR	Yield, mg protein per litre of culture
AgCPR	3.2
AmCPR	5.6
CqCPR	17.0
DmCPR	3.4
HsCPR	8.4
RpCPR	10.3

6.3.4 Alignment of CPRs and analysis of primary amino acid structure

The six expressed CPRs are shown aligned in Figure 6.3. A high degree of sequence identity is evident, particularly those residues highlighted in Table 6.4. Previously observed differences in 2' 5' ADP binding between AgCPR and HsCPR could correspond with differences in binding residues at the NADPH binding domain.

AgCPR residues implicated in NADPH binding include R300, R569 and K570 (binding of adenine-ribose 5' phosphate), S596, R597, K602 and Y604 (binding of adenine-ribose 2' phosphate), and W677 (facilitation of electron transfer to FAD). These residues are identified by homology with the three-dimensional structure of HsCPR [86]. All of these residues are identical in both enzymes with the exception of K570, where HsCPR has an arginine residue at the equivalent position. The differences between 2' AMP binding in AgCPR and HsCPR range from negligible to two times stronger in AgCPR, however 2' 5' ADP binding is 6 – 10 fold higher in HsCPR [90]. The divergent K570 residue, which is implicated in binding at the

adenine 5’ phosphate may explain the difference in nucleotide analogue sensitivities between these two enzymes.

There is minimal divergence in the residues associated with FMN and FAD binding, which is unsurprising given how crucial cofactor positioning is for the function of the CPR enzyme. T474 is a cysteine in HsCPR, a conservative change which allows for hydrogen bonding between FAD and the amino acid residue.

The E216, D217, Y218 sequence is an acidic patch allowing for docking with redox partners. HsCPR has glutamic acid at the D217 position, which is a conservative change. AmCPR, CqCPR, DmCPR, HsCPR and RpCPR all have aspartic acid at the Y218 position, likely corresponding with divergences in redox partners.

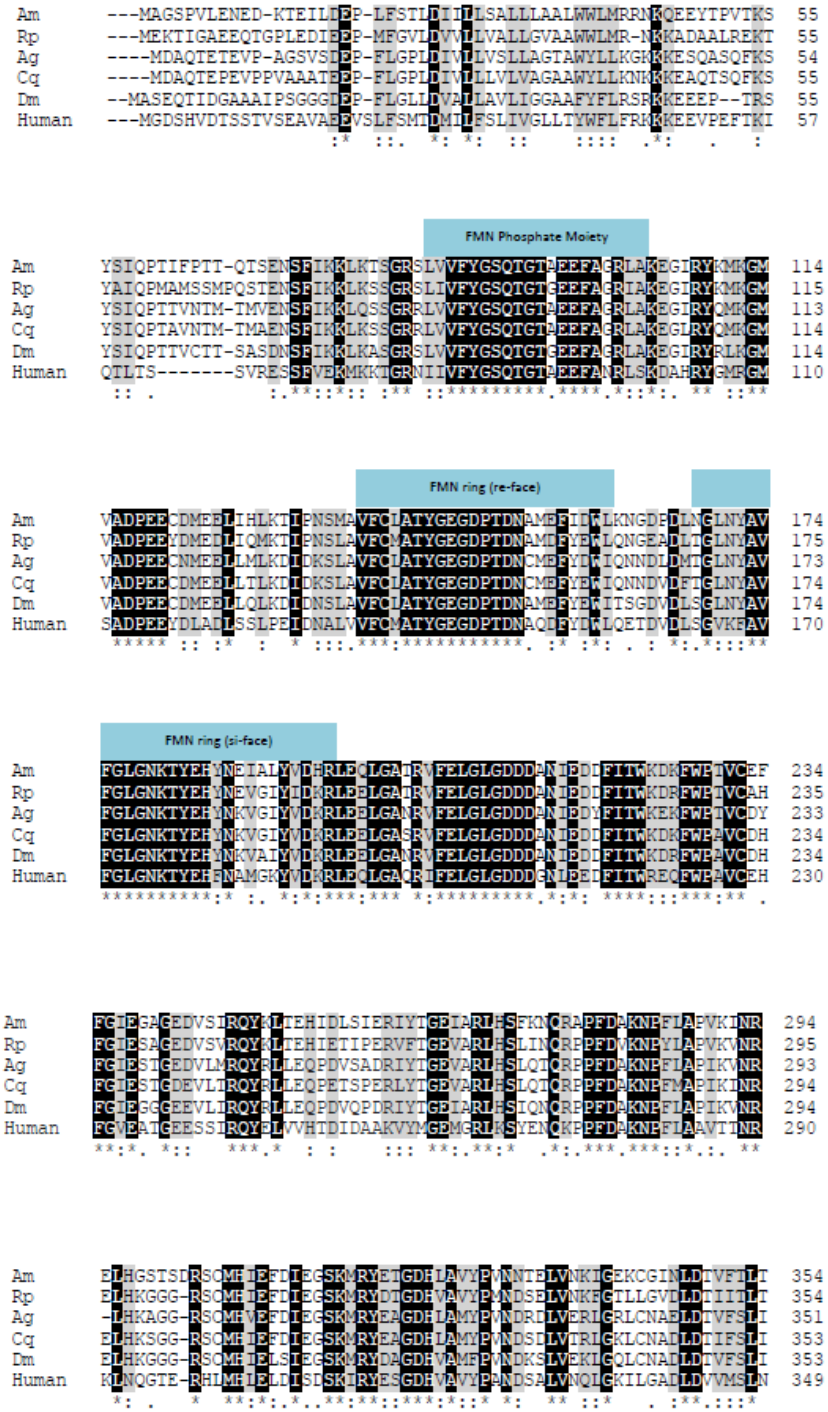
FMN Phosphate Moiety
FMN ring (re-face)
FMN ring (si-face)

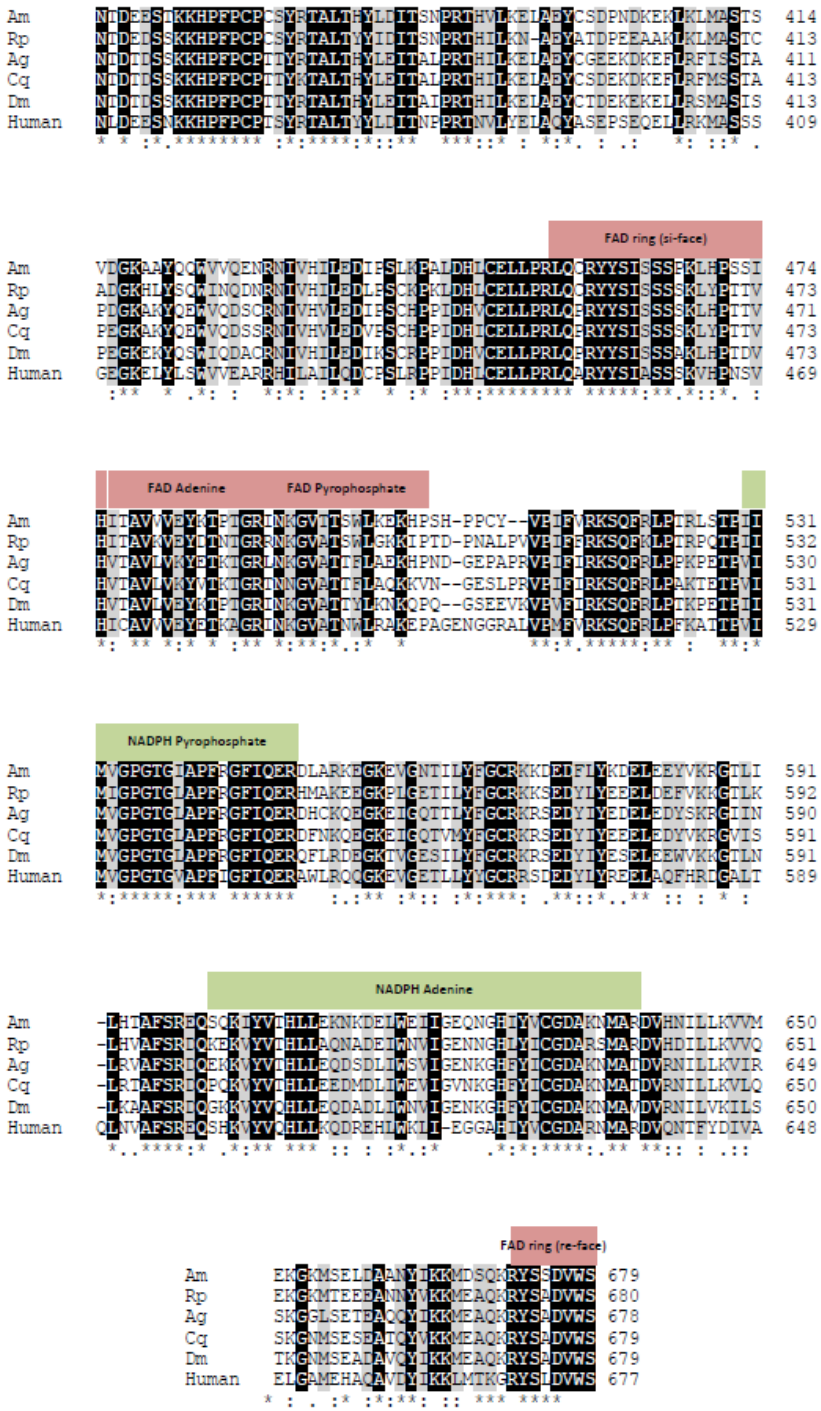

Figure 6.3. **Amino acid alignment of six CPRs showing high conservation between enzymes** Highlighted are known CPR binding motifs. Black shading denotes complete conservation, grey denoted conserved divergences

The c. 6kDa membrane anchor domain (Figure 6.6) is the region of least homology. However they are all predominantly hydrophobic.

```
Am      ---MAGSPVLENED-KTEILDEP-LFSTLDIILLSALLLAALWWLMRRNKQEEYTPVTKSYSI
Rp      ---MEKTIGAEEQTGPLEDIEEP-MFGVLDVVLLVALLGVAAWWLMR-NKKADAALREKTYAI
Ag      ----MDAQTETEVP-AGSVSDEP-FLGPLDIVLLVSLLAGTAWYLLKGKKKESQASQFKSYSI
Cq      ----MDAQTEPEVPPVAAATEEP-FLGPLDIVLLLVLVAGAAWYLLKNKKKEAQTSQFKSYSI
Dm      --MASEQTIDGAAAIPSGGGDEP-FLGLLDVALLAVLIGGAAFYFLRSRKKEEEP--TRSYSI
Human   MINMGDSHVDTSSTVSEAVAEEVSLFSMTDMILFSLIVGLLTYWFLFRKKKEEVPEFTKIQTL
                          :*  ::.  *: *:  ::    ::::  .*:   .   :  ::
```

Figure 6.4. CPR membrane domains with hydrophobic residues highlighted

One of the most important amino acid residues in CPR is the C-terminal tryptophan. This residue stacks against the isoalloxazine ring on FAD, and initially shields it from the nicotinamide cofactor. The residue is the focus of a conformational change in the CPR protein, and this conformational change facilitates hydride transfer from NADPH to FAD.

Table 6.4. Conservation of important residues in CPRs (Amino acid numbering is according to AgCPR sequence)

Residue	**Function**	**Conservation**
T91	Hydrogen bonding to FMN phosphate	Conserved
T93	Hydrogen bonding to FMN phosphate	Conserved
T142	Hydrogen bonding to FMN re face	Conserved

Y143	Stacking with FMN re face	Conserved
G144	Hydrogen bonding with FMN re face	Conserved
G146	Hydrogen bonding with FMN re face	Conserved
N178	Hydrogen bonding with FMN si face	Conserved
Y181	Stacking with FMN si face	Conserved
H183	Hydrogen bonding with FMN si face	Conserved
N185	Hydrogen bonding with FMN si face	Conserved
D210, D211, D212	Acidic residues associated with redox partner binding	Conserved
E216, D217, Y218	Acidic residues associated with redox partner binding	D217E in HsCPR, Y218D in all other CPRs
R300	Binding with 5’ phosphate on adenosine ribose moiety of NADPH	Conserved
R456	Hydrogen bonding with FAD si face	Conserved

Y458	Stacking with FAD si face	Conserved
S459	Hydrogen bonding with FAD si face, stabilises semiquinone form of FAD	Conserved
T474	Hydrogen bonding with FAD adenine	T474C in HsCPR
A475	Hydrogen bonding with FAD adenine	Conserved
V476	Hydrogen bonding with FAD adenine	Conserved
Y480	Stacking with FAD adenine	Conserved
V491	Hydrogen bonding with FAD pyrophosphate	Conserved
T493	Hydrogen bonding with FAD pyrophosphate	Conserved
C567	Cofactor recognition at 2' phosphate, allows conformational change for nicotinamide binding	Conserved
R569	Binds NADPH adenosine ribose 5' phosphate	Conserved

K570	Binds NADPH adenosine ribose 5’ phosphate	K570R in HsCPR
S596	Binds NADPH adenosine ribose 2’ phosphate	Conserved
R597	Binds NADPH adenosine ribose 2’ phosphate	Conserved
K602	Binds NADPH adenosine ribose 2’ phosphate	Conserved
Y604	Binds NADPH adenosine ribose 2’ phosphate	Conserved
C631	Promotes hydride transfer via stabilization of the transient carbocation formed upon release of hydride ion	Conserved
D675	Hydrogen bonding network with S459 and C631 – maintains orientation of FAD for hydride transfer, stabilises semiquinone FAD	Conserved
W677	Stacks with FAD re face, changes conformation to allow close proximity between FAD and NADPH	Conserved

	nicotinamide, facilitates initial cofactor binding and hydride transfer	

6.3.5 Spectral analysis of CPRs

The visible absorption spectra for the six expressed CPRs are shown in Figure 6.5. All produced characteristic diflavin reductase spectra with absorption maxima at 379nm and 454nm. Addition of a stoichiometric amount of NADPH produced a characteristic increase in the 500-650nm regions of the spectra indicating formation of an air-stable flavin semiquinone, as has been seen previously in human and insect CPRs [90, 147, 148]. Increases in absorption in the 340nm – 350nm region are associated with NADPH oxidation to $NADP^+$, after the electrons have been stripped of NADPH by the CPR, and passed to the flavin cofactor [148-150].

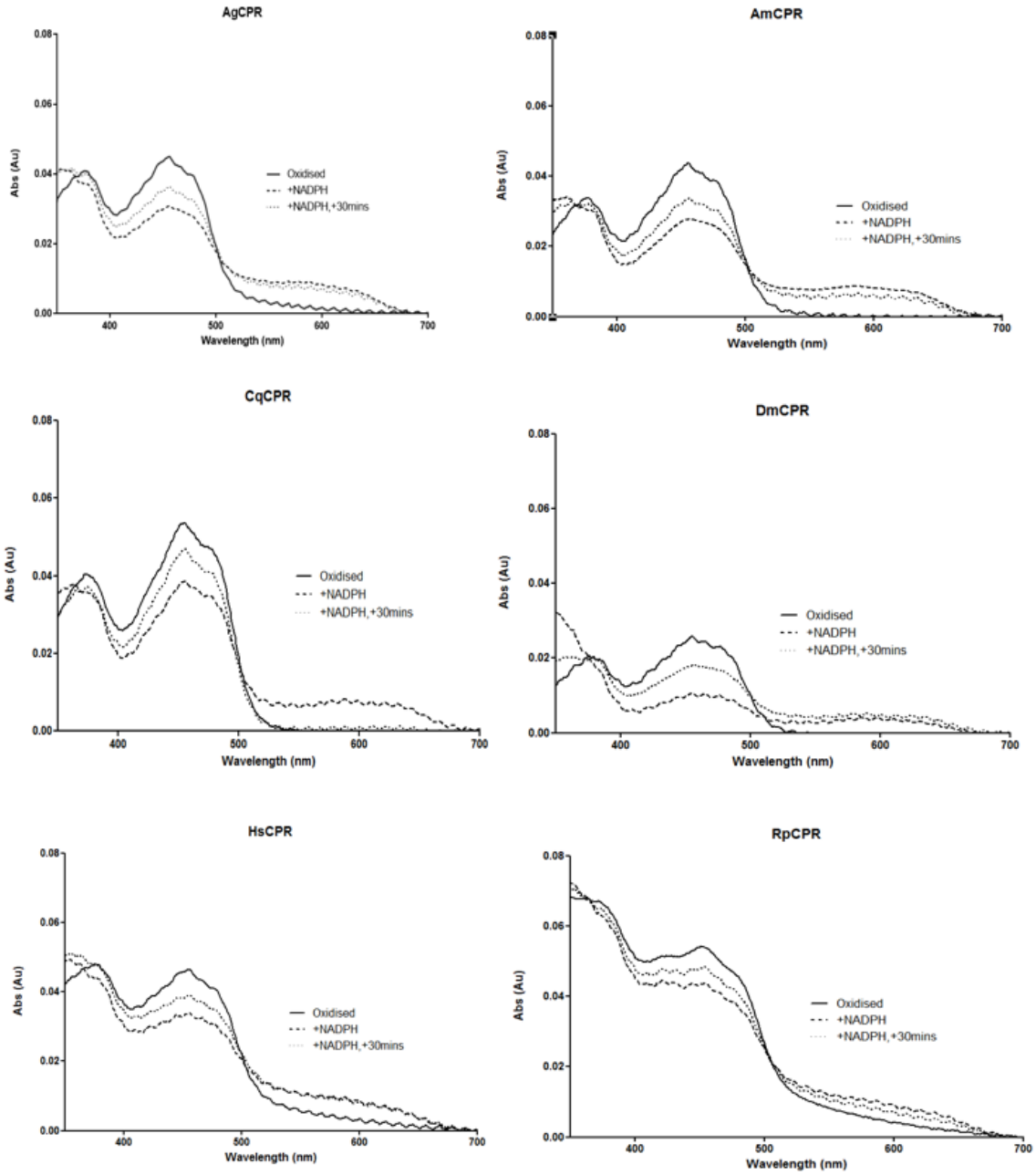

Figure 6.7. Absorption spectra of purified CPRs. Spectra are measured on 1.5 µM enzyme. Traces show the oxidised spectra; the reduced spectra with 1.5 µM NADPH and measured after 10 seconds; and the air-stable semiquinone measured after 30 min.

6.3.6 Cytochrome c kinetics of CPRs

All six of the CPRs catalysed the reduction of cytochrome c following Michaelis-Menten kinetics with respect to cytochrome c concentration. The V_{max}, K_M and K_{cat} values are shown in Figure 6.8 and Table 6.5. The HsCPR K_M for cytochrome c was the lowest; the insect CPRs having 2-7 fold greater K_M values. Amongst the insect K_M values, AgCPR had the lowest K_M, and DmCPR had the highest value.

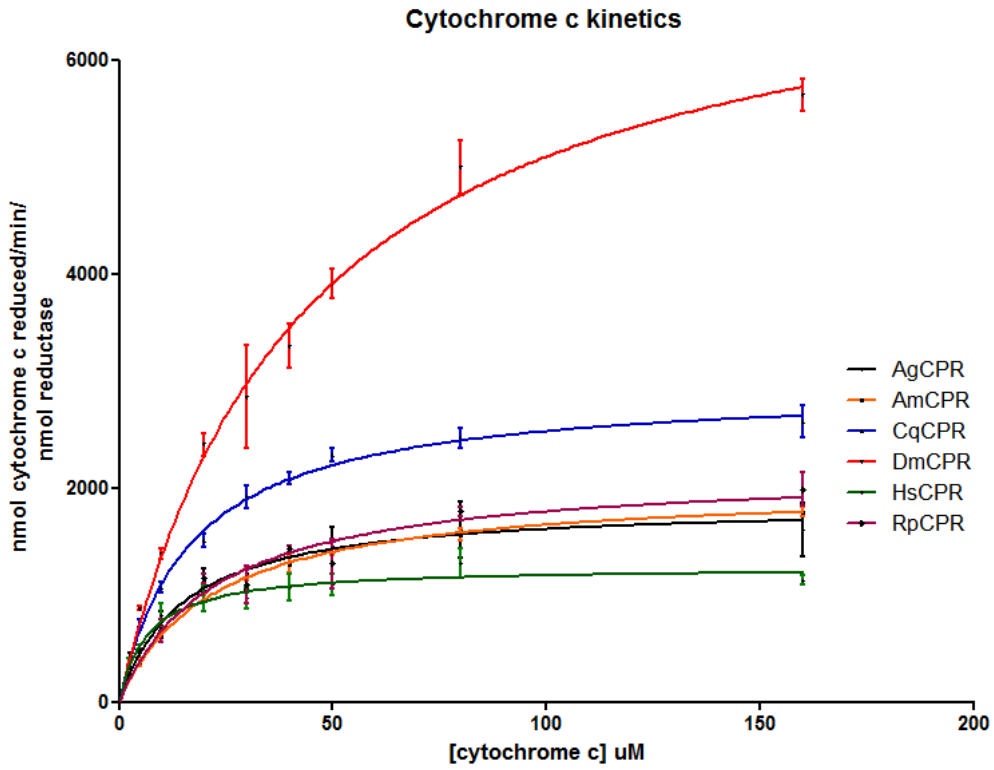

Figure 6.8. Initial reaction rates for CPRs at different concentrations of cytochrome c

Table 6.5. Catalytic parameters for CPRs with respect to cytochrome c concentration

Enzyme	AgCPR	AmCPR	CqCPR	DmCPR	HsCPR	RpCPR
V_{max} (nmol cytochrome c reduced/min/nmol)	1857 (+/- 125)	2019 (+/- 58)	2954 (+/- 79)	7315 (+/- 370)	1262 (+/- 63)	2181 (+/- 151)
$K_{M(\mu M)}$	14.74 (+/- 3.44)	21.75 (+/- 1.87)	16.57 (+/- 1.47)	43.32 (+/- 5.10)	6.63 (+/- 1.52)	22.35 (+/- 4.56)
K_{cat} (s^{-1})	8.42	9.15	13.39	33.16	5.72	9.89

Table 6.6. Catalytic parameters for CPRs with respect to NADPH concentration

Enzyme	AgCPR	AmCPR	CqCPR	DmCPR	HsCPR	RpCPR
V_{max} (nmol cytochrome c reduced/min/nmol)	4123 (+/- 107)	2243 (+/- 85)	3716 (+/- 215)	10559 (+/- 433)	1354 (+/- 56)	2214 (+/- 99)
K_{M} (µM)	12.73 (+/- 1.2)	20.97 (+/- 2.43)	34.17 (+/- 5.03)	30.68 (+/- 3.32)	3.68 (+/- 0.84)	24.98 (+/- 3.17)
K_{cat} (s^{-1})	8.4	9.2	13.4	30.1	5.7	9.9

6.3.7 NADPH kinetics of CPRs

All six of the CPRs catalysed the reduction of cytochrome c following Michaelis-Menten kinetics with respect to NADPH concentration. The V_{max}, K_M and K_{cat} values are shown in Figure 6.8 and Table 6.6. Following a similar trend to the K_M values with respect to cytochrome c, the HsCPR K_M for NADPH was the lowest, and the insect CPRs had 3-8 fold greater K_M values. Amongst the insect K_M values, AgCPR had the lowest K_M, and DmCPR had the highest value.

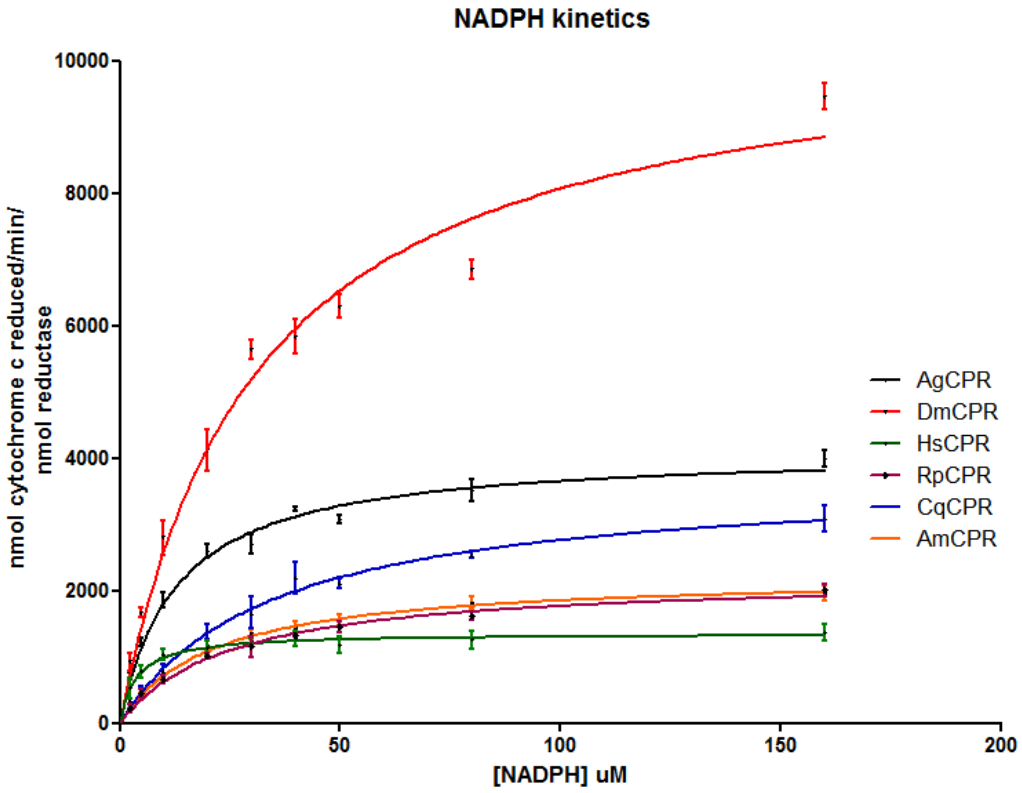

Figure 6.8. Initial reaction rates for CPRs at different concentrations of NADPH

6.3.8 *In vitro* Inhibition of CPRs

In order to investigate differences in inhibition characteristics between the insect and mammal CPRs, four CPR inhibitors were used [90]. Three of these inhibitors, 2'5' ADP, 5' AMP, and $NADP^+$, (see Figure 6.10) are nucleotide analogues of NADPH, which act as competitive inhibitors; binding at the NADPH binding domain [148, 151]. The fourth, DPIC (Figure 6.11), is an irreversible CPR inhibitor, which is thought to mediate inhibition *via* an NADPH dependent mechanism which results in a covalent modification of FMN (Figure 6.12 full mechanism in figure caption) [152].[152]

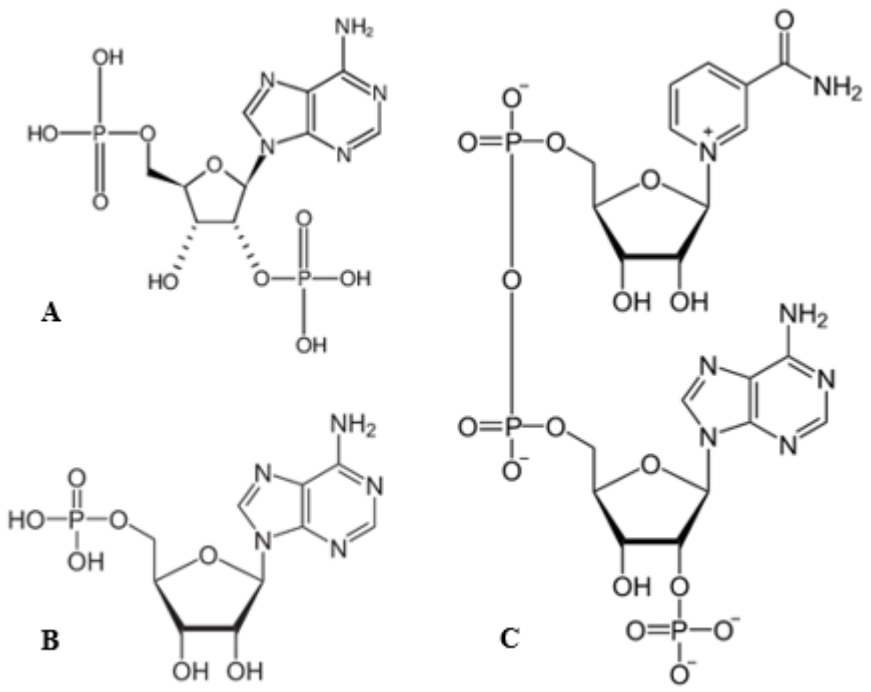

Figure 6.10 – Structures of nucleotide analogue inhibitors of CPRs A – 2’5 adenine diphosphate (2’5’ ADP), B – 5’ adenine monophosphate (5’ AMP), C – nicotinamide adenine dinucleotide phosphate, reduced form ($NADP^+$)

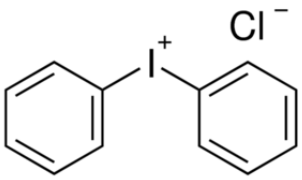

Figure 6.11 – Structure of diphenyliodonium chloride (DPIC) A non-competitive inhibitor of CPRs

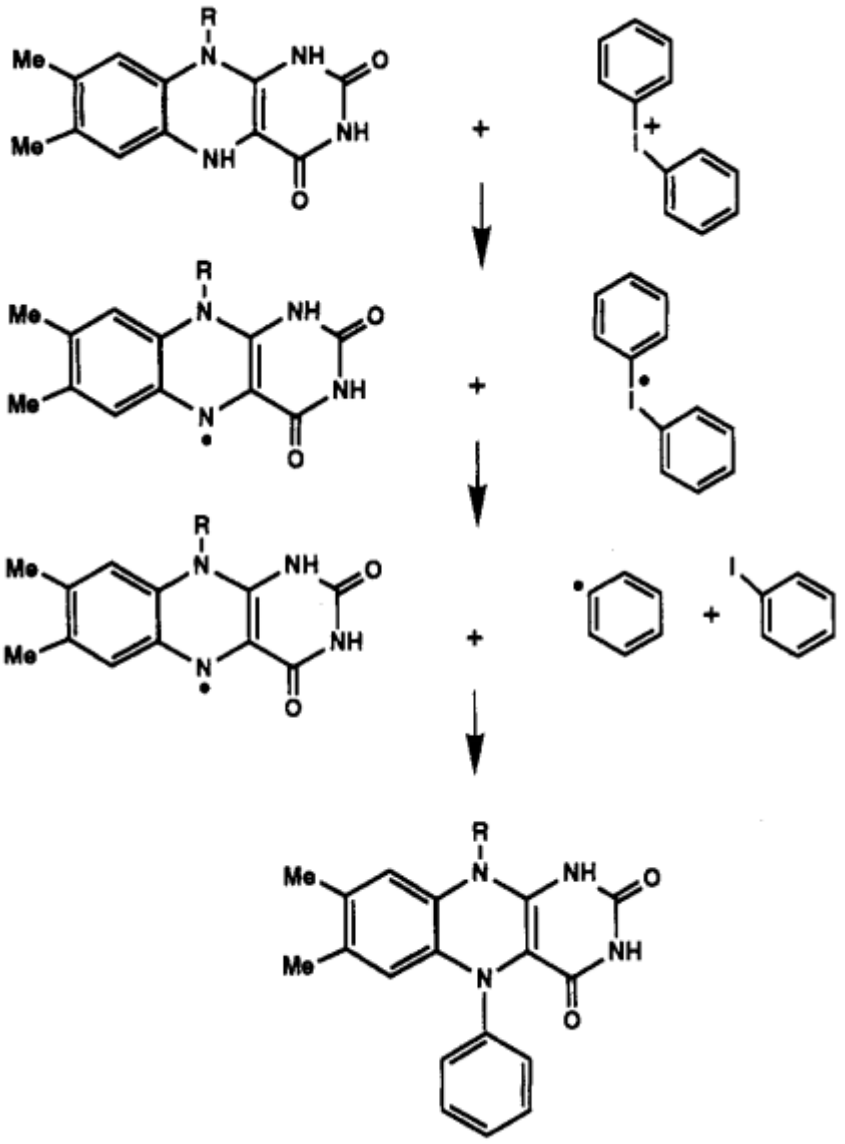

Figure 6.12 – Mechanism of DPIC mediated inhibition of CPR *via* covalent modification of FMN

This mechanism starts with fully reduced enzyme and DPIC. One electron is then transferred from DPIC to the fully reduced FMN, giving a flavin semiquinone and a diphenyliodonium radical. This diphenyliodonium radical then fragments into a phenyl radical and iodobenzene. The phenyl radical can now recombine with the flavin semiquinone, which results in an aromatic group being covalently, and irreversibly attached to the isoalloxazine of FMN [152].

All six CPRs were inhibited by all four inhibitory compounds to varying extents (Figures 6.12-6.17) IC_{50} values are shown in Tables 5.6 and 5.7 and are defined as being the concentration of inhibitor at which activity of the enzyme is reduced by 50% [148].

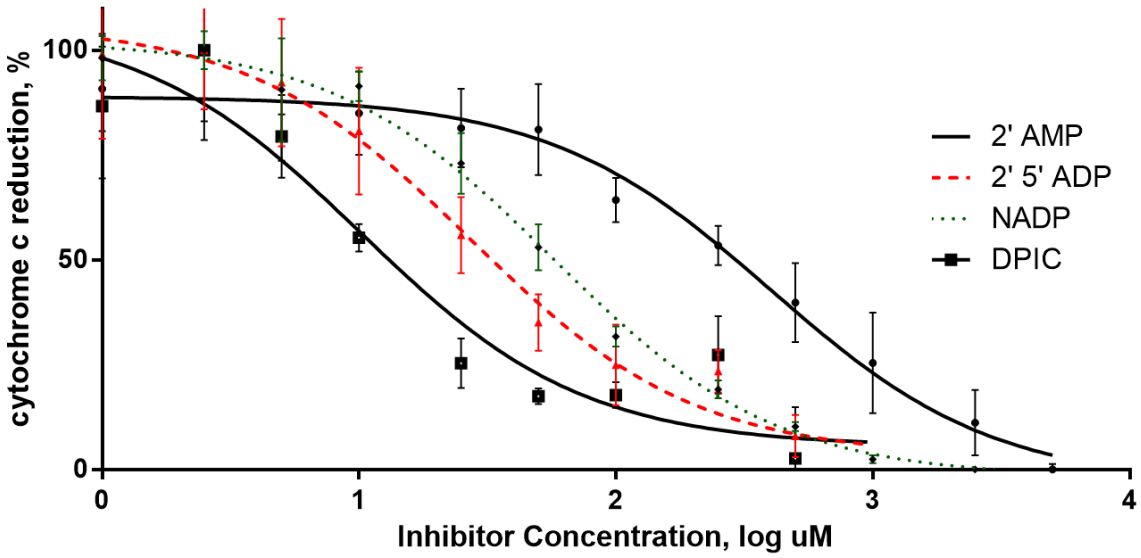

Figure 6.12 IC_{50} curves for AgCPR with CPR inhibitors

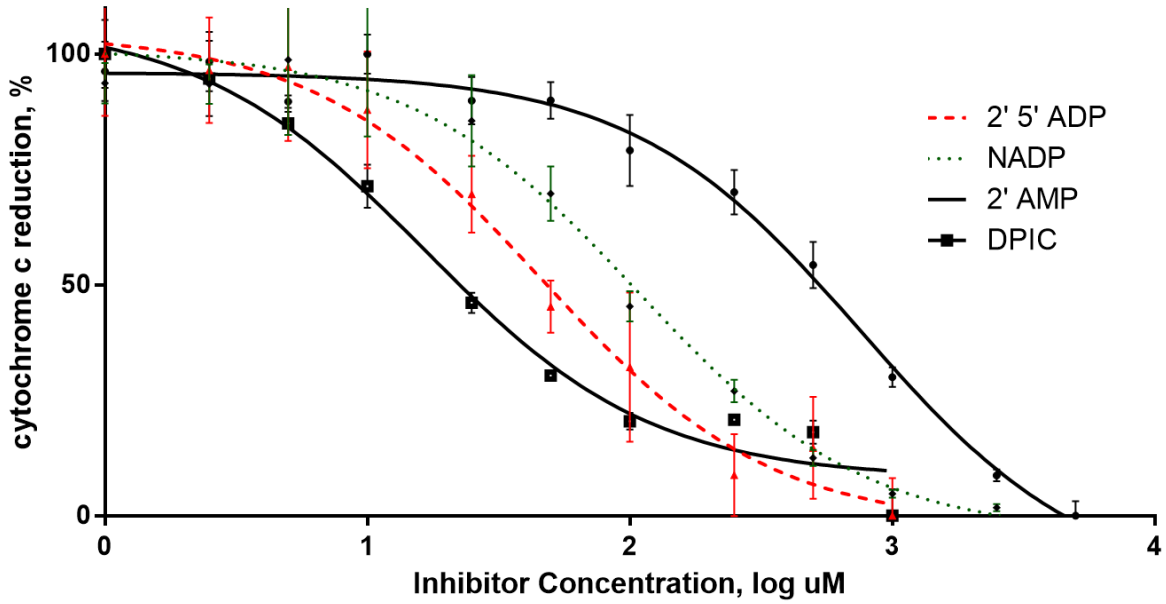

Figure 6.13. IC_{50} curves for AmCPR with CPR inhibitors

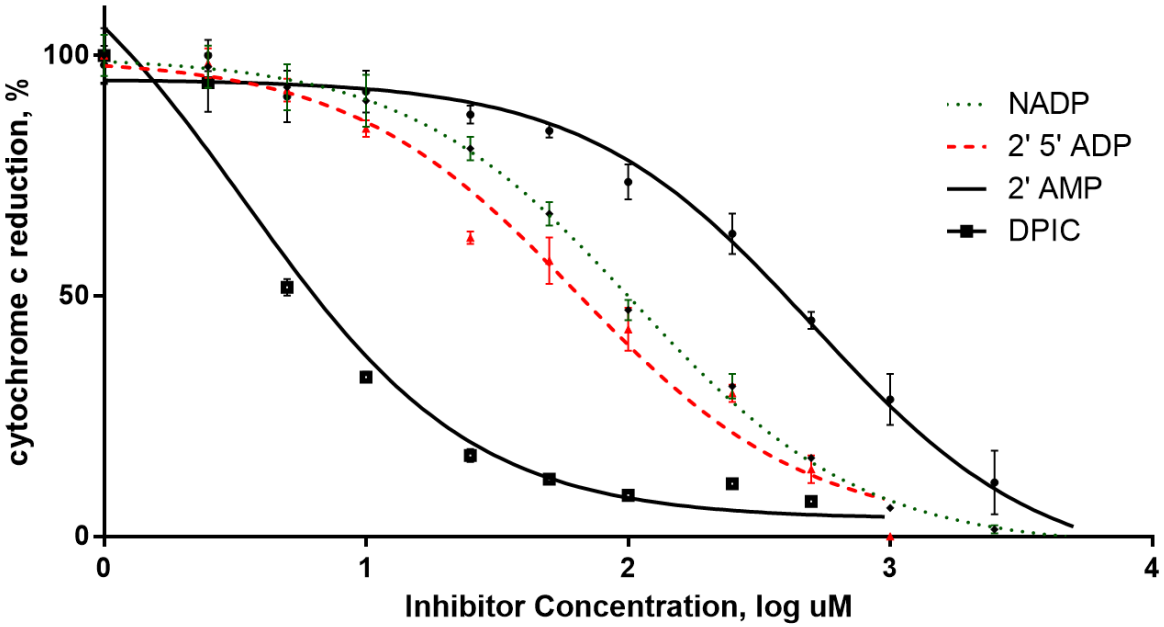

Figure 6.14. IC_{50} curves for CqCPR with CPR inhibitors

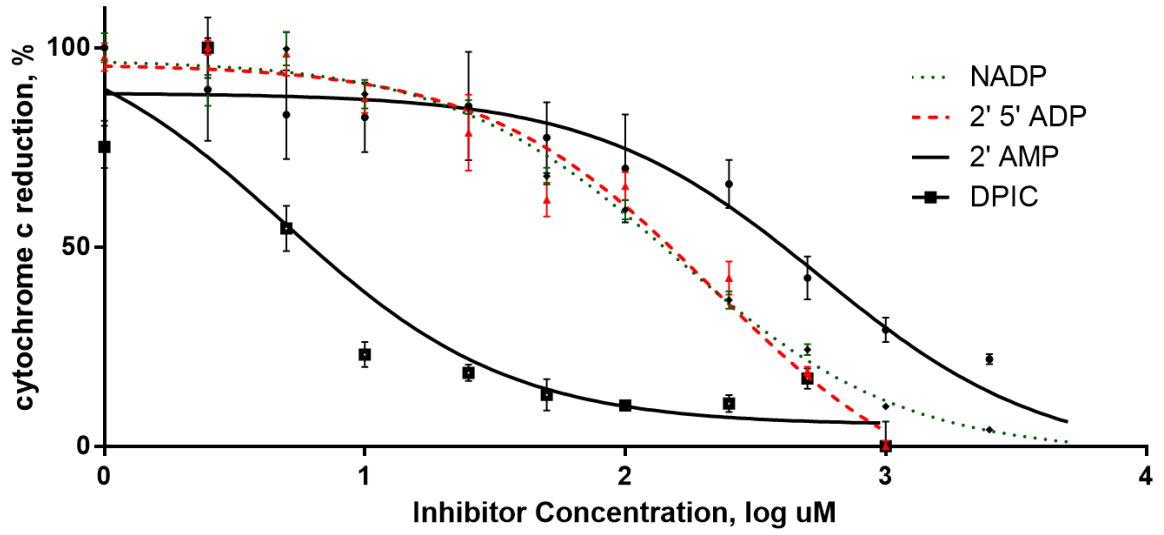

Figure 6.15. IC_{50} curves for DmCPR with CPR inhibitors

Table 6.7 IC_{50} values for CPRs with CPR inhibitors

Inhibitor	AgCPR		AmCPR		CqCPR		DmCPR		HsCPR		RpCPR	
	IC_{50} (μM)	log IC_{50} (μM)	IC_{50} (μM)	log IC_{50} (μM)	IC_{50} (μM)	log IC_{50} (μM)	IC_{50} (μM)	log IC_{50} (μM)	IC_{50} (μM)	log IC_{50} (μM)	IC_{50} (μM)	log IC_{50} (μM)
2' AMP	402.2	2.60 (+/- 0.17)	760.5	2.88 (+/- 0.08)	507.6	2.71 (+/- 0.07)	557.6	2.75 (+/- 0.18)	301.2	2.48 (+/- 0.09)	614.4	2.79 (+/- 0.10)
2' 5' ADP	27.4	1.44 (+/- 0.17)	46.4	1.67 (+/- 0.17)	64.1	1.81 (+/- 0.07)	214.6	2.33 (+/- 0.11)	6.6	0.82 (+/- 0.10)	56.6	1.75 (+/- 0.07)
$NADP^+$	57.1	1.76 (+/- 0.06)	107.8	2.03 (+/- 0.11)	105.1	2.02 (+/- 0.04)	155.1	2.19 (+/- 0.05)	40.2	1.61 (+/- 0.05)	112.3	2.05 (+/- 0.03)
DPIC	10.2	1.01 (+/- 0.21)	16.5	1.21 (+/- 0.09)	3.5	0.54 (+/- 0.09)	4.9	0.69 (+/- 0.19)	61.0	1.79 (+/- 0.17)	7.1	0.85 (+/- 0.16)

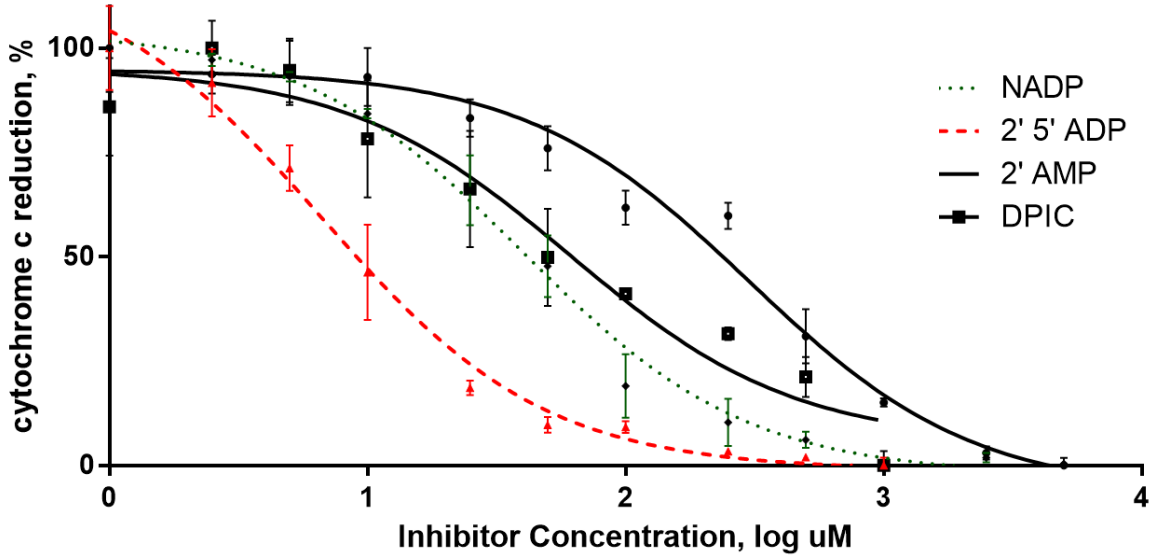

Figure 6.16. IC_{50} curves for HsCPR with CPR inhibitors

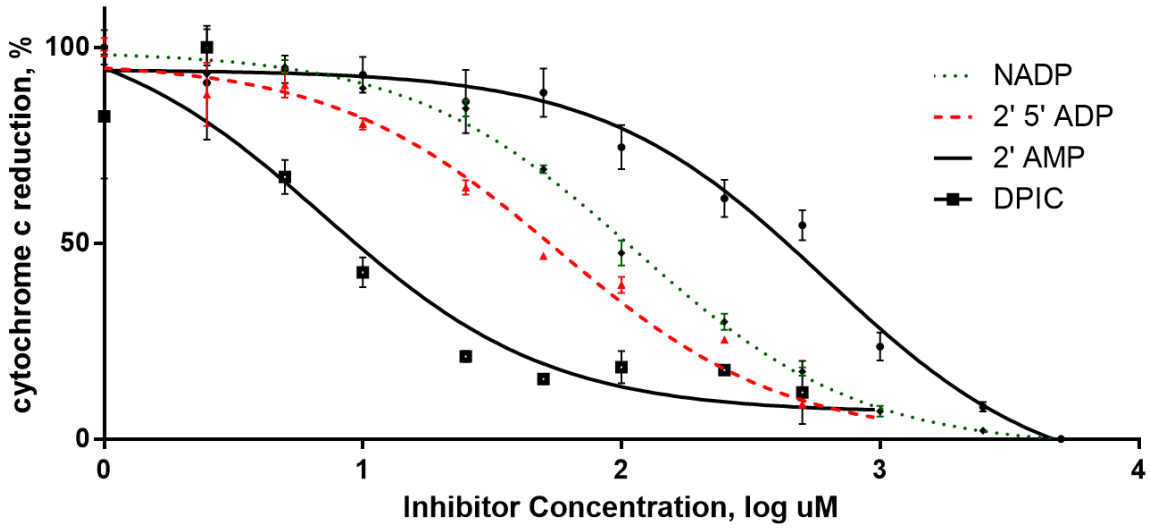

Figure 6.17. IC_{50} curves for RpCPR with CPR inhibitors

Of the competitive nucleotide analogues, 2' AMP was the inhibitor to which all of the CPRs tested were least sensitive, with IC_{50} values ranging from 301 to 760 μM. The nucleotide to which the CPRs were most sensitive was 2'5' ADP, with IC_{50} values ranging from 6 to 214 μM. DmCPR, however, is an exception to this trend, and is more sensitive to $NADP^+$ than 2'5'

ADP (155.1 μM for $NADP^+$ and 214.6 μM for 2'5' ADP). These data collectively differ from the previously found trend for AgCPR where $NADP^+$ is the stronger nucleotide analogue inhibitor [90].

Between the CPRs, there was least difference in sensitivity to 2' AMP. HsCPR and AgCPR were most readily inhibited, and the IC_{50} value found for HsCPR (301.2 μM) was less than half that of AmCPR (760.5μM) and RpCPR (614.4μM).

With respect to $NADP^+$, HsCPR was most sensitive; the IC_{50} (40.2μM) was 2 fold lower than all insect CPRs apart from AgCPR, which had a similar IC_{50} value of 57.1μM and DmCPR (155.1μM), where was the IC_{50} was three fold lower.

2'5' ADP produced the strongest inhibition in all CPRs apart from DmCPR. HsCPR was again, the most sensitive. The IC_{50} value for HsCPR (6.6μM) was four times lower than AgCPR (27.4μM), over 30 times lower than DmCPR (214.6μM), and 7-10 times lower than the other CPRs (46.4 - 64.1μM).

Finally, DPIC is the only inhibitor for which HsCPR is least sensitive. The IC_{50} of HsCPR for DPIC is 61.0 μM, which is 4-20 times higher than the insect IC_{50} values (3.5 – 16.5μM). The sensitivity of insect CPRs to DPIC is also noteworthy in that these values are very low in comparison with nucleotide inhibitors. In CqCPR and DmCPR, the IC_{50} for DPIC is 20 – 30 times lower than the most inhibitory nucleotide.

6.4 Discussion

Cytochrome P450 reductase is the obligate redox partner for endoplasmic cytochromes P450s and haem oxygenase. Thus CPR is an attractive synergist target, because blocking CPR activity would essentially block the activity of both P450s and the HO system [153, 154]. HsCPR and AgCPR have previously been observed to have differences with respect to nucleotide binding, specifically, AgCPR has been observed to have 10 fold weaker binding with 2'5' ADP than HsCPR [90]. This chapter aims to explore whether these differences extend to other insect CPRs, and whether there is any evidence to suggest that there are any differences in activity related with a bloodfeeding habit. In order to examine these questions, CPRs from six different organisms were cloned and expressed. These included three haematophagous insects from two distinct orders (*An. gambiae* and *C. quinquefasciatus* from Diptera, and *R. prolixus* from Hemiptera), two non-haematophagous insects from separate orders, (*A. mellifera* from Hymenoptera, and *D. melanogaster* from Diptera) and one mammal (*H. sapiens*). Two other CPRs were trialled, but their expression was unsuccessful (*Ae. aegypti* and *G. morsitans*).

This study provides the first direct comparison of a range of different insect CPRs with human CPR. Expression of soluble recombinant enzymes have allowed for experimental observations of kinetic parameters of CPRs and to analyse their inhibition by competitive and non-competitive inhibitors. These assays were conducted using the cytochrome c reductase assay; cytochrome c reductase is an artificial electron acceptor that produces a change in absorbance at 550nm associated with a distinct colour change upon reduction.

The V_{max} values had a similar trend in each kinetic analysis, regardless of whether or not the NADPH or cytochrome c concentration was being altered. In both of these kinetic experiments, the HsCPR had the lowest V_{max}, the three haematophagous insect CPRs and AmCPR all had similar V_{max} values. Of note is AgCPR, which had a higher V_{max}^{NADPH} than four of the other CPRs, whereas its $V_{max}^{cyt\ c}$ was only higher than that of HsCPR. DmCPR is a

huge outlier with respect to its V_{max} values. It's V_{max} with respect to both substrates is more than double that of the other CPRs, and it's V_{max}^{NADPH} is approximately an order of magnitude greater than that of HsCPR.

In terms of K_M, again, HsCPR had the lowest values in each kinetic analysis. The $K_M^{cyt\ c}$ values have exactly the same trend as the $V_{max}^{cyt\ c}$ values, with the non-haematophagous and AmCPR having similar kinetic parameters, and the DmCPR having a markedly higher value. The K_M^{NADPH} values are not so straightforward, and there is not so obvious a trend. With the exception of the fact that the K_M^{NADPH} for CqCPR and DmCPR is a full order of magnitude higher than that of HsCPR, the K_M^{NADPH} values are similar, and do not follow the same trend as the V_{max}^{NADPH} values.

When comparing the CPRs, particularly of note was DmCPR, which was revealed to have a much higher maximum velocity than the other CPRs studied (10 fold in some cases), both with respect to NADPH and cytochrome c. Of interest is the fact that K_M, which has a strong association with tightness of binding (i.e. the higher the K_M value, the looser the binding, generally speaking), is lower in those CPRs with lower V_{max} values, implying that those enzymes with a lower maximum reaction velocity have a tighter bind to their substrates. In terms of the NADPH binding, this possibility has previously been considered [151]. The conformational change induced by NADPH binding acts upon the C terminal tryptophan present in all characterised CPRs. Upon NADPH binding, the protein confirmation alters such that the tryptophan moves from its inactive position in which it is shielding the isoalloxazine ring on FAD, facilitating hydride transfer from NADPH to FAD. It has previously been considered that looser NADPH binding might allow for quicker conformational changes and hence quicker hydride transfer and $NADP^+$ clearance [151].

However, as the $K_{M\ cyt\ c}$ values also generally increased alongside an increase in $V_{max\ cyt\ c}$, it must be considered that the loose nucleotide binding pocket hypothesis may not be relevant to this discussion. This is partially corroborated by the fact that the trends are not perfect, for instance, the $K_{M\ NADPH}$ for AgCPR is the second lowest, whereas its $V_{max\ NADPH}$ is the second highest. Other explanations for increased V_{max} values independent of a trend in K_M include more thermodynamically favourable configurations for hydride transfer across the two flavin cofactors. Accurate crystal structures would provide more of an insight into how valid this hypothesis is. Although since hydride transfer from NADPH for FAD has been found to be the rate limiting step in previously studied CPRs, I would suggest that the FAD positioning relative to the C terminal tryptophan is more important. The documented Bi-Bi kinetic mechanism for CPRs and the distinct cytochrome c and NADPH binding sites [86] suggest that the K_M values for each substrate do not experimentally confound one another.

Results showed that all of the insect CPRs had weaker binding for nucleotide analogue inhibitors than HsCPR. Inhibition by 2'5' ADP was between 4 and 32 fold higher in HsCPR than the insect CPRs. Likewise, $NADP^+$ and 2' AMP inhibition was strongest in HsCPR. Variation in nucleotide inhibition amongst the insect CPRs does not follow a trend associated with bloodfeeding. DPIC inhibition is weaker in human CPR than in insect CPRs, but does not follow a trend associated with haematophagy. Overall, the CPRs examined showed variable activities, but none to suggest a viable species selective target, though the DPIC mode of action (covalent modification of FMN) is more inhibitory to insect CPRs than to humans.

Chapter 7 – General Discussion

This study has explored in depth, what was, until now, a hypothetical haem oxygenase in *Anopheles gambiae*. Recombinant AgHO has been cloned, expressed, and used in biochemical assays to verify that it is a canonical haem oxygenase enzyme which catabolises haem into biliverdin. The *in vivo* role of AgHO was examined using an inhibition bioassay. This bioassay revealed a key role in insect physiology in that haem oxygenase inhibition led to a marked decrease in oviposition. This study also biochemically compared the cytochrome P450 reductases of humans and five insects, and found that there were no significant enzymatic differences between the CPRs of haematophagous and non-haematophagous insects.

7.1 Introduction

Malaria is the most important disease in the world, and of its numerous anopheline vectors, *An. gambiae* is the most important because of its wide sub-Saharan distribution, its developing insecticide resistance, and its propensity to spread the most frequently lethal strain of malaria, *Plasmodium falciparum*. Because of its importance, *An. gambiae* is the best organism to study novel targets for insecticides for vector control. Lessons learned from such study of *An. gambiae* can be directly applied to malaria control, and inform strategies for the control of other vectors.

The mosquito bloodmeal is of clear importance. From the point of view of the mosquito life cycle, the bloodmeal is a necessity for egg development and production of progeny. Disease transmission occurs through the bloodmeal also, therefore it has great potential to be a vector control target. Indeed, even outside of vector control, transmission-blocking or “altruistic” vaccines directly rely on the bloodmeal for their effect [155, 156].

As explained in the introductory chapter, haem detoxification methods are a key adaptation of haematophagous insects to survive the threat of massive oxidative stress posed by haem. Of these adaptations, enzymatic degradation by haem oxygenase remains the least well characterised. Addressing this point, and establishing whether or not this haem degradation system could be a viable target for insecticides is the purpose of this thesis.

7.2 *In silico* investigation of AgHO

The high levels of amino acid identity and similarity between AgHO and other HOs indicates that the enzymes are homologous to one another, and these haem oxygenase enzymes share evolutionary history. The extent of this homology and conservation suggest that the HO enzyme is of vital physiological importance, not only to haematophages.

The most highly conserved amino acids of the haem oxygenase protein are those in the enzyme active site, and those which are involved with CPR docking. When comparing known key amino acid residues between AgHO and human HO-1, it is clear that most residues have semi-conservative mutation, conservative mutation or are non-divergent. 4 residues are divergent, two of which are involved with haem binding (somewhat on the periphery of the active site) and two are involved with CPR binding.

Creation of a structural homology model of AgHO reinforces its similarity to HO-1. In essence, the haem oxygenase enzyme in both cases is a binding pocket made up of two α-helices which contain positively charged amino acids which perform two main functions: substrate recognition and orientation, and docking with the FMN domain on CPR.

7.3 Expression of recombinant AgHO

Expression of recombinant AgHO was initially difficult. Of a range of nine successfully cloned AgHO constructs of varying length, only one yielded soluble protein. Heterologous expression of eukaryotic proteins in bacterial systems often leads to insoluble protein products, due to dissimilar expression machinery and potential for formation of inclusion bodies and aggregates [157].

One clone of AgHOΔ31 was used to successfully express soluble enzyme, and unsurprisingly, this construct was the one most similar to previously expressed HOs [76, 80]. This soluble protein was however, catalytically inactive. This is unexpected, considering that previously expressed proteins which were truncated in a similar way were catalytically active. Examination of the structural model shows that the polypeptide removed from the enzyme in the expressing clone extended into an α-helix which appears to be part of the main enzyme unit, as opposed to simply part of an external transmembrane region. 1D-NMR spectroscopy provided confirmation that the AgHOΔ31 was misfolded. This explains the lack of catalytic activity, and the source of this misfolding is most likely due to the truncation being too large.

In order to overcome the difficulties in enzyme expression, a codon-optimised, full length AgHO gene was synthesised. The codon optimisation coupled with the lack of truncation allowed for the successful expression of a catalytically active haem oxygenase enzyme.

7.4 Identification of AgHO reaction products

A series of biochemical tests have been used to prove that AgHO is a canonical haem oxygenase. Haem oxygenases are defined as those enzyme which catabolise molecular haem with the addition of oxygen. The products of this reaction are biliverdin, ferrous iron and carbon monoxide. NADPH is used as a reducing equivalent, and is converted to $NADP^+$ over the

course of this reaction. In order to state that AgHO is a true haem oxygenase, each of these reaction products was identified in turn.

Biliverdin was identified using a straightforward absorption spectroscopy assay. AgHO and a CPR were incubated with NADPH and haem and monitored spectroscopically. Over time, the haem Soret peak was reduced, indicating the breakdown of haem, and a broad peak at 680nm was seen. This broad 680nm peak is characteristic of biliverdin. At the same time, the absorbance at 340nm was seen to be reducing, indicating that NADPH was being converted into NADP.

When haemoproteins bind to carbon monoxide, their absorption spectra change due to changes in electron spin in the haem molecule. This phenomenon was used to examine the production of carbon monoxide by the haem oxygenase reaction. Myoglobin, which is otherwise inert in this reaction system, was added to the haem oxygenase reaction and monitored spectroscopically. Movement of the myoglobin Soret peak to a higher wavelength confirmed the presence of carbon monoxide.

Lastly, ferrozine was used to observe the liberation of ferrous iron over the course of the haem oxygenase reaction. Ferrozine is an organic molecule which acts as a bidentate ligand for certain metal ions, among them, ferrous iron [129]. As it binds metal ions, ferrozine produces a magenta coloured complex, which corresponds with a distinct change in absorption at 562nm. Application of ferrozine to the AgHO assay produced evidence that ferrous iron is released over the course of the reaction.

Ascorbic acid was not used as an artificial reducing agent as it has been in previous HO characterisations [76], instead CPRs were used. Where ascorbate was used previously, a truncated CPR (DmΔCPR) and a truncated HO (DmΔHO) was used initially, and there was little activity. The data in Chapter 4 show that AgHO is compatible with full-length HsCPR

and MdCPR, however less catalytically active when an AgCPR with N-terminal truncation. Together, these findings suggest that the hydrophobic tail regions are key to efficient docking between insect HOs and CPRs. As my study had successful CPR mediated electron transfer, ascorbate was unnecessary.

7.5 Estimation of AgHO optima

The ferrozine assay proved to be the most reliable and repeatable assay due to its distinct absorption maximum. For this reason, it was used to estimate pH and temperature optima for the AgHO reaction.

The pH optimum was found to be close to pH 7.5, which makes perfect sense. Both cytoplasmic and blood pHs are approximately pH 7.4. Activity dropped off rapidly at pH 9, to an extent which suggested enzyme denaturation. The temperature optimum was a very interesting case, being found to be approximately 27.5^{o}C. It is interesting, as this matches previously found data which suggest that the ideal resting temperature, post-bloodmeal is 26-28^{o}C [158].

One of the most valuable insights taken from this part of the study is the application of the Ferrozine assay to haem oxygenase research. The fact that the Fe^{2+}-Ferrozine complex has a constant rate of formation and a known extinction coefficient means that this assay can be used to reliably compare the activities of different haem oxygenases.

With some thought, a ferrozine based assay could be designed to probe the effects of haem oxygenase inhibition by the protoporphyrin inhibitors employed in Chapter 6. One of the problems with assaying these inhibitors is that they have their own absorption profiles which obscure interpretation of the AgHO-haem Soret peak. Also, the standard assay uses an AgHO-haem complex rather than incubating free haem with the enzyme. This is, again, because of

difficulties in interpreting the Soret peak, in this case when AgHO binds haem. Employing ferrozine should avoid these problems.

7.6 The *in vivo* role of AgHO and viability of AgHO as an insecticide target

This project has also involved the development of an AgHO inhibition bioassay, largely based on previous work conducted in the American trypanosomiasis vector, *R. prolixus* [100]. This study differs from the *R. prolixus* study in that here, numerous methods of inhibitor application have been trialled. Application of free protoporphyrin has been seen to be the most reliable and cheapest method of inhibiting haem oxygenase *in vivo*. Another advantage over the *R. prolixus* study is that application of free protoporphyrin gives a clearer insight into the phenotype of an HO-inhibitory insecticide.

This project has found that SnPP and ZnPP being applied in the bloodmeal has an inhibitory effect on oviposition in the mosquito. The exact mode of action is still obscure, but candidates include inhibition of carbon monoxide signalling, lack of nutrients for oogenesis and poor fitness due to oxidative stress. Similarly to the *R. prolixus* study, no effects on mortality were observed. This is likely due to other strategies to ameliorate haem mediated toxicity, such as formation of aggregates or binding proteins, or it could simply be that the dose was not high enough to mediate insect death. Application of a CuPP control showed that the inhibitory effects of the protoporphyrins were on haem oxygenase, rather than other enzyme systems.

Gene knockdown via RNAi would give an additional insight into the *in vivo* role of haem oxygenase, and this is a clear next step for HO research in *Anopheles.* It would have the advantage of eliminating background fitness effects, although the CuPP control to an extent showed the "background" of protoporphyrin application. Again, using these inhibitors in an *in*

vitro AgHO assay would conclusively prove that AgHO inhibition is the mode of action of these compounds in inhibiting oviposition.

A potential advantage of this approach surrounds the relationship between midgut haem and parasites. A focus of this project is the toxicity of haem, so it is significant that it is not only vector species that are vulnerable to haem toxicity, but so are the parasites the vectors transmit. There is strong evidence that haem mediates cell lysis in *Trypanosoma brucei* [159], *Plasmodium berghei* [160] and *P. falciparum* [161]. Inhibition of vector HO may well increase midgut haem concentrations, which might contribute to vector refractoriness by making the midgut a more toxic milieu.

There are potential hurdles to the field use of these inhibitors; they would not be selective to vector species, and would potentially be toxic to other organisms. A method of introducing these inhibitors to vector diet without risking leaking into the environment would have to be devised. These inhibitors are also expensive, and are not very water soluble. The best application for these inhibitors may be a proof of principle for the vector control potential of HO inhibition. An *in silico* approach to rational insecticide design could take over to find a more field suitable HO inhibiting insecticide.

Another potential means of inhibiting AgHO as part of a vector control strategy could be the use of altruistic vaccines. Chapter 3 showed that inactivated AgHO can successfully be used to generate antibodies, and hence an immune response. If these antibodies bind in a position on the enzyme such that they block haem entering the active site, or block AgCPR docking, then AgHO could be a viable altruistic vaccine target. Caution must be taken to ensure that the immune response is not cross-reactive with any of the human HOs, however α-AgHO antibodies have been shown to not have cross-reactivity with GmHO (G. P. G. de Lima,

personal communication), so provided the right AgHO epitopes are used, this should not be a problem.

7.7 Comparison of CPR activities and inhibition profiles

High-throughput expression screening allowed for comparison of six CPRs from a range of organisms: three haematophagous insects, two herbivorous insects and humans. The initial hypothesis in advance of this study was that there are key differences in haematophage CPRs related to their blood feeding habit. This hypothesis was based on previous findings which showed different inhibitor binding profiles between human and *An. gambiae* CPRs [90].

The hypothesis was not found to be true however. Firstly, kinetic assays were performed on the CPRs, with respect to both cytochrome c and NADPH. In terms of V_{max} and K_M parameters, the insect CPRs are somewhat distinct from HsCPR, but there is no clear divergence in activity based on haematophagy. *D. melanogaster* CPR is massively different to the other CPRs, having markedly higher parameters relating to a higher activity.

Four inhibitors were used to obtain IC_{50} values for each CPR: NADP, 2'5' ADP, 2' AMP and DPIC. 2'5' ADP was the inhibitor which had previously been found to have a different inhibitory profile in humans and mosquitoes [90], and a difference in sensitivity was found here also. Again however, the difference was clearer between humans and insects, rather it being a trait restricted to haematophages.

One of the more compelling features of this study is that HsCPR is not particularly sensitive to DPIC, whereas all the insect CPRs are. This finding suggests that the mode of CPR inhibition performed by DPIC (that is covalent binding to FMN, rather than active site competition as with the nucleotide analogues) could be an avenue of future research for insecticides or insecticide synergists.

7.8 Conclusion and perspectives

Drawing from the conclusions found during this study, the following conclusions can be made: (i) the AgHO gene codes for an haem oxygenase enzyme which catalyses the degradation of free haem into biliverdin, carbon monoxide and ferrous iron; (ii) AgHO inhibition in vivo results in decreased oviposition and therefore has potential as an insecticide or synergist target; (iii) there is no association between activity or nucleotide binding characteristics of CPR enzymes and a blood feeding habit, and there is nothing to suggest that there is a viable species selective target.

The results gathered in this project do not go as far as to present AgHO inhibition as a viable insecticide target as yet. There are numerous avenues that can be pursued to achieve a more holistic understanding of AgHO using both *in vitro* and *in vivo* approaches. Crystallisation of AgHO would be of great utility to make more concrete conclusions on the structure of AgHO. The structure would also allow for more detailed comparison with the other crystallised haem oxygenases and would provide a template for rational insecticide design. The expense to produce and light sensitivity of the haem analogues used in Chapter 5 indicate poor suitability for IRS or LLINs. It is unknown whether these compounds would work when not directly ingested, and there are potential issues with lack of species specificity. These difficulties with protoporphyrins suggest that other compounds which target haem oxygenases need to be designed and trialled. The histidine in the haem oxygenase binding site suggests that an imidazole derivative may hold promise. Any likely insecticide candidate would have to then have its target product profile thoroughly tested to ensure suitability for use in the field.

Alongside crystallisation, other potential areas of biochemical characterisation would be to validate the importance of important amino acid residues (such as the histidine mentioned above) involved in propionate binding, Fe^{2+} coordination and CPR docking by using site directed mutagenesis. Also, as mentioned above, *in vitro* validation of the use of α-AgHO

antibodies and whether or not they block the access of haem to the active site, or CPR docking would be a proof of principle approach to an altruistic AgHO vaccine.

Another future research perspective would be to isolate and identify the biliverdin produced by AgHO *in vitro*, and to examine whether the AgBV produced *in vivo* has any pre- or post-hydrolysis modifications as in *R. prolixus* [77] and *Ae. aegypti* [78], and whether the biliverdin produced is exclusively BV-IXα. One option for further study of AgHO inhibition *in vivo* would be to compare the amounts of biliverdin produced by the mosquito when subjected to AgHO inhibition by protoporphyrin analogues. This would provide evidence of the extent of AgHO inhibition. Likewise, analysis of oxidative stress in *An. gambiae* when exposed to protoporphyrin analogues would help to explore the hypothesis that AgHO is working in a detoxification capacity. AgHO knockdown using RNAi would similarly be a powerful tool.

It is important to remember that AgHO does not act alone, in two ways. Firstly, it cannot degrade haem without the assistance of CPR. CPR is somewhat of a generalist redox partner, so if the goal of a novel insecticide were to target the haem degradation pathway, CPR presents an attractive target, not only because its inhibition would indirectly inhibit AgHO, but also because knocking out CPR would knock out the P450 system (and thus, insecticide resistance) [91]. A novel insecticide based on, for example, DPIC would act simultaneously as an insecticide and an insecticide synergist, so should be explored. AgHO also does not act alone considering that haematophages have an array of other strategies to block haem toxicity. The extent that AgHO inhibitors also inhibit haem binding proteins and the formation of haem aggregates should be examined.

References

1. WHO, *World Health Organisation Fact Sheet 387 - Vector-Borne Diseases.* 2014.
2. Gething, P.W., et al., *A new world malaria map: Plasmodium falciparum endemicity in 2010.* Malar J, 2011. **10**(378): p. 1475-2875.
3. WHO, *World Health Organisation Fact Sheet 94 - Malaria.* 2015.
4. Luxemburger, C., et al., *Effects of malaria during pregnancy on infant mortality in an area of low malaria transmission.* American journal of epidemiology, 2001. **154**(5): p. 459-465.
5. Ranson, H., et al., *Pyrethroid resistance in African anopheline mosquitoes: what are the implications for malaria control?* Trends in parasitology, 2011. **27**(2): p. 91-98.
6. Chandrudu, S., et al., *Synthesis and immunological evaluation of peptide-based vaccine candidates against malaria.* 2016.
7. Wellems, T.E. and C.V. Plowe, *Chloroquine-Resistant Malaria.* Journal of Infectious Diseases, 2001. **184**(6): p. 770-776.
8. Dondorp, A.M., et al., *The Threat of Artemisinin-Resistant Malaria.* New England Journal of Medicine, 2011. **365**(12): p. 1073-1075.
9. Liu, N., *Insecticide resistance in mosquitoes: impact, mechanisms, and research directions.* Annual review of entomology, 2015. **60**: p. 537-559.
10. Macdonald, G., *The epidemiology and control of malaria.* The Epidemiology and Control of Malaria., 1957.
11. Smith, D.L., et al., *Ross, Macdonald, and a Theory for the Dynamics and Control of Mosquito-Transmitted Pathogens.* PLoS Pathog, 2012. **8**(4): p. e1002588.
12. Fillinger, U. and S.W. Lindsay, *Larval source management for malaria control in Africa: myths and reality.* Malar J, 2011. **10**(353): p. 10.1186.
13. Yapabandara, A. and C. Curtis, *Control of Vectors and Incidence of Malaria in an Irrigated Settlement Scheme in Sri Lanka When Using the Insect Growth Regulator Pyriproxyfen.* Journal of the American Mosquito Control Association, 2004. **20**(4): p. 395-400.
14. Mbare, O., S.W. Lindsay, and U. Fillinger, *Dose–response tests and semi-field evaluation of lethal and sub-lethal effects of slow release pyriproxyfen granules (Sumilarv® 0.5 G) for the control of the malaria vectors Anopheles gambiae sensu lato.* Malar J, 2013. **12**(1): p. 94.
15. Curtis, C., *Malaria control through anti-mosquito measures.* Journal of the Royal Society of Medicine, 1989. **82**(Suppl 17): p. 18.
16. Clarke, S.E., et al., *Do untreated bednets protect against malaria?* Transactions of the Royal Society of Tropical Medicine and Hygiene, 2001. **95**(5): p. 457-462.
17. Gamage-Mendis, A.C., et al., *Clustering of malaria infections within an endemic population: risk of malaria associated with the type of housing construction.* The American journal of tropical medicine and hygiene, 1991. **45**(1): p. 77-85.
18. Nauen, R., *Insecticide resistance in disease vectors of public health importance.* Pest Management Science, 2007. **63**(7): p. 628-633.
19. Sadasivaiah, S., Y. Tozan, and J.G. Breman, *Dichlorodiphenyltrichloroethane (DDT) for indoor residual spraying in Africa: how can it be used for malaria control?* The American journal of tropical medicine and hygiene, 2007. **77**(6 Suppl): p. 249-263.
20. Coats, J.R., *Mechanisms of toxic action and structure-activity relationships for organochlorine and synthetic pyrethroid insecticides.* Environmental Health Perspectives, 1990. **87**: p. 255.

21. Fukuto, T.R., *Mechanism of action of organophosphorus and carbamate insecticides.* Environmental Health Perspectives, 1990. **87**: p. 245.
22. David, J.-P., et al., *Role of cytochrome P450s in insecticide resistance: impact on the control of mosquito-borne diseases and use of insecticides on Earth.* Philosophical Transactions of the Royal Society of London B: Biological Sciences, 2013. **368**(1612): p. 20120429.
23. Mulligan, F.S. and C.H. Schaefer, *Efficacy of a juvenile-hormone mimic, pyriproxyfen, for mosquito control in dairy waste-water lagoons.* Journal of the American Mosquito Control Association, 1990. **6**(1): p. 89-92.
24. Caputo, B., et al., *The "auto-dissemination" approach: a novel concept to fight Aedes albopictus in urban areas.* PLoS Negl Trop Dis, 2012. **6**(8): p. e1793.
25. Ohashi, K., et al., *Efficacy of pyriproxyfen-treated nets in sterilizing and shortening the longevity of Anopheles gambiae (Diptera: Culicidae).* Journal of Medical Entomology, 2012. **49**(5): p. 1052-1058.
26. Shapiro, A., et al., *Juvenile hormone and juvenile hormone esterase in adult females of the mosquito Aedes aegypti.* Journal of insect physiology, 1986. **32**(10): p. 867-877.
27. Bhatt, S., et al., *The effect of malaria control on Plasmodium falciparum in Africa between 2000 and 2015.* Nature, 2015. **526**(7572): p. 207-211.
28. Hemingway, J. and H. Ranson, *Insecticide resistance in insect vectors of human disease.* Annual Review of Entomology, 2000. **45**(1): p. 371-391.
29. Hemingway, J., et al., *The molecular basis of insecticide resistance in mosquitoes.* Insect Biochemistry and Molecular Biology, 2004. **34**(7): p. 653-665.
30. Hemingway, J., et al., *The Innovative Vector Control Consortium: improved control of mosquito-borne diseases.* Trends in Parasitology, 2006. **22**(7): p. 308-312.
31. Ranson, H. and N. Lissenden, *Insecticide Resistance in African Anopheles Mosquitoes: A Worsening Situation that Needs Urgent Action to Maintain Malaria Control.* Trends in Parasitology, 2016. **32**(3): p. 187-196.
32. Ribeiro, J.M.C., *Blood-feeding arthropods - live syringes or invertebrate pharmacologists.* Infectious Agents and Disease-Reviews Issues and Commentary, 1995. **4**(3): p. 143-152.
33. Lehane, M., *Biology of Blood-Sucking Insects*. 2nd ed. 2005, Cambridge: Cambridge University Press.
34. Valenzuela, J.G., et al., *The salivary apyrase of the blood-sucking sand fly Phlebotomus papatasi belongs to the novel Cimex family of apyrases.* Journal of Experimental Biology, 2001. **204**(2): p. 229-237.
35. Ribeiro, J. and J.G. Valenzuela, *Purification and cloning of the salivary peroxidase/catechol oxidase of the mosquito Anopheles albimanus.* Journal of Experimental Biology, 1999. **202**(7): p. 809-816.
36. Isawa, H., et al., *A mosquito salivary protein inhibits activation of the plasma contact system by binding to factor XII and high molecular weight kininogen.* Journal of Biological Chemistry, 2002. **277**(31): p. 27651-27658.
37. Ortiz de Montellano, P.R., *Cytochrome P450: Structure, Mechanism and Biochemistry*. 2005.
38. Atamna, H. and K. Boyle, *Amyloid-β peptide binds with heme to form a peroxidase: Relationship to the cytopathologies of Alzheimer's disease.* Proceedings of the National Academy of Sciences of the United States of America, 2006. **103**(9): p. 3381-3386.
39. Klatt, P., K. Schmidt, and B. Mayer, *Brain nitric oxide synthase is a haemoprotein.* Biochemical Journal, 1992. **288**(Pt 1): p. 15.

40. Schmitt, T.H., W.A. Frezzatti, and S. Schreier, *Hemin induced lipid membrane disorder and increased permeability - a molecular model for the mechanism of cell lysis.* Archives of Biochemistry and Biophysics, 1993. **307**(1): p. 96-103.
41. Tappel, A.L., *Unsaturated lipid oxidation catalyzed by hematin compounds.* Journal of Biological Chemistry, 1955. **217**(2): p. 721-733.
42. Aft, R.L. and G.C. Mueller, *Hemin-mediated oxidative-degradation of proteins.* Journal of Biological Chemistry, 1984. **259**(1): p. 301-305.
43. Aft, R.L. and G.C. Mueller, *Hemin-mediated DNA strand scission.* Journal of Biological Chemistry, 1983. **258**(19): p. 2069-2072.
44. Ryter, S.W. and R.M. Tyrrell, *The Heme synthesis and degradation pathways: role in oxidant sensitivity - Heme oxygenase has both pro- and antioxidant properties.* Free Radical Biology and Medicine, 2000. **28**(2): p. 289-309.
45. VanderZee, J., D.P. Barr, and R.P. Mason, *ESR spin trapping investigation of radical formation from the reaction between hematin and tert-butyl hydroperoxide.* Free Radical Biology and Medicine, 1996. **20**(2): p. 199-206.
46. Cannon, J.B., et al., *Kinetics of the interaction of hemin liposomes with heme binding proteins.* Biochemistry, 1984. **23**(16): p. 3715-3721.
47. Tipping, E., B. Ketterer, and L. Christodoulides, *Interactions of small molecules with phospholipid bilayers. Binding to egg phosphatidylcholine of some uncharged molecules (2-acetylaminofluorene, 4-dimethylaminoazobenzene, estrone and testosterone) that bind to ligandin and aminoazo-dye-binding protein-A.* Biochemical Journal, 1979. **180**(2): p. 319-326.
48. Gwadz, R.W., *Regulation of blood meal size in the mosquito.* Journal of insect physiology, 1969. **15**(11): p. 2039-2044.
49. Friend, W., C. Choy, and E. Cartwright, *The effect of nutrient intake on the development and the egg Production of Rhodnius prolixus Ståhl (Hemiptera: Reduviidae).* Canadian journal of zoology, 1965. **43**(6): p. 891-904.
50. Rosomer, W.S., *The vector alimentar system*, in *Biology of Disease Vectors*, W.H. Marquardt, Editor. 2004, Academic Press.
51. Graca-Souza, A.V., et al., *Adaptations against heme toxicity in blood-feeding arthropods.* Insect Biochemistry and Molecular Biology, 2006. **36**(4): p. 322-335.
52. Slater, A.F.G., et al., *An iron carboxylate bond links the heme units of malaria pigment.* Proceedings of the National Academy of Sciences of the United States of America, 1991. **88**(2): p. 325-329.
53. Pagola, S., et al., *The structure of malaria pigment beta-haematin.* Nature, 2000. **404**(6775): p. 307-310.
54. Pascoa, V., et al., *Aedes aegypti peritrophic matrix and its interaction with heme during blood digestion.* Insect Biochemistry and Molecular Biology, 2002. **32**(5): p. 517-523.
55. Okuda, K., et al., *Morphological and enzymatic analysis of the midgut of Anopheles darlingi during blood digestion.* Journal of Insect Physiology, 2005. **51**(7): p. 769-776.
56. Oliveira, M.F., et al., *Haemozoin formation in the midgut of the blood-sucking insect Rhodnius prolixus.* Febs Letters, 2000. **477**(1-2): p. 95-98.
57. Lane, N.J. and J.B. Harrison, *Unusual cell-surface modification - double plasma membrane.* Journal of Cell Science, 1979. **39**(OCT): p. 355-372.
58. Sullivan, D.J., I.Y. Gluzman, and D.E. Goldberg, *Plasmodium hemozoin formation mediated by histidine-rich proteins.* Science, 1996. **271**(5246): p. 219-222.
59. Bendrat, K., B.J. Berger, and A. Cerami, *Heme polymerisation in malaria.* Nature, 1995. **378**(6553): p. 138-138.

60. Dorn, A., et al., *A Comparison and Analysis of Several Ways to Promote Haematin (Haem) Polymerisation and an Assessment of Its Initiation In Vitro.* Biochemical Pharmacology, 1998. **55**(6): p. 737-747.
61. Oliveira, P.L., et al., *A heme-binding protein from hemolymph and oocytes of the bloodsucking insect, Rhodnius prolixus - isolation and characterisation.* Journal of Biological Chemistry, 1995. **270**(18): p. 10897-10901.
62. Dansa-Petretski, M., et al., *Antioxidant role of Rhodnius prolixus heme-binding protein - protection against heme-induced lipid peroxidation.* Journal of Biological Chemistry, 1995. **270**(18): p. 10893-10896.
63. Maya-Monteiro, C.M., et al., *HeLp, a heme lipoprotein from the hemolymph of the cattle tick, Boophilus microplus.* Journal of Biological Chemistry, 2000. **275**(47): p. 36584-36589.
64. Maya-Monteiro, C.M., et al., *HeLp, a heme-transporting lipoprotein with an antioxidant role.* Insect Biochemistry and Molecular Biology, 2004. **34**(1): p. 81-87.
65. Vincent, S.H., *Oxidative effects of heme and porphyrins on proteins and lipids.* Seminars in Hematology, 1989. **26**(2): p. 105-113.
66. Holt, R.A., et al., *The genome sequence of the malaria mosquito Anopheles gambiae.* Science, 2002. **298**(5591): p. 129-+.
67. Ribeiro, J.M.C., *A catalogue of Anopheles gambiae transcripts significantly more or less expressed following a blood meal.* Insect Biochemistry and Molecular Biology, 2003. **33**(9): p. 865-882.
68. Marinotti, O., et al., *Microarray analysis of genes showing variable expression following a blood meal in Anopheles gambiae.* Insect Molecular Biology, 2005. **14**(4): p. 365-373.
69. Dana, A.N., et al., *Gene expression patterns associated with blood-feeding in the malaria mosquito Anopheles gambiae.* BMC Genomics, 2005. **6**(January 14).
70. Sanders, H.R., et al., *Blood meal induces global changes in midgut gene expression in the disease vector, Atedes aegypti.* Insect Biochemistry and Molecular Biology, 2003. **33**(11): p. 1105-1122.
71. da-Silva, W.S., et al., *Mitochondrial bound hexokinase activity as a preventive antioxidant Defense - Steady-state ADP formation as a regulatory mechanism of membrane potential and reactive oxygen species generation in mitochondria.* Journal of Biological Chemistry, 2004. **279**(38): p. 39846-39855.
72. Paes, M.C., M.B. Oliveira, and P.L. Oliveira, *Hydrogen peroxide detoxification in the midgut of the blood-sucking insect, Rhodnius prolixus.* Archives of Insect Biochemistry and Physiology, 2001. **48**(2): p. 63-71.
73. Kumar, S., et al., *The role of reactive oxygen species on Plasmodium melanotic encapsulation in Anopheles gambiae.* Proceedings of the National Academy of Sciences of the United States of America, 2003. **100**(24): p. 14139-14144.
74. Graca-Souza, A.V., M.A.C. Silva-Neto, and P.L. Oliveira, *Urate synthesis in the blood-sucking insect Rhodnius prolixus - Stimulation by hemin is mediated by protein kinase C.* Journal of Biological Chemistry, 1999. **274**(14): p. 9673-9676.
75. Lima, V.L.A., et al., *The Antioxidant Role of Xanthurenic Acid in the Aedes aegypti Midgut during Digestion of a Blood Meal.* Plos One, 2012. **7**(6).
76. Zhang, X.H., et al., *Unique features of recombinant heme oxygenase of Drosophila melanogaster compared with those of other heme oxygenases studied.* European Journal of Biochemistry, 2004. **271**(9): p. 1713-1724.
77. Paiva-Silva, G.O., et al., *A heme-degradation pathway in a blood-sucking insect.* Proceedings of the National Academy of Sciences of the United States of America, 2006. **103**(21): p. 8030-8035.

78. Pereira, L.O.R., et al., *Biglutaminyl-biliverdin IX alpha as a heme degradation product in the dengue fever insect-vector Aedes aegypti.* Biochemistry, 2007. **46**(23): p. 6822-6829.
79. McCoubrey, W.K., T. Huang, and M.D. Maines, *Isolation and characterization of a cDNA from the rat brain that encodes hemoprotein heme oxygenase-3.* European Journal of Biochemistry, 1997. **247**(2): p. 725-732.
80. Schuller, D.J., et al., *Crystal structure of human heme oxygenase-1.* Nature Structural Biology, 1999. **6**(9): p. 860-867.
81. Tenhunen, R., H.S. Marver, and R. Schmid, *Microsomal heme oxygenase - characterization of enzyme.* Journal of Biological Chemistry, 1969. **244**(23): p. 6388-&.
82. Wang, J. and P.R.O. de Montellano, *The Binding Sites on Human Heme Oxygenase-1 for Cytochrome P450 Reductase and Biliverdin Reductase.* Journal of Biological Chemistry, 2003. **278**(22): p. 20069-20076.
83. Schacter, B.A., et al., *Immunochemical evidence for an association of heme oxygenase with microsomal electron transport system.* Journal of Biological Chemistry, 1972. **247**(11): p. 3601-&.
84. Sano, S., et al., *On the mechanism of the chemical and enzymatic oxygenations of alpha-oxyprotohemin-IX to Fe biliverdin-IX-alpha.* Proceedings of the National Academy of Sciences of the United States of America, 1986. **83**(3): p. 531-535.
85. Kayser, H. and K. Dettner, *Biliverdin IX gamma in beetles (Dytiscidae, Laccophilinae).* Comparative Biochemistry and Physiology B-Biochemistry & Molecular Biology, 1984. **77**(3): p. 639-643.
86. Wang, M., et al., *Three-dimensional structure of NADPH–cytochrome P450 reductase: Prototype for FMN- and FAD-containing enzymes.* Proceedings of the National Academy of Sciences, 1997. **94**(16): p. 8411-8416.
87. Paine, M.J.I.S., Nigel S.; Munro, Andrew W.; Gutierrez, Aldo; Roberts, Gordon C. K.; Wolf, C. Roland, *Electron Transfer Partners of Cytochrome P450*, in *Cytochrome P450: Structure, Mechanism, and Biochemistry*, P.R. Ortiz de Montellano, Editor. 2005, Springer US: Boston, MA. p. 115-148.
88. Sugishima, M., et al., *Structural basis for the electron transfer from an open form of NADPH-cytochrome P450 oxidoreductase to heme oxygenase.* Proceedings of the National Academy of Sciences, 2014. **111**(7): p. 2524-2529.
89. Scott, J.G., *Cytochromes P450 and insecticide resistance.* Insect Biochemistry and Molecular Biology, 1999. **29**(9): p. 757-777.
90. Lian, L.-Y., et al., *Biochemical Comparison of Anopheles gambiae and Human NADPH P450 Reductases Reveals Different 2'-5'-ADP and FMN Binding Traits.* PLoS ONE, 2011. **6**(5): p. e20574.
91. Lycett, G., et al., *Anopheles gambiae P450 reductase is highly expressed in oenocytes and in vivo knockdown increases permethrin susceptibility.* Insect molecular biology, 2006. **15**(3): p. 321-327.
92. Henderson, C.J., et al., *Inactivation of the hepatic cytochrome P450 system by conditional deletion of hepatic cytochrome P450 reductase.* Journal of Biological Chemistry, 2003. **278**(15): p. 13480-13486.
93. Zhu, F., et al., *RNA interference of NADPH-cytochrome P450 reductase results in reduced insecticide resistance in the bed bug, Cimex lectularius.* PloS one, 2012. **7**(2): p. e31037.
94. Maines, M.D. and A. Kappas, *Metals as regulators of heme metabolism.* Science, 1977. **198**(4323): p. 1215-1221.

95. Maines, M.D., *The heme oxygenase system: A regulator of second messenger gases.* Annual Review of Pharmacology and Toxicology, 1997. **37**: p. 517-554.
96. Whitten, J.M., *Comparative anatomy of the tracheal system*. Smith, Ray F., Thomas E. Mittler and Carroll N. Smith. 1972. 373-402.
97. van Holde, K.E. and K.I. Miller, *Hemocyanins*, in *Advances in Protein Chemistry*, F.M.R.J.T.E. C.B. Anfinsen and S.E. David, Editors. 1995, Academic Press. p. 1-81.
98. Maines, M.D., *Zinc protoporphyrin is a selective inhibitor of heme oxygenase activity in the neonatal rat.* Biochimica Et Biophysica Acta, 1981. **673**(3): p. 339-350.
99. Rebeiz, C.A., J.A. Juvik, and C.C. Rebeiz, *Porphyric insecticides.* Pesticide Biochemistry and Physiology, 1988. **30**(1): p. 11-27.
100. Caiaffa, C.D., et al., *Sn-protoporphyrin inhibits both heme degradation and hemozoin formation in Rhodnius prolixus midgut.* Insect Biochemistry and Molecular Biology, 2010. **40**(12): p. 855-860.
101. Arnold, K., et al., *The SWISS-MODEL workspace: a web-based environment for protein structure homology modelling.* Bioinformatics, 2006. **22**(2): p. 195-201.
102. Kiefer, F., et al., *The SWISS-MODEL Repository and associated resources.* Nucleic Acids Research, 2009. **37**(suppl 1): p. D387-D392.
103. Guex, N., M.C. Peitsch, and T. Schwede, *Automated comparative protein structure modeling with SWISS-MODEL and Swiss-PdbViewer: A historical perspective.* ELECTROPHORESIS, 2009. **30**(S1): p. S162-S173.
104. Biasini, M., et al., *SWISS-MODEL: modelling protein tertiary and quaternary structure using evolutionary information.* Nucleic Acids Research, 2014. **42**(W1): p. W252-W258.
105. Schrödinger, L., *The PyMOL Molecular Graphics System, Version 1.7.4.* 2015.
106. Wilks, A. and P.O. de Montellano, *Rat liver heme oxygenase. High level expression of a truncated soluble form and nature of the meso-hydroxylating species.* Journal of Biological Chemistry, 1993. **268**(30): p. 22357-22362.
107. Wilks, A., et al., *Expression and characterization of truncated human heme oxygenase (hHO-1) and a fusion protein of hHO-1 with human cytochrome P450 reductase.* Biochemistry, 1995. **34**(13): p. 4421-4427.
108. Zhu, W., A. Wilks, and I. Stojiljkovic, *Degradation of heme in gram-negative bacteria: the product of the hemO gene of Neisseriae is a heme oxygenase.* Journal of bacteriology, 2000. **182**(23): p. 6783-6790.
109. Wilks, A. and M.P. Schmitt, *Expression and Characterization of a Heme Oxygenase (Hmu O) from Corynebacterium diphtheriae - Iron acquisition requires oxidative cleavage of the heme macrocycle.* Journal of Biological Chemistry, 1998. **273**(2): p. 837-841.
110. Yoshida, T. and G. Kikuchi, *Purification and properties of heme oxygenase from rat liver microsomes.* Journal of Biological Chemistry, 1979. **254**(11): p. 4487-91.
111. Sugishima, M., et al., *Crystal structure of rat heme oxygenase-1 in complex with heme.* FEBS Letters, 2000. **471**(1): p. 61-66.
112. Hirotsu, S., et al., *The crystal structures of the ferric and ferrous forms of the heme complex of HmuO, a heme oxygenase of Corynebacterium diphtheriae.* Journal of Biological Chemistry, 2004. **279**(12): p. 11937-11947.
113. Gasteiger, E., et al., *Protein identification and analysis tools on the ExPASy server*. 2005: Springer.
114. Wilding, C.S., et al., *High, clustered, nucleotide diversity in the genome of Anopheles gambiae revealed through pooled-template sequencing: implications for high-throughput genotyping protocols.* BMC genomics, 2009. **10**(1): p. 320.

115. Wilks, A., *Heme oxygenase: Evolution, structure, and mechanism.* Antioxidants & Redox Signaling, 2002. **4**(4): p. 603-614.
116. Liu, Y., et al., *Replacement of the Distal Glycine 139 Transforms Human Heme Oxygenase-1 into a Peroxidase.* Journal of Biological Chemistry, 2000. **275**(44): p. 34501-34507.
117. Hofman, K.S., W, *TMbase-A database of membrane spanning protein segments.* Biol. Chem. Hoppe-Seyler, 1993. **374**: p. 166.
118. Braz, G.R.C., et al., *Heme biosynthesis and oogenesis in the blood-sucking bug, Rhodnius prolixus.* Insect Biochemistry and Molecular Biology, 2001. **31**(4–5): p. 359-364.
119. Zhou, G., et al., *Fate of blood meal iron in mosquitoes.* Journal of Insect Physiology, 2007. **53**(11): p. 1169-1178.
120. Yuda, M., et al., *cDNA Cloning, Expression and Characterization of Nitric-oxide Synthase from the Salivary Glands of the Blood-Sucking Insect Rhodnius prolixus.* European Journal of Biochemistry, 1996. **242**(3): p. 807-812.
121. Ranson, H., et al., *Molecular analysis of multiple cytochrome P450 genes from the malaria vector, Anopheles gambiae.* Insect Molecular Biology, 2002. **11**(5): p. 409-418.
122. Tijet, N., C. Helvig, and R. Feyereisen, *The cytochrome P450 gene superfamily in Drosophila melanogaster: Annotation, intron-exon organization and phylogeny.* Gene, 2001. **262**(1–2): p. 189-198.
123. Wilks, A. and P. Moënne-Loccoz, *Identification of the Proximal Ligand His-20 in Heme Oxygenase (Hmu O) from Corynebacterium diphtheriae OXIDATIVE CLEAVAGE OF THE HEME MACROCYCLE DOES NOT REQUIRE THE PROXIMAL HISTIDINE.* Journal of Biological Chemistry, 2000. **275**(16): p. 11686-11692.
124. Lambeth, D.O. and G. Palmer, *The Kinetics and Mechanism of Reduction of Electron Transfer Proteins and Other Compounds of Biological Interest by Dithionite.* Journal of Biological Chemistry, 1973. **248**(17): p. 6095-6103.
125. Yoshida, T. and G. Kikuchi, *Purification and properties of heme oxygenase from pig spleen microsomes.* Journal of Biological Chemistry, 1978. **253**(12): p. 4224-4229.
126. Yoshida, T. and G. Kikuchi, *Features of the reaction of heme degradation catalyzed by the reconstituted microsomal heme oxygenase system.* Journal of Biological Chemistry, 1978. **253**(12): p. 4230-4236.
127. Berry, E.A. and B.L. Trumpower, *Simultaneous determination of hemes a, b, and c from pyridine hemochrome spectra.* Analytical Biochemistry, 1987. **161**(1): p. 1-15.
128. Bar, I.G., F., *Pyridine Hemochromagen Assay for Determining the Concentration of Heme in Purified Protein Solutions.* Bio-Protocol, 2015. **5**(18): p. e1594.
129. Stookey, L.L., *Ferrozine---a new spectrophotometric reagent for iron.* Analytical Chemistry, 1970. **42**(7): p. 779-781.
130. Wilks, A., et al., *Heme oxygenase (HO-1): His-132 stabilizes a distal water ligand and assists catalysis.* Biochemistry, 1996. **35**(3): p. 930-936.
131. Soldano, A., et al., *Heme-iron utilization by Leptospira interrogans requires a heme oxygenase and a plastidic-type ferredoxin-NADP+ reductase.* Biochimica et Biophysica Acta (BBA) - General Subjects, 2014. **1840**(11): p. 3208-3217.
132. Blanford, S., A.F. Read, and M.B. Thomas, *Thermal behaviour of Anopheles stephensi in response to infection with malaria and fungal entomopathogens.* Malar J, 2009. **8**(72).
133. Oliveira, M.F., et al., *Haemozoin in Schistosoma mansoni.* Molecular and biochemical parasitology, 2000. **111**(1): p. 217-221.

134. Magalhaes, T., *What is the association of heme aggregates with the peritrophic matrix of adult female mosquitoes.* Parasit Vectors, 2014. **7**: p. 362.
135. Devenport, M., et al., *Identification of the Aedes aegypti peritrophic matrix protein AeIMUCI as a heme-binding protein.* Biochemistry, 2006. **45**(31): p. 9540-9549.
136. Teale, F., *Cleavage of the haem-protein link by acid methylethylketone.* Biochimica et biophysica acta, 1959(35): p. 543.
137. Drummond, G.S. and A. Kappas, *Prevention of neonatal hyperbilirubinemia by tin protoporphyrin IX, a potent competitive inhibitor of heme oxidation.* Proceedings of the National Academy of Sciences, 1981. **78**(10): p. 6466-6470.
138. Yoshinaga, T., S. Sassa, and A. Kappas, *Purification and properties of bovine spleen heme oxygenase. Amino acid composition and sites of action of inhibitors of heme oxidation.* Journal of Biological Chemistry, 1982. **257**(13): p. 7778-85.
139. Maines, M.D., *Heme oxygenase: function, multiplicity, regulatory mechanisms, and clinical applications.* The FASEB Journal, 1988. **2**(10): p. 2557-2568.
140. De Block, M. and R. Stoks, *Compensatory growth and oxidative stress in a damselfly.* Proceedings of the Royal Society of London B: Biological Sciences, 2008. **275**(1636): p. 781-785.
141. Benveniste, I., et al., *Multiple forms of NADPH-cytochrome P450 reductase in higher plants.* Biochemical and Biophysical Research Communications, 1991. **177**(1): p. 105-112.
142. Smith, G., D.G. Tew, and C.R. Wolf, *Dissection of NADPH-cytochrome P450 oxidoreductase into distinct functional domains.* Proceedings of the National Academy of Sciences, 1994. **91**(18): p. 8710-8714.
143. Zhao, Q., et al., *Crystal structure of the FMN-binding domain of human cytochrome P450 reductase at 1.93 [Angstrom capital A, ring] resolution.* Protein science, 1999. **8**(02): p. 298-306.
144. Shen, A.L., et al., *Structural analysis of the FMN binding domain of NADPH-cytochrome P-450 oxidoreductase by site-directed mutagenesis.* Journal of Biological Chemistry, 1989. **264**(13): p. 7584-7589.
145. Yasukochi, Y. and B.S. Masters, *Some properties of a detergent-solubilized NADPH-cytochrome c(cytochrome P-450) reductase purified by biospecific affinity chromatography.* Journal of Biological Chemistry, 1976. **251**(17): p. 5337-44.
146. Bird, L., *OPPF-UK Standard Protocols: Cloning and Expression Screening*, OPPF, Editor. 2012, Oxford Protein Production Facility: Online.
147. Sarapusit, S., et al., *NADPH-cytochrome P450 oxidoreductase from the mosquito Anopheles minimus: kinetic studies and the influence of Leu86 and Leu219 on cofactor binding and protein stability.* Archives of biochemistry and biophysics, 2008. **477**(1): p. 53-59.
148. Murataliev, M.B., et al., *Kinetic mechanism of cytochrome P450 reductase from the house fly (Musca domestica).* Insect Biochemistry and Molecular Biology, 1999. **29**(3): p. 233-242.
149. Iyanagi, T., N. Makino, and H. Mason, *Redox properties of the reduced nicotinamide adenine dinucleotide phosphate-cytochrome P-450 and reduced nicotinamide adenine dinucleotide-cytochrome b5 reductases.* Biochemistry, 1974. **13**(8): p. 1701-1710.
150. Daff, S., et al., *Redox control of the catalytic cycle of flavocytochrome P-450 BM3.* Biochemistry, 1997. **36**(45): p. 13816-13823.
151. Murataliev, M.B. and R. Feyereisen, *Interaction of NADP(H) with oxidized and reduced P450 reductase during catalysis. Studies with nucleotide analogues.* Biochemistry, 2000. **39**(17): p. 5066-5074.

152. Tew, D.G., *Inhibition of cytochrome P450 reductase by the diphenyliodonium cation. Kinetic analysis and covalent modifications.* Biochemistry, 1993. **32**(38): p. 10209-10215.
153. Nikou, D., H. Ranson, and J. Hemingway, *An adult-specific CYP6 P450 gene is overexpressed in a pyrethroid-resistant strain of the malaria vector, Anopheles gambiae.* Gene, 2003. **318**: p. 91-102.
154. Müller, P., et al., *Field-Caught Permethrin-Resistant <italic>Anopheles gambiae</italic> Overexpress CYP6P3, a P450 That Metabolises Pyrethroids.* PLoS Genet, 2008. **4**(11): p. e1000286.
155. Carter, R., *Transmission blocking malaria vaccines.* Vaccine, 2001. **19**(17): p. 2309-2314.
156. Wu, Y., et al., *Phase 1 trial of malaria transmission blocking vaccine candidates Pfs25 and Pvs25 formulated with montanide ISA 51.* PloS one, 2008. **3**(7): p. e2636.
157. Khow, O. and S. Suntrarachun, *Strategies for production of active eukaryotic proteins in bacterial expression system.* Asian Pacific Journal of Tropical Biomedicine, 2012. **2**(2): p. 159-162.
158. Blanford, S., A.F. Read, and M.B. Thomas, *Thermal behaviour of Anopheles stephensi in response to infection with malaria and fungal entomopathogens.* Malaria Journal, 2009. **8**(1): p. 1-9.
159. Meshnick, S.R., K.P. Chang, and A. Cerami, *Heme lysis of bloodstream forms of Trypanosoma brucei.* Biochemical Pharmacology, 1977. **26**(20): p. 1923-1928.
160. Orjih, A.U., et al., *Hemin lyses malaria parasites.* Science, 1981. **214**(4521): p. 667-669.
161. Fitch, C.D., et al., *Lysis of Plasmodium falciparum by ferriprotoporphyrin IX and a chloroquine-ferriprotoporphyrin IX complex.* Antimicrobial Agents and Chemotherapy, 1982. **21**(5): p. 819-822.

Appendices

Appendix 3.1 – Phylogram of haem oxygenases

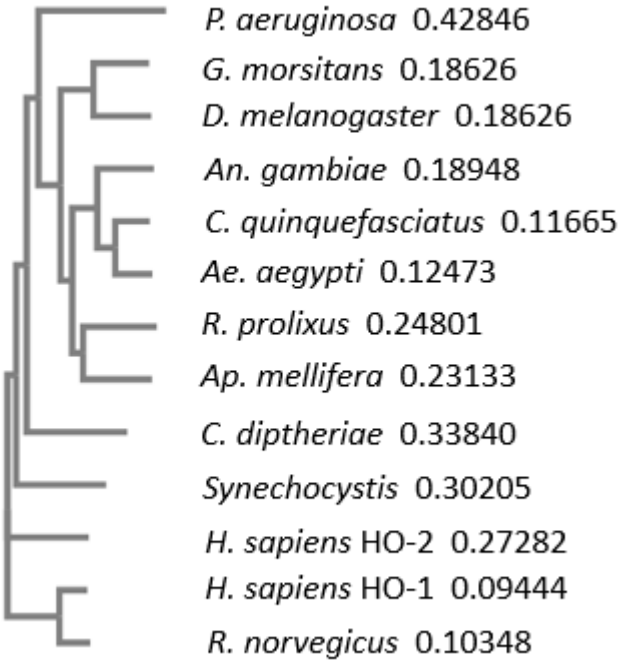

Phylogram generated using ClustalW Phylogeny. Shown distance values are in units of number of substitutions as a proportion of the length of the alignment.

Appendix 3.2 – Primers designed

Primer name	Primer function	Primer sequence (5' – 3')

pJETF	Initial amplification from cDNA for blunt end ligation into pJET1.2. Forward primer. *Nde*I restriction site.	GAGACATATGGCACAAAATGTG CCTTTTTCG
pJETR	Initial amplification from cDNA for blunt end ligation into pJET1.2. Reverse primer. *Hin*dIII restriction site.	AAGCTTTCACAACGTTTGCTCTT GCTCGTG
pOPINFF	Amplification from pJET1.2 for ligation into pOPIN-F. Forward primer	AAGTTCTGTTTCAGGGCCCGATG GCACAAAATGTGCCTTTTTCG
pOPINFR	Amplification from pJET1.2 for ligation into pOPIN-F. Reverse primer, full length.	ATGGTATAGAAAGCTTTACAACG TTTGCTCTTGCTCGTG
pOPINFRA	Amplification from pJET1.2 for ligation into pOPIN-F. Reverse primer, AgHOΔ10.	ATGGTATAGAAAGCTTTAGTTTC GCACGACGTACTGC
pOPINFRB	Amplification from pJET1.2 for ligation into pOPIN-F. Reverse primer, AgHOΔ15.	ATGGTATAGAAAGCTTTACTGCA TTAATATGATGGCAGC
pOPINFRC	Amplification from pJET1.2 for ligation into pOPIN-F. Reverse primer, AgHOΔ31.	ATGGTATAGAAAGCTTTAACGCA TGTTGGCCGAACCAAC
pOPINFRD	Amplification from pJET1.2 for ligation into pOPIN-F. Reverse primer, AgHOΔ46.	ATGGTATAGAAAGCTTTAGTGTT GTTCAGTTCGAACACTTTC
pOPINFRE	Amplification from pJET1.2 for ligation into pOPIN-F. Reverse primer, AgHOΔ60.	ATGGTATAGAAAGCTTTACGCTG GCGCGTTTCCTCGTCCAG
pOPINFRF	Amplification from pJET1.2 for ligation into pOPIN-F. Reverse primer, AgHOΔ73.	ATGGTATAGAAAGCTTTACCACA ATTTTGCGCAAACGTTG
pOPINFRG	Amplification from pJET1.2 for ligation into pOPIN-F. Reverse primer, AgHOΔ83.	ATGGTATAGAAAGCTTTAGTAAA TGCTGTGATCTTCGAATG
pOPINFRH	Amplification from pJET1.2 for ligation into pOPIN-F. Reverse primer, AgHOΔ95.	ATGGTATAGAAAGCTTTACATCC GGGACCGGTTCTGCATCC

Appendix 3.3 – AgHO truncation designs

Truncation	Protein size (aa)	Residues removed (aa)	New C terminus	Approximate protein size (kDa)
AgHO	249	0	EQEQTL	29.2
AgHOΔ10	239	10	QYVVRN	27.9
AgHOΔ15	234	15	AIILMQ	27.3
AgHOΔ31	218	31	GSANMR	25.6
AgHOΔ46	203	46	VFELNN	24.0
AgHOΔ60	189	60	DEETRQ	22.2
AgHOΔ73	176	73	RLRKIV	20.7
AgHOΔ83	166	83	EDHSIY	19.4
AgHOΔ95	154	95	AEPVPD	18.1

Appendix 3.4 –AgHOΔ31 expression time course

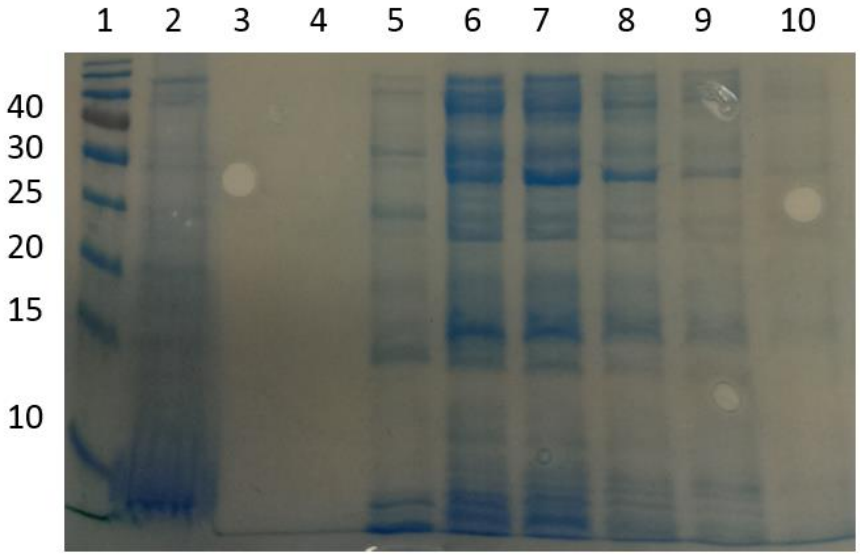

SDS-PAGE gel. Lanes: 1, Molecular weight markers; 2, purified AgHOΔ31 control (failed); 3, empty (dye only); 4, empty (dye only); 5, uninduced control; 6, 60 hours post induction; 7, 48 hours post-induction; 8, 36 hours post-induction; 9, 24 hours no induction; 10, 12 hours no induction. 48 hours is the optimal length of time for expression of AgHOΔ31

Appendix 3.5 – Confirmation of antibody binding

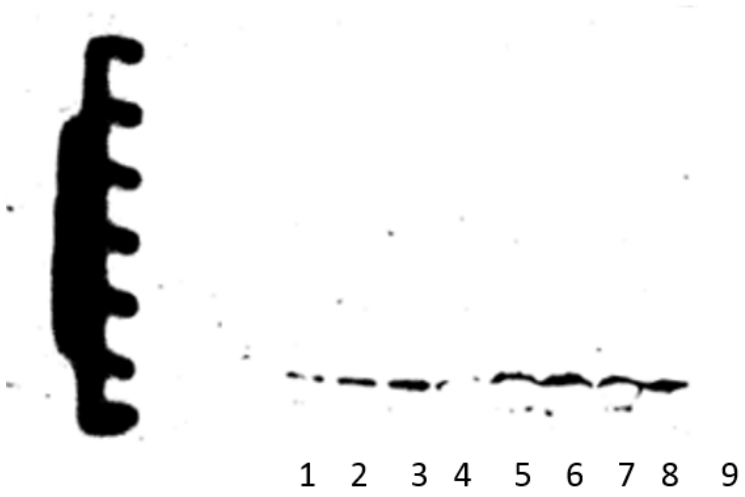

Western blot. Lanes 1 – 8 contain 15µL 0.1mg mL^{-1} AgHO. Lane 9 contains uninduced *E. coli* lysate. Primary antibody is α-AgHO (1:1000 concentration). Secondary antibody is HRP conjugated goat α-rabbit IgG (1:5000) concentration. Exposure time is 10 seconds. Pictured left is overexposed size ruler.

Appendix 3.6 - Codon optimised AgHO

ORF	Protected sites	Protected areas	Motifs to avoid
19-768 [ATG...TAA]	1-6 NdeI [CATATG] 7-12 NcoI [CCATGG] 13-18 BamHI [GGATCC] 17-22 NcoI [CCATGG] 769-774 EcoRI [GAATTC] 775-780 HindIII [AAGCTT] 781-786 KpnI [GGTACC]		NdeI [CATATG] NcoI [CCATGG] BamHI [GGATCC] NcoI [CCATGG] EcoRI [GAATTC] HindIII [AAGCTT] KpnI [GGTACC]

```
                                M  A  Q  N  V  P  F  S  K  Q  M  R  I  A  T  R  E
1.    CATATGCCATGGGGATCCATGGCACAGAATGTTCCGTTTAGCAAACAAATGCGTATTGCCACCCGTGAA
      I  H  N  V  S  D  A  L  V  N  A  K  L  A  F  A  L  Y  D  S  R  V  W
70.   ATTCATAATGTTAGTGATGCACTGGTGAATGCCAAACTGGCATTTGCACTGTATGATAGCCGTGTTTGG
      A  E  G  L  L  I  F  Y  D  V  F  K  H  L  E  Q  R  V  P  H  D  F  L
139.  GCAGAAGGTCTGCTGATCTTTTATGATGTGTTCAAACATCTGGAACAGCGTGTTCCGCATGATTTTCTG
      P  P  E  M  H  R  T  A  Q  F  E  Q  D  L  R  Y  Y  L  G  E  G  W  L
208.  CCTCCGGAAATGCATCGTACCGCACAGTTTGAACAGGATCTGCGTTATTATCTGGGTGAAGGTTGGCTG
      E  R  H  T  P  K  A  E  V  R  A  Y  L  K  H  L  Q  E  L  E  Q  E  N
277.  GAACGTCATACCCCGAAAGCCGAAGTTCGTGCATATCTGAAACATCTGCAAGAACTGGAACAAGAAAAT
      A  N  L  L  L  A  Y  V  Y  H  L  Y  M  G  L  L  S  G  G  Q  I  L  Q
346.  GCAAATCTGCTGCTGGCCTATGTGTATCATCTGTATATGGGTCTGCTGAGCGGTGGTCAGATTCTGCAG
      K  R  R  S  I  G  R  R  I  N  P  F  R  R  A  D  A  E  P  V  P  D  A
415.  AAACGTCGTAGCATTGGTCGTCGTATTAATCCGTTTCGTCGTGCAGATGCAGAACCGGTTCCGGATGCA
      A  V  T  T  F  E  D  H  S  I  Y  E  L  K  Q  R  L  R  K  I  V  D  D
484.  GCAGTTACCACCTTTGAAGATCATAGCATCTATGAACTGAAACAGCGTCTGCGTAAAATCGTGGATGAT
      F  G  A  R  L  D  E  E  T  R  Q  R  M  L  D  E  S  R  K  V  F  E  L
553.  TTTGGTGCACGTCTGGATGAAGAAACCCGTCAGCGTATGCTGGATGAAAGCCGTAAAGTTTTTGAACTG
      N  N  T  I  I  R  T  V  E  G  V  G  S  A  N  M  R  I  V  R  Y  I  A
622.  AACAACACCATTATTCGCACCGTTGAAGGTGTTGGTAGCGCAAATATGCGTATTGTTCGTTATATTGCA
      M  A  I  A  A  I  I  L  M  Q  Y  V  V  R  N  Q  F  G  H  E  Q  E  Q
691.  ATGGCGATTGCAGCCATTATTCTGATGCAGTATGTTGTGCGTAATCAGTTTGGTCATGAACAAGAACAG
      T  L  *
760.  ACCCTGTAAGAATTCAAGCTTGGTACC
```

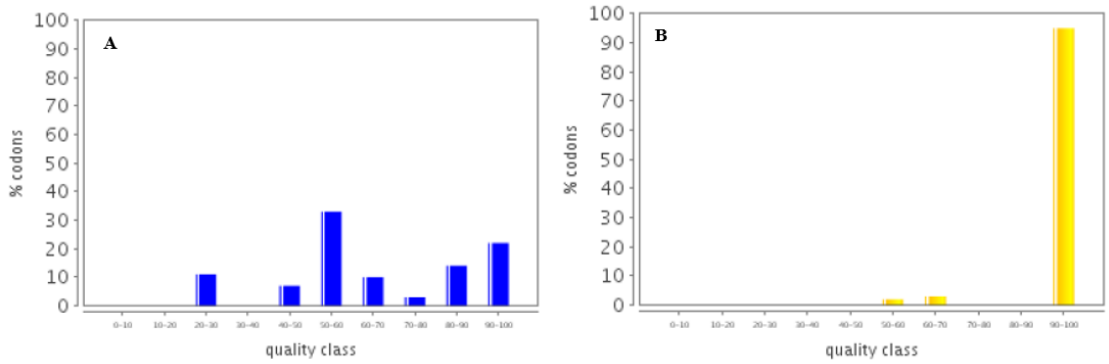

Synthetic AgHO codon optimisation "Quality classes" are on a semi-arbitrary scale. The quality value of the most frequently used codon for the given amino acid in *E. coli* is assigned a value of 100. The other codons are assigned a quality value proportionate to their frequency of appearance in the *E. coli* coding genome. **A** – Codon quality classes for AgHO derived from *An. gambiae* cDNA in *E. coli*. **B** – Codon quality classes for synthetic codon optimised AgHO.

Appendix 6.1 – CPR Coding DNA sequences

AgCPR

```
ATGGACGCCCAGACAGAAACGGAAGTGCCCGCGGGAAGCGTGAGCGACGAACCGTTCCTC
GGCCCGCTTGACATCGTCCTGCTCGTCAGTCTGCTGGCCGGCACTGCCTGGTATCTGCTC
AAGGGCAAGAAAAAGGAAAGCCAAGCTAGTCAGTTTAAATCCTACTCGATCCAGCCGACG
ACGGTGAACACGATGACGATGGTGGAGAACTCGTTCATCAAGAAGCTACAGTCCTCGGGC
CGCCGGCTCGTAGTGTTTTACGGTTCCCAAACAGGCACGGCAGAGGAATTTGCCGGTCGC
CTGGCGAAGGAAGGAATCCGCTACCAAATGAAGGGCATGGTCGCCGACCCAGAGGAGTGC
AATATGGAAGAGCTGCTGATGCTGAAGGACATCGACAAATCGTTGGCCGTGTTTTGCTTA
GCGACGTACGGCGAGGGCGACCCGACGGACAACTGCATGGAGTTCTACGACTGGATTCAA
AACAACGATCTAGATATGACCGGTTTGAATTACGCGGTGTTTGGCCTTGGCAACAAAACG
TACGAGCACTACAACAAGGTCGGCATCTACGTGGACAAGCGTCTCGAGGAGCTCGGTGCG
AACAGACTGCACAAGGCGGGCGGCCGGTCCTGCATGCACGTCGAGTTCGACATCGAGGGC
TCGAAGATGCGGTACGAGGCGGGCGACCATCTCGCGATGTACCCGGTGAACGATCGCGAT
CTGGTCGAGCGGCTCGGCCGGCTGTGCAATGCCGAGCTCGATACGGTCTTCTCGCTCATC
AACACCGACACGGACAGCAGCAAGAAGCATCCGTTCCCGTGCCCCACCACCTACCGGACC
GCGCTCACCCACTATCTGGAGATAACGGCGCTGCCGCGCACCCACATCCTGAAGGAGCTG
GCCGAGTACTGCGGCGAGGAGAAGGACAAGGAGTTCCTGCGCTTCATCTCGTCGACCGCG
CCCGACGGCAAGGCGAAGTACCAGGAGTGGGTGCAGGACAGCTGCCGCAACATCGTGCAC
GTGCTCGAGGACATCCCGTCCTGCCATCCGCCGATCGATCACGTGTGCGAGCTGCTGCCC
CGGCTGCAGCCCCGCTACTACTCGATCTCCTCCTCGTCCAAGCTGCACCCGACGACGGTG
CACGTGACCGCGGTGCTGGTGAAGTACGAGACGAAGACGGGCCGGCTGAACAAGGGCGTC
GCGACGACCTTCCTCGCGGAGAAGCACCCGAACGATGGGGAGCCGGCACCGCGCGTACCA
ATCTTCATCCGCAAGAGCCAGTTCCGGTTGCCGCCCAAGCCGGAAACGCCCGTGATCATG
GTGGGGCCCGGCACCGGGCTGGCACCGTTCCGGGGCTTCATCCAGGAGCGGGACCACTGC
AAGCAGGAGGGCAAGGAGATTGGCCAGACGACGCTGTACTTTGGCTGCCGCAAGCGCTCC
GAGGACTACATCTACGAGGATGAACTGGAAGACTACTCCAAGCGCGGCATCATCAACCTT
CGCGTTGCGTTCTCGCGCGACCAGGAGAAGAAGGTGTACGTGACGCACCTGCTCGAGCAG
GACTCGGACCTCATATGGAGCGTGATCGGCGAGAACAAGGGACACTTTTACATCTGCGGT
GATGCGAAAAATATGGCCACCGATGTGCGAAACATTCTGCTGAAGGTCATCCGCTCGAAG
GGTGGGCTCAGCGAAACCGAGGCCCAGCAGTACATCAAAAAGATGGAAGCCCAAAAACGA
TACTCGGCGGACGTGTGGAGCTAA
```

AmCPR

```
ATGGCAGGTTCTCCAGTATTGGAGAATGAGGATAAAACAGAGATTCTTGATGAACCTCTC
TTTAGCACTCTTGATATTATCCTTCTCAGTGCTCTTTTATTGGCTGCCCTATGGTGGTTG
ATGCGCCGAAACAAACAAGAGGAATATACACCTGTCACAAAATCTTATTCTATTCAGCCA
ACAATATTTCCTACAACGCAAACATCAGAAAATTCATTTATAAAAAAATTGAAAACTTCT
GGACGAAGTTTAGTAGTATTTTATGGTAGTCAAACTGGAACTGCAGAAGAATTTGCCGGT
AGGTTAGCCAAGGAAGGTATTCGATACAAAATGAAAGGCATGGTGGCTGATCCAGAAGAA
TGTGATATGGAAGAATTAATACATCTCAAAACAATACCAAACAGTATGGCAGTATTCTGT
TTAGCAACTTATGGAGAAGGTGATCCTACAGACAATGCTATGGAATTTATTGATTGGCTA
AAAAATGGTGATCCTGATTTAAATGGATTAAATTATGCGGTATTTGGTCTTGGAAATAAA
ACATATGAACATTATAATGAAATAGCTTTATATGTTGATCATAGATTAGAACAACTTGGT
GCTACTCGTGTCTTTGAACTTGGTTTGGGAGATGATGATGCTAATATAGAAGATGATTTT
ATTACATGGAAAGATAAATTTTGGCCAACAGTTTGTGAATTCTTTGGAATTGAAGGTGCA
GGAGAAGATGTTAGTATTAGACAGTATAAACTAACAGAACATATCGATTTATCAATTGAA
CGCATTTATACTGGTGAAATAGCTCGTCTTCATTCATTTAAGAATCAAAGAGCACCATTT
GATGCAAAAAATCCTTTCCTAGCTCCAGTAAAAATAAATCGTGAACTTCATGGTTCAACT
TCAGATAGATCATGTATGCATATAGAATTTGATATAGAAGGATCAAAAATGCGATATGAA
ACTGGTGATCATTTAGCAGTATATCCTGTAAATAATACGGAATTAGTAAATAAAATTGGA
GAAAAATGTGGTATAAATTTAGATACAGTGTTTACTCTTACAAATACAGATGAGGAATCT
```

ACCAAGAAGCATCCATTTCCTTGTCCATGTTCTTACAGAACTGCTTTGACACATTATTTA
GATATTACTAGTAATCCACGCACTCATGTTCTGAAAGAATTAGCAGAATATTGTAGTGAT
CCAAATGATAAAGAAAAATTAAAATTAATGGCATCAACCAGTGTGGATGGTAAAGCTGCT
TATCAGCAATGGGTAGTTCAAGAAAATAGAAATATTGTACATATTTTAGAAGATATTCCT
AGCTTGAAGCCGGCCTTGGATCATCTTTGCGAACTTTTACCAAGATTGCAATGTCGATAT
TATTCAATTTCCTCATCTCCTAAGTTACACCCATCTTCAATTCATATTACTGCAGTTGTT
GTGGAATATAAAACACCAACAGGTAGAATTAACAAAGGTGTAACTACTAGCTGGTTAAAA
GAAAAACATCCTTCACATCCACCATGTTATGTTCCTATTTTTGTTCGAAAATCTCAATTT
CGTTTACCAACTCGATTATCAACTCCTATTATCATGGTTGGTCCAGGTACTGGAATAGCA
CCATTTAGAGGTTTTATACAAGAACGTGATCTTGCAAGAAAAGAAGGAAAAGAAGTAGGA
AATACAATTTTATATTTTGGATGTAGAAAAAAAGATGAAGATTTTCTTTATAAAGATGAA
CTTGAAGAATATGTAAAAAGAGGTACTTTAATTTTACATACTGCATTTAGTAGAGAACAA
TCTCAGAAAATATATGTTACACATCTACTAGAAAAAAATAAAGACGAATTGTGGGAAATT
ATTGGAGAACAAAATGGACATATCTATGTGTGTGGTGATGCAAAAAATATGGCACGAGAT
GTACACAATATTTTATTAAAAGTTGTGATGGAAAAGGGAAAAATGTCGGAATTAGATGCA
GCGAATTATATCAAGAAAATGGATTCGCAAAAACGTTATTCAAGTGACGTATGGAGTTGA

CqCPR

ATGGACGCACAGACAGAGCCGGAAGTGCCCCCGGTGGCGGCGGCAACCGAGGAGCCCTTC
CTGGGCCCGCTAGACATTGTCCTGCTGCTGGTGCTGGTGGCCGGTGCAGCATGGTACCTG
CTCAAGAACAAGAAGAAGGAAGCCCAGACTAGTCAGTTCAAGTCGTACTCGATACAGCCC
ACCGCCGTCAACACGATGACCATGGCGGAGAACTCCTTCATCAAGAAGCTGAAGTCGTCC
GGTCGACGGCTGGTGGTGTTCTACGGCTCGCAGACCGGAACCGCCGAGGAGTTCGCCGGG
CGGTTGGCGAAGGAGGGCCTGCGCTACCAGATGAAGGGTATGGTGGCCGACCCGGAGGAG
TGCGACATGGAAGAGCTGCTGACGCTCAAGGACATCGACAAGTCGCTGGCGGTGTTCTGC
TTGGCCACGTACGGCGAGGGTGATCCCACCGACAACTGCATGGAGTTCTACGAGTGGATC
CAGAACAACGACGTGGACTTTACCGGGTTGAACTACGCGGTCTTTGGGCTTGGCAACAAA
ACGTACGAGCACTATAACAAGGTTGGAATCTATGTCGACAAACGGCTGGAGGAGTTGGGA
GCAAGTCGTGTCTTCGAGCTGGGACTTGGAGATGATGACGCGAACATTGAGGATGACTTC
ATCACGTGGAAGGACAAGTTCTGGCCAGCAGTGTGCGACCATTTTGGAATCGAAAGTACC
GGCGACGAGGTGTTGACGCGTCAGTACCGTCTGCTTGAGCAGCCGGAGACCTCGCCGGAA
CGTCTGTACACCGGTGAGGTGGCCCGCCTGCACTCGCTCCAGACGCAGCGCCCGCCGTTC
GATGCCAAGAATCCGTTCATGGCTCCGATCAAGATTAACCGCGAGCTGCACAAGTCCGGT
GGCCGTTCGTGCATGCACATCGAGTTCGATATCGAGGGATCGAAGATGCGCTACGAAGCT
GGTGATCATCTGGCGATGTACCCGGTGAACGATTCGGACTTGGTGACCCGATTGGGCAAG
CTGTGCAATGCCGACCTGGATACGATCTTCTCGCTGATCAACACCGATACGGACAGTAGC
AAGAAACATCCGTTCCCTTGCCCAACGACGTACAAAACGGCGCTGACGCACTACCTGGAG
ATCACCGCGCTGCCGAGAACTCACATCCTGAAGGAGTTGGCCGAATACTGCAGCGACGAA
AAGGACAAGGAGTTCCTGCGGTTCATGTCTTCCACGGCACCCGAAGGCAAGGCCAAGTAC
CAGGAATGGGTTCAGGACAGCAGCCGTAACATTGTGCACGTACTGGAAGACGTCCCGTCC
TGCCATCCACCGATTGACCACATCTGCGAGCTGCTTCCGAGACTGCAGCCCCGCTACTAC
TCGATCTCTTCGTCTTCCAAGCTGTACCCTACCACGGTGCACGTCACGGCCGTTCTGGTC
AAGTACGTCACCAAGACCGGACGTACCAACAACGGCGTCGCTACGACATTCCTGGCCCAG
AAGAAGGTTAACGGAGAATCGCTGCCGCGGGTGCCGATCTTCATCCGCAAGAGCCAGTTC
CGGTTACCGGCGAAAACGGAAACCCCGGTCATCATGGTCGGCCCGGGAACCGGGTTGGCT
CCCTTCCGAGGCTTTATCCAGGAGCGAGATTTCAACAAGCAGGAAGGCAAGGAAATCGGC
CAGACCGTCATGTACTTTGGCTGTCGCAAACGGTCCGAGGATTACATCTATGAAGAGGAA
CTCGAAGACTACGTCAAGCGCGGCGTAATCAGCCTGAGGACAGCCTTCTCGCGTGACCAA
CCGCAAAAGGTGTACGTTACGCATCTGCTAGAGGAAGACATGGACCTGATCTGGGAAGTG
ATAGGTGTCAACAAGGGTCACTTCTACATTTGCGGTGACGCCAAGAACATGGCCACCGAC
GTGCGGAACATTCTGCTCAAGGTGCTGCAATCCAAGGGCAACATGAGCGAGAGTGAAGCG
ACGCAGTACGTCAAGAAGATGGAAGCCCAGAAGCGGTACTCGGCCGACGTGTGGAGTTAA

DmCPR

ATGGCCAGCGAGCAAACGATTGATGGAGCAGCCGCAATTCCCAGCGGCGGCGGCGACGAA
CCCTTCCTGGGACTGCTGGACGTGGCCCTATTGGCGGTGCTAATCGGCGGCGCAGCCTTC
TACTTCCTGCGTAGCCGCAAGAAGGAGGAGGAGCCAACCAGGAGCTATTCCATACAACCC
ACCACAGTGTGCACCACCAGTGCGTCGGACAATTCGTTCATCAAGAAGCTCAAGGCATCC
GGACGCAGTCTGGTCGTCTTCTATGGCTCACAGACCGGAACCGGCGAGGAGTTCGCCGGC
CGTCTGGCCAAGGAGGGCATTCGTTACCGTCTGAAGGGCATGGTTGCCGATCCCGAGGAA
TGCGACATGGAGGAGCTGCTGCAGCTGAAGGACATCGACAACTCGCTGGCGGTCTTTTGC
CTGGCCACCTACGGCGAGGGAGATCCCACTGACAACGCCATGGAGTTCTACGAGTGGATC
ACCAGCGGCGATGTCGATCTGAGCGGGCTAAATTATGCGGTCTTTGGCTTGGGCAACAAG
ACCTATGAGCACTACAACAAGGTGGCCATCTATGTGGACAAGCGACTGGAGGAGCTGGGC
GCCAACCGGGTCTTTGAACTGGGACTGGGCGACGATGATGCCAACATCGAGGATGACTTC
ATCACGTGGAAGGATCGCTTCTGGCCCGCCGTGTGCGATCACTTCGGCATCGAGGGCGGC
GGCGAGGAAGTGCTCATCCGCCAGTACCGTTTGCTAGAACAGCCAGATGTGCAGCCTGAC
CGCATTTACACGGGAGAGATCGCCCGCCTGCACTCGATTCAGAACCAGCGCCCGCCCTTC
GACGCCAAGAACCCATTCCTGGCCCCCATCAAGGTGAACCGCGAGCTGCACAAGGGCGGT
GGCCGCTCCTGCATGCACATTGAGCTGAGCATCGAGGGTTCCAAGATGCGCTACGATGCC
GGAGATCATGTGGCCATGTTCCCTGTTAACGACAAGAGTCTGGTGGAGAAGCTCGGCCAG
CTGTGCAACGCCGATCTGGATACTGTGTTCTCGCTGATCAACACCGATACGGACAGCAGC
AAGAAGCACCCATTCCCTTGCCCCACTACGTACCGCACCGCTCTGACCCACTACCTGGAA
ATTACGGCCATACCCCGCACACACATCCTCAAGGAGCTCGCTGAGTATTGTACTGACGAG
AAGGAGAAGGAGTTGCTGCGCAGCATGGCCTCCATCAGTCCCGAAGGAAAGGAGAAATAC
CAGAGCTGGATCCAAGACGCCTGTCGCAACATCGTCCACATTCTGGAGGACATCAAATCC
TGTCGCCCACCCATCGATCACGTTTGCGAGCTGCTGCCCCGCTTGCAGCCTCGTTACTAC
TCCATCTCGTCGTCTGCTAAGCTGCACCCCACTGATGTCCACGTTACAGCCGTTCTCGTG
GAGTACAAGACGCCGACGGGACGCATCAACAAGGGCGTAGCCACCACATATCTGAAGAAC
AAGCAGCCGCAGGGCAGTGAGGAAGTAAAGGTTCCGGTATTCATCCGCAAGTCGCAGTTC
CGTTTGCCTACGAAGCCAGAGACACCTATCATAATGGTGGGTCCTGGCACTGGCTTGGCC
CCCTTCCGCGGATTCATTCAGGAGCGACAATTCCTTCGCGATGAGGGCAAGACCGTGGGC
GAGTCGATTCTCTACTTCGGTTGCCGTAAGCGCAGTGAGGACTACATCTACGAATCCGAG
TTGGAGGAGTGGGTTAAGAAGGGCACTCTCAACCTGAAGGCCGCCTTTTCTCGTGACCAG
GGCAAGAAGGTCTACGTGCAGCATCTGCTCGAGCAGGACGCAGATCTTATATGGAACGTG
ATTGGCGAGAATAAGGGGCACTTCTACATATGCGGTGATGCAAAGAACATGGCCGTGGAC
GTTAGGAACATTTTAGTGAAAATTTTGTCCACTAAGGGTAACATGAGCGAGGCTGACGCC
GTGCAGTATATCAAGAAGATGGAGGCTCAGAAGCGCTACTCGGCCGATGTCTGGAGCTAA

HsCPR

ATGATCAACATGGGAGACTCCCACGTGGACACCAGCTCCACCGTGTCCGAGGCGGTGGCC
GAAGAAGTATCTCTTTTCAGCATGACGGACATGATTCTGTTTTCGCTCATCGTGGGTCTC
CTAACCTACTGGTTCCTCTTCAGAAAGAAAAAAGAAGAAGTCCCCGAGTTCACCAAAATT
CAGACATTGACCTCCTCTGTCAGAGAGAGCAGCTTTGTGGAAAAGATGAAGAAAACGGGG
AGGAACATCATCGTGTTCTACGGCTCCCAGACGGGGACTGCAGAGGAGTTTGCCAACCGC
CTGTCCAAGGACGCCCACCGCTACGGGATGCGAGGCATGTCAGCGGACCCTGAGGAGTAT
GACCTGGCCGACCTGAGCAGCCTGCCAGAGATCGACAACGCCCTGGTGGTTTTCTGCATG
GCCACCTACGGTGAGGGAGACCCCACCGACAATGCCCAGGACTTCTACGACTGGCTGCAG
GAGACAGACGTGGATCTCTCTGGGGTCAAGTTCGCGGTGTTTGGTCTTGGGAACAAGACC
TACGAGCACTTCAATGCCATGGGCAAGTACGTGGACAAGCGGCTGGAGCAGCTCGGCGCC
CAGCGCATCTTTGAGCTGGGGTTGGGCGACGACGATGGGAACTTGGAGGAGGACTTCATC
ACCTGGCGAGAGCAGTTCTGGCCGGCCGTGTGTGAACACTTTGGGGTGGAAGCCACTGGC
GAGGAGTCCAGCATTCGCCAGTACGAGCTTGTGGTCCACACCGACATAGATGCGGCCAAG
GTGTACATGGGGGAGATGGGCCGGCTGAAGAGCTACGAGAACCAGAAGCCCCCCTTTGAT

GCCAAGAATCCGTTCCTGGCTGCAGTCACCACCAACCGGAAGCTGAACCAGGGAACCGAG
CGCCACCTCATGCACCTGGAATTGGACATCTCGGACTCCAAAATCAGGTATGAATCTGGG
GACCACGTGGCTGTGTACCCAGCCAACGACTCTGCTCTCGTCAACCAGCTGGGCAAAATC
CTGGGTGCCGACCTGGACGTCGTCATGTCCCTGAACAACCTGGATGAGGAGTCCAACAAG
AAGCACCCATTCCCGTGCCCTACGTCCTACCGCACGGCCCTCACCTACTACCTGGACATC
ACCAACCCGCCGCGTACCAACGTGCTGTACGAGCTGGCGCAGTACGCCTCGGAGCCCTCG
GAGCAGGAGCTGCTGCGCAAGATGGCCTCCTCCTCCGGCGAGGGCAAGGAGCTGTACCTG
AGCTGGGTGGTGGAGGCCCGGAGGCACATCCTGGCCATCCTGCAGGACTGCCCGTCCCTG
CGGCCCCCCATCGACCACCTGTGTGAGCTGCTGCCGCGCCTGCAGGCCCGCTACTACTCC
ATCGCCTCATCCTCCAAGGTCCACCCCAACTCTGTGCACATCTGTGCGGTGGTTGTGGAG
TACGAGACCAAGGCTGGCCGCATCAACAAGGGCGTGGCCACCAACTGGCTGCGGGCCAAG
GAGCCTGCCGGGGAGAACGGCGGCCGTGCGCTGGTGCCCATGTTCGTGCGCAAGTCCCAG
TTCCGCCTGCCCTTCAAGGCCACCACGCCTGTCATCATGGTGGGCCCCGGCACCGGGGTG
GCACCCTTCATAGGCTTCATCCAGGAGCGGGCCTGGCTGCGACAGCAGGGCAAGGAGGTG
GGGGAGACGCTGCTGTACTACGGCTGCCGCCGCTCGGATGAGGACTACCTGTACCGGGAG
GAGCTGGCGCAGTTCCACAGGGACGGTGCGCTCACCCAGCTCAACGTGGCCTTCTCCCGG
GAGCAGTCCCACAAGGTCTACGTCCAGCACCTGCTAAAGCAAGACCGAGAGCACCTGTGG
AAGTTGATCGAAGGCGGTGCCCACATCTACGTCTGTGGGGATGCACGGAACATGGCCAGG
GATGTGCAGAACACCTTCTACGACATCGTGGCTGAGCTCGGGGCCATGGAGCACGCGCAG
GCGGTGGACTACATCAAGAAACTGATGACCAAGGGCCGCTACTCCCTGGACGTGTGGAGC
TAG

RpCPR

ATGGAAAAAACTATAGGCGCGGAAGAGCAGACGGGACCGTTGGAAGACATTGAAGAACCA
ATGTTTGGCGTGTTGGATGTGGTATTATTGGTAGCTTTACTTGGAGTAGCCGCTTGGTGG
CTTATGAGGAATAAAAAAGCTGATGCAGCGCTTAGAGAGAAAACTTACGCCATACAACCA
ATGGCAATGAGCTCAATGCCACAAAGTACAGAAAATTCTTTTATTAAAAAGTTAAAATCA
AGTGGACGAAGCCTCATAGTATTCTATGGTAGCCAGACTGGTACTGGTGAAGAATTCGCT
GGACGTATTGCTAAAGAAGGGATTAGGTATAAAATGAAAGGAATGGTTGCCGATCCAGAA
GAATATGATATGGAAGATCTAATTCAAATGAAGACAATACCAAACTCATTAGCCGTTTTC
TGTATGGCAACCTATGGTGAAGGCGATCCAACTGATAATGCCATGGATTTCTATGAATGG
CTTCAGAATGGTGAAGCAGATCTTACAGGGCTTAATTATGCTGTCTTTGGTTTGGGTAAC
AAAACTTACGAGCACTATAATGAAGTTGGTATCTACATTGACAAAAGGTTAGAAGAACTA
GGAGCAACTAGAGTATTTGAACTAGGACTTGGGGATGATGATGCTAACATTGAAGATGAC
TTTATTACTTGGAAAGACAGATTTTGGCCGACAGTTTGTGCCCATTTTGGTATAGAATCT
GCGGGAGAAGATGTCTCTGTAAGGCAATACAAACTCACCGAACATATAGAGACAATACCA
GAGCGAGTGTTCACCGGAGAAGTGGCTAGACTGCATTCACTCATCAATCAGAGACCACCA
TTCGACGTGAAGAACCCTTACTTAGCGCCAGTAAAAGTTAATAGAGAATTACATAAAGGT
GGTGGAAGATCTTGTATGCATATTGAATTTGACATTGAAGGATCTAAAATGCGATATGAC
ACTGGGGACCATGTAGCCGTATATCCAATGAATGACTCAGAATTAGTCAATAAGTTTGGC
ACATTACTTGGAGTTGATTTAGACACTATTATTACCTTAACAAACACTGACGAGGATTCT
AGTAAAAAACATCCATTCCCTTGTCCGTGTTCCTATAGGACCGCTTTGACGTATTATATT
GACATAACATCTAATCCACGTACTCATATTCTTAAAAACGCAGAGTATGCCACAGATCCT
GAGGAAGCAGCAAAATTGAAGCTGATGGCAAGTACTTGTGCAGATGGTAAACATTTGTAC
AGCCAGTGGATAAATCAAGATAATAGAAATATTGTTCATATATTAGAGGACTTGCCTTCT
TGTAAACCCAAATTGGATCATCTTTGCGAATTATTGCCGAGGTTACAATGCCGTTATTAC
TCAATATCATCGTCATCCAAGCTCTATCCTACCACAGTGCACATTACAGCTGTAAAAGTG
GAATATGATACTAACACCGGGCGTAGAAACAAAGGTGTTGCTACATCATGGTTAGGAAAA
AAAATACCAACGGACCCTAATGCCCTTCCTGTTGTTCCTATCTTTTTCAGGAAATCACAA
TTCAAATTGCCCACAAGACCTCAGACGCCAATAATTATGATAGGGCCTGGTACAGGTTTA
GCCCCATTTAGAGGATTCATACAAGAACGACATATGGCCAAAGAAGAAGGCAAACCTCTA
GGAGAAACTATCCTATATTTTGGATGCAGAAAGAAATCAGAAGATTATCTTTACGAAGAA
GAACTTGATGAATTTGTGAAGAAGGGGACGTTGAAATTACATGTGGCATTTTCACGTGAT
CAAAAAGAAAAAGTATACGTTACACATCTTTTAGCACAAAATGCTGATGAAATTTGGAAC

GTCATTGGTGAAAACAATGGACATTTATATATCTGCGGTGATGCCAGATCGATGGCACGC
GATGTGCACGATATACTATTAAAAGTGGTACAAGAAAAGGGGAAAATGACTGAAGAAGAG
GCTAATAATTATGTAAAAAAGATGGAAGCACAAAAGAGATATTCAGCTGATGTTTGGAGT
TAA

Appendix 6.2 – Primers for preliminary amplification

These primers were used to create a full length CPR insert to be cloned into pJET1.2 and used as a template for further amplification.

Primer Name	**Primer Function**	**Primer Sequence (5' – 3')**
AaF	*Ae. aegypti* forward	ATGGACGCACAGACGGAAC
AaR	*Ae. aegypti* reverse	TTAACTCCACACGTCGGCC
AgF	*An. gambiae* forward	ATGGACGCCCAGACAGAAAC
AgR	*An. gambiae* reverse	TTAGCTCCACACGTCCGC
AmF	*A. mellifera* forward	ATGATGTTTTATATGTACATATGTTTATGTG
AmR	*A. mellifera* reverse	TCAACTCCATACGTCACTTGAATAAC
CqF	*C. quinquefasciatus* forward	ATGGACGCACAGACAGAG
CqR	*C. quinquefasciatus* reverse	TTAACTCCACACGTCGGC
DmF	*D. melanogaster* forward	ATGGCCAGCGAGCAAACG
DmR	*D. melanogaster* reverse	TTAGCTCCAGACATCGGCC
GmF	*G. morsitans* forward	ATGACTGATGAGAAAATCGAAAACG
GmR	*G. morsitans* reverse	CTACCCACATATGTAAAAGTGG
HsF	*H. sapiens* forward	ATGATCAACATGGGAGACTCC
HsR	*H. sapiens* reverse	CTAGCTCCACACGTCCAG
RpF	*R. prolixus* forward	ATGGAAAAAACTATAGGCGCGG
RpR	*R. prolixus* reverse	TTAACTCCAAACATCAGCTGAATATC

Appendix 6.3 – pOPINF CPR Primers

CPR	Forward Primer		Reverse Primer	
	Sequence (5'-3')	**Melting temperature (°C)**	**Sequence (5'-3')**	**Melting temperature (°C)**
AaCPR full length	AAGTTCTGTTTCAGGGCCCGGACGCACAGACG GAACCGGAG	73.5	ATGGTCTAGAAAGCTTTATTAACTCCACACG TCGGCCGAGTATCGC	69.9
AaCPR truncated	AAGTTCTGTTTCAGGGCCCGACGATGACCATG GCGGAGAACTCG	72.9	ATGGTCTAGAAAGCTTTATTAACTCCACACG TCGGCCGAGTATCGC	69.9
AgCPR full length	AAGTTCTGTTTCAGGGCCCGGACGCCCAGACA GAAACGGAAGTG	72.9	ATGGTCTAGAAAGCTTTATTAGCTCCACACG TCCGCCGAG	68.6
AgCPR truncated	AAGTTCTGTTTCAGGGCCCGGACGCCCAGACA GAAACGGAAGTG	72.9	ATGGTCTAGAAAGCTTTATTAGCTCCACACG TCCGCCGAG	68.6
AmCPR full length	AAGTTCTGTTTCAGGGCCCGGCAGGTTCTCCA GTATTGGAGAATGAGG	72.2	ATGGTCTAGAAAGCTTTATCAACTCCATACG TCACTTGAATAACGTTTTTG	66.2
AmCPR truncated	AAGTTCTGTTTCAGGGCCCGACATCAGAAAAT TCATTTATAAAAAAATTGAAAACTTCTG	66.7	ATGGTCTAGAAAGCTTTATCAACTCCATACG TCACTTGAATAACGTTTTTG	66.2

CqCPR full length	AAGTTCTGTTTCAGGGCCCGGACGCACAGACA GAGCCGGAAGTGC	74.6	ATGGTCTAGAAAGCTTTATTAACTCCACACG TCGGCCGAGTACC	69.2
CqCPR truncated	AAGTTCTGTTTCAGGGCCCGACGATGACCATG GCGGAGAACTCC	72.9	ATGGTCTAGAAAGCTTTATTAACTCCACACG TCGGCCGAGTACC	69.2
DmCPR full length	AAGTTCTGTTTCAGGGCCCGGCCAGCGAGCAA ACGATTGATGGAGC	73.5	ATGGTCTAGAAAGCTTTATTAGCTCCAGACA TCGGCCGAGTAGCG	70
DmCPR truncated	AAGTTCTGTTTCAGGGCCCGACCACCAGTGCG TCGGACAATTCG	72.9	ATGGTCTAGAAAGCTTTATTAGCTCCAGACA TCGGCCGAGTAGCG	70
GmCPR full length	AAGTTCTGTTTCAGGGCCCGACTGATGAGAAA ATCGAAAACGTTGTTAGCGG	70.9	ATGGTCTAGAAAGCTTTACTACCCACATATG TAAAAGTGGCCGTTATTTTCACC	68.4
GmCPR truncated	AAGTTCTGTTTCAGGGCCCGACTGCAGCAGTT ACAGAAAATTCGTTTATTAAGAAATTG	69.5	ATGGTCTAGAAAGCTTTACTACCCACATATG TAAAAGTGGCCGTTATTTTCAC	67.7
HsCPR full length	AAGTTCTGTTTCAGGGCCCGATCAACATGGGA GACTCCCACGTGG	72.7	ATGGTCTAGAAAGCTTTACTAGCTCCACACG TCCAGGGAGTAGC	70.1
HsCPR truncated	AAGTTCTGTTTCAGGGCCCGACCTCCTCTGTCA GAGAGAGCAGCTTTG	73.1	ATGGTCTAGAAAGCTTTACTAGCTCCACACG TCCAGGGAGTAGC	70.1

RpCPR full length	AAGTTCTGTTTCAGGGCCCGGAAAAAACTATA GGCGCGGAAGAGCAGAC	72.1	ATGGTCTAGAAAGCTTTATTAACTCCAAACA TCAGCTGAATATCTCTTTTGTG	66.1
RpCPR truncated	AAGTTCTGTTTCAGGGCCCGATGCCACAAAGT ACAGAAAATTCTTTTATTAAAAAGTTAA	67.4	ATGGTCTAGAAAGCTTTATTAACTCCAAACA TCAGCTGAATATCTCTTTTGTGC	66.9

Appendix 6.4 – CPR Truncations

Enzyme	Truncated protein size (aa)	Residues removed (aa)	Approximate truncated protein size (kDa)
AgCPR	613	66	65000
AmCPR	613	67	67500
CqCPR	613	67	67700
DmCPR	613	67	67700
HsCPR	618	63	68000
RpCPR	613	68	67700